

An investigation of cholesterol pathways in castration-resistant prostate cancer: the role of scavenger receptor class B type I (SR-BI)

by

Alexis Twiddy

BSc and BPhE Queen's University, 2007

A THESIS SUBMITTED IN PARTIAL FULFILLMENT OF
THE REQUIREMENTS FOR THE DEGREE OF

MASTER OF SCIENCE

in

THE FACULTY OF GRADUATE STUDIES

(Pharmaceutical Sciences)

THE UNIVERSITY OF BRITISH COLUMBIA
(Vancouver)

November 2011

© Alexis Twiddy, 2011

ABSTRACT

Background. Scavenger Receptor Class B Type I (SR-BI) facilitates influx of cholesterol to the cell from lipoproteins in the circulation. This influx of cholesterol is important for many cellular functions, including synthesis of androgens. Castration-resistant prostate cancer tumors are able to synthesize androgens *de novo* in order to supplement the loss of exogenous sources often as a result of androgen deprivation therapy. By removing a source of cholesterol, silencing of SR-BI may impact the ability of prostate cancer cells, particularly those of castration-resistant state, to maintain the intracellular supply of androgens.

Methods. SR-BI expression was knocked down in LNCaP (androgen-dependent) and C4-2 (castration-resistant) cells using small interfering RNA. The effect of down-regulation of SR-BI on cell toxicity, cell viability, and expression of various proteins was examined using a LDH assay, a MTS assay and western blotting in both cell types. In addition, cholesterol synthesis activity was measured using the radiolabeled precursor, ^{14}C -acetate and cellular cholesterol, testosterone and PSA concentrations were assessed using fluorometric and colorimetric assays.

Results. Basal SR-BI and HSL protein expression was higher in C4-2 cells than LNCaP cells. Silencing of SR-BI expression by greater than 85% reduced PSA secretion in LNCaP and C4-2 SRBI-KD cells by 55% and 58% compared to negative control cells, respectively. SR-BI-KD C4-2 cells demonstrated significantly reduced cell viability

(>25%) compared the NC cells as well as an increased cholesterol synthesis 6 days post-transfection.

Conclusions. The down-regulation of SR-BI significantly impacted PSA production of both prostate cancer cell lines, as well as the viability of C4-2 cells in the presence and absence of HDL. Although corresponding changes in cholesterol and testosterone concentrations were not observed, the data suggest that silencing SR-BI and thereby reducing cholesterol influx impacts cholesterol pathways, as evidenced by a compensatory up-regulation of *de novo* cholesterol synthesis. This may affect substrate availability to the androgen synthesis pathway or may implicate a separate role of SR-BI in prostate cancer cells.

PREFACE

A portion of the data and introductory information presented in the following thesis has been published in peer-reviewed journals.

A version of Chapter 1 has been published. Twiddy AL, Leon CG, and Wasan KM. (2011) Cholesterol as a potential target in castration-resistant prostate cancer. *Pharm Res* 2011;28(3):423-437. I wrote this review paper.

Portions of the data, methodology and discussion found in Chapter 3, 4 and 5 have been published online in 'Prostate'. Twiddy AL, Cox ME, and Wasan KM. Knockdown of Scavenger Receptor Class B Type I (SR-BI) reduces prostate specific antigen secretion and viability of prostate cancer cells. *Prostate*. 2011 Oct 24. doi: 10.1002/pros.21499. [Epub ahead of print]. I conducted all the experiments presented in this paper and wrote the article.

TABLE OF CONTENTS

ABSTRACT.....	ii
PREFACE.....	iv
TABLE OF CONTENTS.....	v
LIST OF TABLES	vii
LIST OF FIGURES	viii
LIST OF ABBREVIATIONS	xii
ACKNOWLEDGMENTS	xiii
CHAPTER 1 INTRODUCTION	1
1.1 OVERVIEW	2
1.2 THE PROSTATE, ANDROGENS AND THE ANDROGEN RECEPTOR.....	3
1.3 CRPC AND <i>DE NOVO</i> ANDROGEN SYNTHESIS.....	7
3.3.1 CRPC EXPERIMENTAL MODELS.....	9
1.4 PROSTATE CANCER AND CHOLESTEROL	11
1.4.1 DIETARY CHOLESTEROL AND PROSTATE CANCER	12
1.4.2 LIPOPROTEINS AND ANDROGEN-DEPRIVATION THERAPY.....	13
1.5 SOURCES OF CELLULAR CHOLESTEROL	15
1.5.1 CHOLESTEROL SYNTHESIS	15
1.5.2 METABOLISM OF INTRACELLULAR CHOLESTEROL	17
1.5.3 CHOLESTEROL TRANSPORT-EFFLUX AND INFLUX.....	19
1.5.3.1 ATP-BINDING CASSETTE TRANSPORTER SUBFAMILY A1	19
1.5.3.2 LOW-DENSITY LIPOPROTEIN RECEPTOR	20
1.5.3.3 SCAVENGER RECEPTOR CLASS B TYPE I.....	21
1.6 CHOLESTEROL IN STEROIDOGENIC TISSUES	23
1.7 NEW ANDROGEN RECEPTOR-SIGNALING THERAPIES	24
1.7.2 STATINS AS PROSTATE CANCER THERAPEUTICS.....	27
1.8 OBJECTIVE	29
1.9 SIGNIFICANCE OF THE RESEARCH	30
1.10 HYPOTHESIS	30
CHAPTER 2 AIMS	31
2.1 SPECIFIC AIMS.....	32
2.2 RATIONALE.....	33
CHAPTER 3 MATERIALS AND METHODS.....	36
3.1 MATERIALS AND REAGENTS	37
3.1.1 ANTIBODIES.....	37
3.2 CELL CULTURE	38
3.3 PROTEIN QUANTIFICATION.....	38
3.4. SIRNA TRANSFECTION PROTOCOL.....	40
3.5 CELL CYTOTOXICITY AND VIABILITY	42
3.5.1 LDH ASSAY	42
3.5.2 MTS ASSAY	43
3.6 WESTERN BLOTTING.....	45
3.7 CHOLESTEROL ANALYSES	46
3.7.1 CHOLESTEROL QUANTIFICATION.....	46
3.7.2 CHOLESTEROL SYNTHESIS (HMGCR ACTIVITY) ASSAY	48
3.8 TESTOSTERONE ASSAY	49
3.9 PROSTATE SPECIFIC ANTIGEN ASSAY	51
3.9.1 BASAL PSA AND RESPONSE TO DHT.....	52
3.10 STATISTICAL ANALYSES	53

CHAPTER 4 RESULTS	54
4.1 AIM 1 EXPERIMENTS	55
4.1.1 PSA SECRETION IN THE PRESENCE AND ABSENCE OF DHT.....	55
4.1.2 BASAL PROTEIN EXPRESSION.....	56
4.1.2.2 BASAL SR-BI AND HSL EXPRESSION.....	58
4.2 AIM 2 EXPERIMENTS	59
4.2.1 SIRNA-INDUCED SILENCING OF SR-BI.....	59
4.2.2 CYTOTOXICITY OF SR-BI SILENCED CELLS	61
4.2.3 CELL VIABILITY OF SR-BI SILENCED CELLS	63
4.3 AIM 3 EXPERIMENTS	64
4.3.1 CELLULAR CHOLESTEROL IN SR-BI SILENCED CELLS.....	64
4.3.2 PROTEIN EXPRESSION IN SR-BI SILENCED CELLS.....	67
4.3.2.1 INFLUX AND EFFLUX TRANSPORTERS.....	67
4.3.2.2. CHOLESTEROL METABOLISM ENZYMES	68
4.3.2.3 CHOLESTEROL SYNTHESIS- HMGCR EXPRESSION	71
4.3.3 CHOLESTEROL SYNTHESIS ACTIVITY	71
4.4 AIM 4 EXPERIMENTS	73
4.4.1 PSA SECRETION IN SR-BI SILENCED CELLS	73
4.4.2 INTRACELLULAR TESTOSTERONE IN SR-BI SILENCED CELLS.....	76
4.4.3 STAR AND AR PROTEIN EXPRESSION IN SR-BI SILENCED CELLS	78
CHAPTER 5 DISCUSSION	80
5.1 BASAL SR-BI IN LNCAP AND C4-2	81
5.2 SR-BI SILENCING AFFECTS CELL VIABILITY	84
5.3 SR-BI SILENCING AFFECTS CHOLESTEROL SYNTHESIS	85
5.4 SR-BI SILENCING-INDUCED EFFECTS ON PSA	88
5.5 SR-BI MEDIATED SIGNAL TRANSDUCTION.....	91
5.6 LIMITATIONS OF CURRENT RESEARCH AND FUTURE STUDIES.....	94
5.7 CONCLUSIONS.....	96
5.8 SIGNIFICANCE OF FINDINGS	97
REFERENCES.....	98
APPENDICES	117
APPENDIX A: PROTEIN CONTENT IN CELL LINES.....	118
APPENDIX B: SIRNA METHOD DEVELOPMENT	119
APPENDIX C: SIRNA METHOD DEVELOPMENT	120
APPENDIX D: LIPOPROTEIN METHOD DEVELOPMENT	121
APPENDIX E: LDL-INDUCED VIABILITY	122
APPENDIX F: INTRACELLULAR CHOLESTEROL	123
APPENDIX G: CHOLESTEROL SYNTHESIS DAY 3	124
APPENDIX H: FUTURE STUDIES	125

LIST OF TABLES

Table 1: Antibody specifications used in western blotting techniques.....	38
--	-----------

LIST OF FIGURES

Figure 1: Classical and backdoor steroidogenic pathways (Adapted from (12)).....	8
Figure 2A-D: LNCaP xenograft <i>ex vivo</i> cholesterol synthesis activity (A), ACAT2 (B) and SR-BI (C) protein expression and testosterone (C) concentrations in androgen-dependent (AD), nadir/castrate and castration-resistant (CRPC) tumour samples (adapted from (50)). *, **, p<.05 as compared to AD and Nadir, respectively.	17
Figure 3: Plasma membrane topology of Scavenger Receptor Class B Type I (103).	21
Figure 4: A typical BSA standard curve is shown. This standard curve plots absorbance at 650nm against known concentrations of BSA ($\mu\text{g/mL}$). The equation of the line is determined and sample protein concentrations are extrapolated by solving for x.	40
Figure 5: A typical Amplex® Red cholesterol assay standard curve is shown. This standard curve plots fluorescence (excitation of 530 nm and emission of 590 nm) of known concentrations of cholesterol ($\mu\text{g/mL}$). The equation of the line is determined and sample cholesterol concentrations are determined by solving for x.	47
Figure 6: A typical testosterone standard curve is shown. This standard curve plots absorbance (450 nm-540 nm) corrected for non-specific binding (NSB) against known log-transformed testosterone concentrations. The equation of the sigmoidal line is determined using 4-parametric linear regression model.	50
Figure 7: A typical PSA standard curve is shown. This standard curve plots absorbance at 450nm against known concentrations of PSA (ng/mL) as provided. The equation of the line is determined and sample PSA concentrations are determined by solving for x.	52
Figure 8: PSA secretion (ng/mL) per μg of protein in LNCaP and C4-2 cells untreated (-DHT) and treated (+DHT) with 10nM DHT in 5% CSS for 72 hours. Columns, mean (n=6 for LNCaP and n=12 for C4-2); bars, +/-SD. *, p<.05, -DHT vs +DHT of each group, #, p<.05, -DHT LNCaP vs -DHT C4-2.	56
Figure 9: Basal protein expression derived from Western blots of proteins involved in cholesterol influx (SR-BI, LDLrec), efflux (ABC-A1), synthesis (HMGCR), metabolism (ACAT-1, ACAT-2 and HSL), transport into mitochondria (stAR) and the androgen receptor (AR) in LNCaP (grey) and C4-2 cells (black). All values are shown normalized to expression in LNCaP cells. Columns, mean (n is specified below the respective proteins); bars, +/-SEM. *, p<.05, LNCaP vs C4-2.	57
Figure 10A-D: Basal protein expression of SR-BI (A) and HSL (C) in LNCaP and C4-2 cells normalized to expression in LNCaP cells. Representative blots of each protein are shown for SR-BI (B) and HSL (D) with the respective actin bands. Columns, mean (n=8 for SR-BI and n=4 for HSL); bars, +/-SEM. *, p<.05.	58
Figure 11A-B: Silencing of SR-BI protein expression in C4-2 (A) and LNCaP (B) cells at Day 1, 3 and 6 post-transfection with negative control (NC) and SR-BI (SRBI-KD) siRNA. Data is shown as the fold change in SR-BI expression from the expression in a pre-transfection control for each cell type. NC was not significantly different than Blank (not shown). Inset diagrams demonstrate representative blots analyzed in each cell type. Columns, mean (n=6); bars, +/-SEM. *, p<.05, NC versus SRBI-KD.	60

- Figure 12A-B:** Cell cytotoxicity is demonstrated as % cytotoxicity based on a 100% cytotoxic control, representing the amount of LDH in the media of C4-2 (A) and LNCaP (B) cells treated with SR-BI siRNA (SRBI-KD, black bars) and a negative control siRNA (NC, grey bars) at Day 1, 3 and 6 post-transfection. Values are controlled for day 0 cytotoxicity. Columns, mean (n=5); bars, +/-SEM..... 62
- Figure 13A-D:** Cell viability is demonstrated as fold change in viability from the pre-transfection (Day 0) control in C4-2 (A) and LNCaP (B) cells treated with SR-BI siRNA (SRBI-KD, black columns), a negative control siRNA (NC, grey columns) at Day 1, 3 and 6 post-transfection. C&D: Measures were taken 24hrs after the addition of 10ug/mL HDL (+HDL) which was added immediately post-transfection on Day 0 to NC (grey columns) and SRBI-KD (black columns) cells. Columns, mean (n=6 for A/B, n=3 for C/D); bars, +/-SEM. *, p<.05, SRBI-KD vs NC (A/B) and NC+HDL vs NC (C). 64
- Figure 14A-D:** Total cholesterol is shown as µg cholesterol per µg protein in whole cell lysates of C4-2 (A) and LNCaP (B) cells treated with SR-BI siRNA (SRBI-KD, black triangles) and negative control (NC, grey boxes) siRNA at Day 0 (pre-transfection) and Day 1, 3 and 6 post-transfection. Free cholesterol (FC, dotted lines) and cholesteryl ester (CE, broken lines) concentration (µg FC or CE/µg of protein) is shown in C4-2 (C) and LNCaP (D) cells. Curve, mean (n=5); error bars, +/-SEM..... 66
- Figure 15A-D:** Expression of LDLrec in C4-2 (A) and LNCaP (B) cells at Day 1, 3 and 6 post-transfection with negative control (NC) and SR-BI (SRBI-KD) siRNA. Expression of ABC-A1 is shown in C4-2 (C) and LNCaP (D) cells. Data is shown as the fold change in LDLrec and ABC-A1 expression from the respective protein expression in a pre-transfection control for each cell type. Inset diagrams demonstrate representative blots analyzed in each cell type. Columns, mean (n=6 for LDLrec and n=5 for ABC-A1); bars, +/-SEM..... 68
- Figure 16A-F:** Expression of ACAT-1 and ACAT-2 in C4-2 (A,C) and LNCaP (B,D) cells at Day 1, 3 and 6 post-transfection with negative control (NC) and SR-BI (SRBI-KD) siRNA. Expression of HSL is shown in C4-2 (E) and LNCaP (F) cells. Data is shown as the fold change in ACAT-1, ACAT-2 and HSL expression from the respective protein expression in a pre-transfection control for each cell type. Inset diagrams demonstrate representative blots analyzed in each cell type. Columns, mean (n=6; ACAT-1/2 and n=4; HSL); bars, +/-SEM. *, p<.05. NC versus SRBI-KD. 70
- Figure 17A-B:** Expression of HMGCR in C4-2 (A) and LNCaP (B) cells at Day 1, 3 and 6 post-transfection with negative control (NC) and SR-BI (SRBI-KD) siRNA. Data is shown as the fold change in HMGCR expression from the expression in a pre-transfection control for each cell type. Inset diagrams demonstrate representative blots analyzed in each cell type. Columns, mean (n=5); bars, +/-SEM. 71
- Figure 18:** Cholesterol synthesis was measured by following the incorporation of ¹⁴C-acetate into cellular cholesterol as measured by scintillation counting after separation by thin layer chromatography in C4-2 and LNCaP cells at Day 0 (white columns) and Day 6 post-transfection with negative control siRNA (NC, grey columns) and SR-BI siRNA (SRBI-KD, black columns). All values are corrected by ³H-cholesterol control counts (dpm) and by ug of protein in a given sample. Columns, mean (n=3); bars, +/- SEM. *, p<.05 Day 6 NC vs Day 6 SRBI-KD..... 73
- Figure 19A-B:** PSA secretion is demonstrated as concentration in the media of C4-2 (A) and LNCaP (B) cells treated with SR-BI siRNA (SRBI-KD, black triangles), a negative control siRNA (NC, grey squares) at Day 0 (pre-transfection) and Day 1, 3 and 6 post-transfection. Values were adjusted for the amount of protein in the respective samples. Curve, mean (n=5); bars, +/-SEM. *, p<.05 Day 6 NC versus Day 6 SRBI-KD. 75

Figure 20A-B: Intracellular testosterone concentration (ng/mL) is shown in C4-2 (A) and LNCaP (B) cells treated with SRBI siRNA (SRBI-KD, black triangles) and a negative control siRNA (NC, grey squares) at Day 0 (pre-transfection) and Day 1, 3 and 6 post-transfection. Values were adjusted for the amount of protein (μg) in the respective samples. Curve, mean (n=5); bars, +/-SEM. *, p<.05 Day 3 NC versus Day 3 SRBI-KD..... 77

Figure 21A-D: Expression of stAR in C4-2 (A) and LNCaP (B) cells at Day 1, 3 and 6 post-transfection with negative control (NC) and SR-BI (SRBI-KD) siRNA. Expression of AR is shown in C4-2 (C) and LNCaP (D) cells. Data is shown as the fold change of stAR and AR expression from the respective protein expression in a pre-transfection control for each cell type. Inset diagrams demonstrate representative blots analyzed in each cell type. Columns, mean (n=3 for stAR and n=6 for AR); bars, +/-SEM. 79

Figure 22: Diagram of cellular cholesterol (●) pathways- synthesis, metabolism, influx and efflux. Cholesterol moves to mitochondria where stAR initiates androgen synthesis by shuttling cholesterol into the intermitochondrial space. Androgens (T) bind to the AR and cause gene transcription (Adapted from (156)). 82

Figure 23: A depiction of one possible SR-BI-mediated effect on cell signaling pathways. Src is activated by SR-BI thereby eliciting downstream phosphorylation and consequent activation of ERK1/2 and Akt which then induce cellular events (adapted from (188)). 93

Figure A: Picograms of protein per cell; LNCaP (grey column) and C4-2 (black column). Columns, mean (n=3); bars, +/- SEM..... 118

Figure B. A-D: Cell cytotoxicity is displayed in C4-2 (A) and LNCaP (B) cells treated with 1 and 10nM final concentration of negative control (NC, grey columns) and SR-BI (SRBI-KD, black columns) siRNA with 1-7.5uL of RNAiMax; a cationic delivery system. Values are expressed as fold change in LDH release (cytotoxicity) from an untreated control group. The lowest cytotoxic dose with the least difference between NC and SRBI-KD (1 or 10nM siRNA + 2.5 or 5.0uL RNAiMax) groups were tested using western blots for the most efficient and persistent reduction in SR-BI expression. The optimal dose of 10nM final concentration of siRNA with 5.0uL of RNAiMax was chosen. In addition, 25nM and 50nM siRNA with a different cationic delivery system (Lipofectamine® 2000) were tested but are not shown here because they were quickly ruled out due to lack of expression changes and significant toxicity..... 119

Figure C. A-B: Cell viability of cells grown in 5% CSS as opposed to 1%FBS is demonstrated as fold change in viability from the pre-transfection (Day 0) control in C4-2 (A) and LNCaP (B) cells treated with SR-BI siRNA (SRBI-KD, black columns), a negative control siRNA (NC, grey columns) at Day 1, 3 and 6 post-transfection. Columns, mean (n=2); bars, +/-SEM. 120

Figure D. A-D: Cell viability of LNCaP and C4-2 cells in response to increasing doses of HDL (A, C4-2 and B, LNCaP) and LDL (C, C4-2 and D, LNCaP) is demonstrated as fold change from untreated controls (Blank). Measures were taken using an MTS assay 24hrs after the addition of 0-50μg/mL HDL or 0-31.3μg/mL LDL. Columns, mean (n=3); bars, +/-SEM.121

Figure E. A-B: Cell viability is demonstrated as fold change from Day 0 (white column) in C4-2 (A) and LNCaP (B) cells as above. Measures were taken 24hrs after the addition of 6.25ug LDL (+LDL) which was added immediately post-transfection to NC (grey columns) and SRBI-KD (black columns) cells. Columns, mean (n=3); bars, +/-SEM..... 122

Figure F. A-D: Total cholesterol is shown as μg cholesterol per μg protein in intracellular samples of C4-2 (A) and LNCaP (B) cells treated with SR-BI siRNA (SRBI-KD, black

triangles) and negative control (NC, grey boxes) siRNA at Day 0 (pre-transfection) and Day 1, 3 and 6 post-transfection. Free cholesterol (FC, dotted lines) and cholesteryl ester (CE, broken lines) concentration ($\mu\text{g FC or CE}/\mu\text{g of protein}$) is shown in C4-2 (C) and LNCaP (D) cells. Curve, mean (n=3); error bars, +/-SD. 123

Figure G. Cholesterol synthesis was measured by following the incorporation of ^{14}C -acetate into cellular cholesterol as measured by scintillation counting after separation by thin layer chromatography in C4-2 at Day 0 (light grey column) and Day 3 and 6 post-transfection with negative control siRNA (NC, grey columns) and SR-BI siRNA (SRBI-KD, black columns). All values are corrected by ^3H -cholesterol control counts (dpm) and the amount of protein in each sample well (μg). Columns, mean (n=3); bars, +/- SEM. *, p<.05 Day 6 SRBI-KD vs Day 6 NC. 124

Figure H. A-C: Depicted in this figure is SR-BI expression (A), cell viability (B) and PSA secretion (C) results from a 2-dose siRNA protocol in C4-2 cells. Cells were treated with 10nM NC and SR-BI siRNA for 5 hours and then again, 24 hours following the first transfection. Western blot, MTS and PSA assays were completed 1, 3 and 6 days after the 2nd transfection. The expression data shows an improved silencing at Day 1 (SRBI-KD cells), a greater reduction in cell viability at Day 6 (SRBI-KD) and similar PSA secretion as compared to the single dose protocol. Columns/curves, mean (n=1)..... 125

LIST OF ABBREVIATIONS

ABC-A1	ATP-binding cassette transporter-subfamily A1
ACAT	Acyl-Coenzyme A:cholesterol acyltransferase
AR	Androgen Receptor
C4-2	LNCaP-derived castration-resistant cell line
CaP	Prostate Cancer
CEs	Cholesteryl esters
CRPC	Castration-resistant prostate cancer
DHT	Dihydrotestosterone
HDL	High-density lipoprotein
HMGCR	3-hydroxy-3-methylglutaryl-Coenzyme A reductase
HSL	Hormone sensitive lipase
LDL	Low-density lipoprotein
LDLrec	Low-density lipoprotein receptor
LNCaP	Lymph node metastatic prostate adenocarcinoma cell-line, androgen-dependent
NC	Negative control siRNA transfected cells
SR-BI	Scavenger receptor Class B Type I
SRBI-KD	SR-BI siRNA transfected cells
stAR	Steroidogenic acute regulatory protein

ACKNOWLEDGMENTS

I would like to thank Dr. Kishor Wasan, my supervisor, for his invaluable advice, critical scientific eye and constant encouragement and patience throughout my degree. Also, thank you Dr. Wasan for your contagious enthusiasm for science which has made for a wonderful learning environment that fostered my own scientific exploration.

I would also like to thank my committee members, Dr. Michael Cox, Dr. John Hill, Dr. Marc Levine and Dr. Larry Lynd for the incredible input and support provided over the course of this project.

I would also like to acknowledge Dr. Carlos Leon for his guidance and technical support from the onset of this work.

Finally, I would very much like to thank my lab members past and present; Kris, Steve, Sheila, Jackie, Jo-Ann, Jenny, Pavel, Olena, Fady and Jin-Ying, for their help troubleshooting and all the wonderful advice they have provided.

I would like to acknowledge the Canadian Institute for Health Research for their financial support.

CHAPTER 1 INTRODUCTION

1.1 OVERVIEW

Prostate cancer (CaP) is the most frequently diagnosed cancer among North American men as well as the third leading cause of cancer-related deaths in the same cohort (1,2). In Canada in 2011, an estimated 25,500 men will be diagnosed and 4,100 will die of CaP (3). Unfortunately, it is thought that incidence rates will continue to rise in the coming years due to the aging baby boomer population (1,4). In addition to being older than 65, it appears that a familial history, African heritage, obesity, diet and lifestyle may put an individual at higher risk of having CaP (5). The only viable treatment option for prostate cancer that has metastasized beyond the confines of the prostate is androgen deprivation therapy (ADT). This treatment serves to cut-off androgen sources in the body, namely the testes (6) and is carried out through chemical or surgical castration of the testes-the major sources of androgens in males. The premise of this androgen depletion is to remove the principal driving force behind growth, proliferation and differentiation in the prostate; androgens. Although this treatment is initially very successful and leads to tumour regression, more than 80% of these cancers will re-emerge (7). Unfortunately, the cancer that recurs is more aggressive, evasive and deadly, likely due to the clonal selection and adaptive responses that occur in the low androgen environment (6). Consequently, this form of CaP does not respond to hormone therapy, resulting in a very negative prognosis (6). This recurrent form of CaP has been termed androgen-independent, hormone-refractory and androgen-insensitive, among others. Recently, the term most universally used term is castration-resistant prostate cancer (CRPC). CRPC is the preferred term by our group and others, as it reflects the knowledge that the re-emergent CaP is not independent of androgens or their influence, as was once

believed.

The recurrence of CaP in the castration-resistant form arises due to an array of interrelated and complex molecular changes, many of which remain incompletely understood (6,8). In the last few decades, extensive research has been directed toward elucidation of these mechanisms. As a result, a number of pathogenic pathways have been proposed. Interestingly, many involve the persistence or re-emergence of androgens, the androgen receptor (AR) and androgen-regulated genes in the progression to CRPC (6). This continued reliance on the androgen receptor warrants a more in depth look at targeting this signaling axis in CRPC.

1.2 THE PROSTATE, ANDROGENS AND THE ANDROGEN RECEPTOR

The prostate is an exocrine gland in the male reproductive system. It is situated inferior to the bladder, anterior to the rectum and it encircles a distal portion of the urethra. The main function of the prostate is the production and secretion of an alkaline fluid into the seminal mixture so as to neutralize the acidity encountered by sperm in the vaginal tract. The prostate is composed of four histologically distinct zones: the peripheral, central, transitional and anterior fibromuscular. The peripheral zone is the largest and most frequent location affected by CaP; CaP that is associated with greater biological aggressiveness and thus a greater likelihood of dissemination (9).

The normal growth, development and secretory function of the prostate, as well as

many other sex-related characteristics are controlled by androgens, including testosterone and dihydrotestosterone (DHT), which are a subclass of steroid hormones (10). Similarly, androgens have been implicated in the growth and proliferation of CaP, a discovery that earned Charles Huggins the 1966 Nobel Prize (11). Huggins found that in dogs with advanced metastatic CaP that treatment with castration or addition of estrogens caused a regression of tumour growth. It is because of these initial experiments that therapeutic intervention has largely been directed towards removal of androgen sources.

Androgens are primarily synthesized by the Leydig cells of the testes through a series of enzymatic bioconversions from a common precursor, cholesterol (Figure 1- adapted from (12)). The cells of the zona reticularis in the adrenal gland also produces a small amount of testosterone, in addition to the androgen precursors, dehydroepiandrosterone (DHEA) and androstenedione (AED), that can be converted into testosterone in other tissues. These biosynthetic pathways all begin with cholesterol, therefore all steroid hormones share a similar cyclopentanophenanthrene 4-ring structure with varying modifications (13). The androgen synthesis pathway is initiated in the mitochondria of steroidogenic cells (14,15). In order for steroidogenesis to occur, cholesterol must be moved across the mitochondrial membrane into the mitochondrial matrix; the location of steroidogenic enzymes. The transport of cholesterol from the outer mitochondrial membrane to the inner mitochondrial membrane is facilitated by steroidogenic acute regulatory protein (stAR) (16,17). Once in the mitochondrial space, cholesterol is transformed by CYP11A1, also called P450 side-chain cleavage enzyme or desmolase, into the steroid precursor pregnenolone (18). CYP11A1 has been deemed the determinant enzyme for steroidogenic potential, as it is the first and rate-limiting step in

steroid synthesis (13,19). The androgen synthesis process is similar in all steroidogenic tissues, with some tissue-specific variations, but essentially pregnenolone continues along the classical pathway through a number of enzymatic steps terminating mainly in testosterone (Figure 1).

Once synthesized, androgens exert their effects on the prostate and in CaP by binding to the androgen receptor (AR), a ligand-activated nuclear receptor (10). The AR is expressed in many different human tissues. The main androgens involved in AR binding are testosterone and DHT. DHT is a more potent androgen that is the product of testosterone reduction facilitated by the action of two isoforms of steroid 5- α reductase, SRD5A1 and 5A2 (18). These enzymes are highly active in prostatic cells making their reaction product, DHT, the predominant androgen in the prostate (20). Androgens bind to the AR in the cytosol, where it is generally found linked to a large group of stabilizing protein chaperones, including a large heat shock protein (HSP) complex (21). The binding of DHT to AR stimulates release of the large HSP chaperone complex after which the DHT-AR unit homodimerizes with an additional DHT-AR complex. The homodimer then translocates to the nucleus where it can interact with androgen response elements and thereby, initiate transcription of multiple target genes involved in cell growth, proliferation and survival (10,22). One such target gene is prostate specific antigen (PSA), which is a serine protease whose function is to solubilize seminal fluid. PSA is used as a biomarker for CaP screening and progression and serves as a valuable indicator of response to androgens in experimental models, as discussed in the next section (23). Although there is considerable debate with regard to the utility of PSA in the

diagnosis of CaP, it is thought to be the most useful non-invasive screening tool for early detection of CaP.

Hormone therapy is the first-line therapy for disseminated CaP that has spread beyond the confines of the prostate. The most commonly used ADT is chemical castration which targets the androgen-AR signaling pathway discussed above. Chemical castration acts on the leutinizing hormone-releasing hormone (LHRH) in the hypothalamus, subsequently affecting the release of leutinizing hormone (LH) and follicular stimulating hormone (FSH) from the pituitary. LH and FSH are the responsible for stimulating androgen production in the testes. This feedback loop was first described by Schally and Guillemin winning them the 1977 Nobel prize in medicine and was termed the hypothalamic-pituitary-gonadal axis (24). LHRH agonists such as Lupron® or Zoladex®, are given at low levels causing an initial up-regulation of androgen production, termed a 'flare' due to compensatory measures in the negative androgen feedback loop (25). This is followed by a regression in androgen production, which may take up to one month to take effect. Thus, there is an intermediary period in this treatment process in which circulating androgens are high and often an additional therapy to counteract the androgen flare effect is necessary generally by administering either anti-androgens or AR-antagonists, such as Casodex®. The combination of castration with anti-androgen treatment is termed maximal androgen blockade (26). Although this treatment elicits significant tumour regression, it seems that CaP, in time, will recur as CRPC.

1.3 CRPC AND *DE NOVO* ANDROGEN SYNTHESIS

The importance of androgens and the AR in the development of CaP was discovered in the middle of the twentieth century when it was observed that removal of androgens decreased AR activity and expression, resulting in subsequent regression of tumors (11). In the last decade, this same relationship between androgens and the AR has been shown to remain important in the progression to and survival of CRPC. As mentioned previously, CRPC cells have the ability to synthesize androgens *de novo* (6,27-29). This has been demonstrated by following radiolabelled precursors, including acetic acid, through the androgen synthesis pathway within *ex vivo* CRPC tumors. Additionally, a number of groups have found that CRPC tumors not only possess the necessary steroidogenic enzymes for intracellular androgen creation, but also, have detected alterations in the expression of genes encoding many of these enzymes (27,29). These alterations included an up-regulated mRNA of CYP17A1, HSD3B1, HSD3B2 (3 β -Hydroxy steroid dehydrogenase 1 and 2), AKR1C1, AKR1C3 (aldo-keto reductase 1C1 and 3) and SRD5A1 (steroid 5 α -reductase type 1) (Figure 1). CYP17A1 acts to modify pregnenolone and progesterone, while HSD3B1 and 2 convert pregnenolone to progesterone. AKR1C1 and 3 catalyze the biosynthetic steps from androstenedione to testosterone and SRD5A1 converts progesterone to pregnan-3,20-dione. In addition, some of these enzymes are part of the backdoor pathway that diverts reactants from the classical pathway and facilitates creation of DHT without the requirement of testosterone as a direct precursor (27-30).

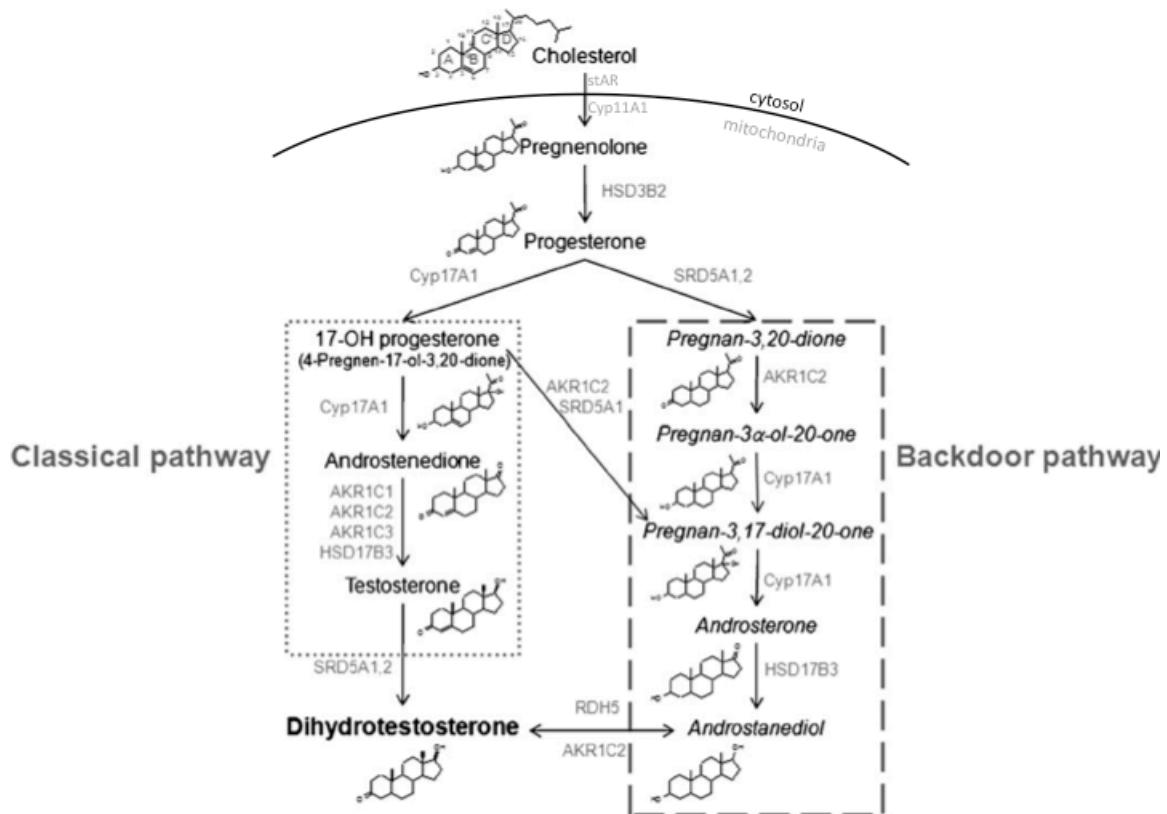


Figure 1: Classical and backdoor steroidogenic pathways (Adapted from (12)).

These findings are relevant because it was accepted for years that recurrent tumors were surviving in a virtually androgen-null environment as reflected by measures taken from the serum. Despite castrate androgen levels in the circulation, concentrations within tumours persist, likely due to *de novo* synthesis or conversion of adrenal precursors, in levels sufficient to activate the AR (27,31-37). Testosterone levels within metastases of castrated men have been documented at three times higher than the levels within primary tumors of eugonadal men (28). Similarly, intraprostatic DHT in castrated men was found to be reduced by only 20% compared to untreated men (37). Furthermore, it was

demonstrated through the use of short-hairpin RNA, that knockdown of the AR and thus, inhibition of the androgen-AR pathway, results in lack of tumor progression after castration and even regression of growth in the CRPC cell line, C4-2 (35,38). These findings indicate that the AR still requires ligand binding in order to exert its transcriptional effect on growth, proliferation, and survival of CRPC cells. Some recent studies suggest that this ligand is provided by residual sources of androgen in the body, namely the adrenal glands, rather than via *de novo* androgen synthesis within the tumor cells. This was based on the finding that DHEA and androstenedione levels also seem to persist intratumorally in castrated men (37). Also, the enzymes converting testosterone to DHT- SRD5A1 and 2, and DHEA to androstenedione- HSD3B1 and 2, were upregulated to a greater extent than other enzymes in the synthesis pathway (39,40). However, it has also been demonstrated that an adrenalectomy paired with ADT does not limit CaP progression, suggesting limited involvement of adrenal precursors (41,42). Regardless of the source, intratumoral *de novo* androgen synthesis or adrenal precursor conversion, it is apparent that the biologically relevant levels present after castration are likely contributing to the survival and progression of CRPC tumors. Therefore, investigating the source of the upstream precursor cholesterol for the generation of androgens in a castrate environment may be therapeutically relevant.

3.3.1 CRPC EXPERIMENTAL MODELS

In order to study these mechanisms effectively, it is important to have a reliable experimental model. Cell lines have been cultured from different human CaP samples in

order to capture different stages of the disease for study *in vitro*. These include the commonly used androgen-sensitive CaP cell line derived from lymph node metastases, LNCaP, as well as a lineage-derived second generation subline of LNCaP cells, C4-2(43). LNCaP cells are androgen receptor positive for both mRNA and protein. These cells also possess a mutation in the phosphatase and tensin homolog (PTEN) gene- a common tumour suppressor. C4-2 cells were derived by subcutaneous co-inoculation of LNCaP and a human osteosarcoma cell line twice over in castrated mice thus producing a castration-resistant cell line. The generation of a subline of LNCaP and an osteosarcoma cell line reflects not only the proclivity of CaP to metastasize to bone, but also the influence that the bone stromal environment can exert on progression to androgen-independence (44). The LNCaP and C4-2 cell lines also have a T877A mutation in the AR that results from a threonine replaced by an alanine at residue 877. In addition, the castration-resistant cell lines PC-3, derived from bone metastases and DU145 derived from brain metastases, both AR negative and are, along with LNCaP, three of the first and most commonly used CaP cell lines. DuCaP and VCaP were derived from the same patient taken from dura mater and vertebral metastases, respectively; both express a wild type AR (43,45-47). The cell lines implemented in the study of CaP are often selected based on their unique characteristics.

An animal model that has been developed to allow for study of CaP as it progresses from androgen-dependence to castration-resistance is the murine prostate xenograft model (48). The most widely used xenograft model is the LNCaP xenograft model. LNCaP cells are inoculated subcutaneously in severe combined immunodeficient

(SCID) mice and tumor growth in the normal androgen environment, termed androgen-dependent tumors (AD), is permitted until a predetermined tumor volume is attained. This tumor growth is marked by a continuous rise in PSA levels. At this point, the mice are castrated and a consequent fall in PSA levels is observed. The tumors are considered to be nadir when PSA drops to basal levels. Any surviving tumor cells in the mice tend to have a recurrence in growth after approximately six weeks. Again, this tumor growth is marked by a rebound in PSA levels, at which point the tumors are called castration-resistant CaP (CRPC) (48). The LNCaP xenograft model was used by our group to examine certain points in cholesterol regulation between the different stages of disease. The findings of which, will be discussed in the following sections have provided much of the impetus for this project (49-52).

1.4 PROSTATE CANCER AND CHOLESTEROL

Cholesterol is an essential molecule that has been studied extensively since it was discovered over two centuries ago. Due to its presence in all the cells of the body, cholesterol predictably has many important biological roles, including maintenance of membrane structure, signal transduction and provision of precursor to bile and androgen synthesis (53). Consequently, cholesterol has been implicated in the pathogenesis of many disease states, most notably cardiovascular disease, but also in many forms of cancer, including CaP (54). Focus has been directed towards cholesterol in CaP for more than fifty years following the findings of increased cholesterol content in prostatic adenomas in 1942 (54,55). This cholesterol accumulation is thought to be due to dysregulation of the complex pathways of cholesterol homeostasis. Cancer is

characterized by a rapid and unregulated proliferation of cells. It has been proposed that the increased levels of cholesterol in CaP may support cell proliferation by contributing cholesterol for membrane composition and signal transduction (56,57). In addition, we propose that cholesterol dysregulation may also provide precursor for *de novo* synthesis of androgens that stimulate cell division within castration-resistant tumors.

Cholesterol is obtained by humans from two major sources- from the diet and from *de novo* synthesis within the cells of the body, namely liver cells (53). Cholesterol in the circulation from either source is contained in soluble packages called lipoproteins. Lipoproteins, in general, consist of a neutral core of lipids surrounded by a monolayer of polarized phospholipids, often with proteins on the surface called apoproteins (58). The size and density of particles is variable, from the large and triglyceride-rich chylomicrons to the smaller high-density lipoproteins (HDL) (58). Lipoproteins are predominantly formed in the liver and the intestine and are then released into the circulation where they undergo further enzymatic transformations, as well as interacting with lipoprotein transporters that facilitate uptake of lipid contents. The most predominant lipoproteins in the circulation are low-density lipoproteins (LDL) and HDL. Both HDL and LDL contain high amounts of cholesterol and cholesteryl esters (58).

1.4.1 DIETARY CHOLESTEROL AND PROSTATE CANCER

The first source of cholesterol for humans is through dietary consumption. Although one cannot ingest enough food to support the daily cholesterol requirement in the body, meats and dairy provide a significant amount of cholesterol. Many

epidemiological studies over the years have examined dietary cholesterol consumption and its link to CaP incidence. This research focus was stimulated by the finding that obesity and the characteristics associated with obesity, including the high fat and high calorie diet of the Western world, have been linked to many cancers, including CaP (59-61). In addition to being correlated with the overall incidence of CaP, the Western diet has also been linked to metastatic progression of CaP (62-65). One particular study associated serum cholesterol levels with grade of cancer and found that men with higher cholesterol (>240 mg/dl) were more likely than men with desirable (<200 mg/dL) or borderline levels (200-240 mg/dL) to develop high-grade or rapidly-growing metastatic CaP (66). This finding was particularly prominent among men with higher body mass index. However, many other studies correlating serum cholesterol and CaP incidence have demonstrated the opposite finding (67-70), indicating a need to perhaps look directly at tumor cholesterol levels which may not be reflective of serum levels. A few recent studies in a xenograft model demonstrate interesting results with dietary variation. Using the androgen-dependent, LNCaP and the castration-resistant brain metastases-derived, DU145, to grow tumor xenografts in mice, data indicate that a diet with increased fat content induces proliferation and growth of the tumors, while inducing cholesterol accumulation in these tumors (51,52). However, the exact relationship between cholesterol, tumor growth and CaP incidence has yet to be fully elucidated.

1.4.2 LIPOPROTEINS AND ANDROGEN-DEPRIVATION THERAPY

Interestingly, due to the intricate relationship between androgen and cholesterol, the anabolic action of androgens consequently can impact overall fat mass and lipid profile

(71,72). Thus, the effects caused by androgen-deprivation therapy in men have been the topic of significant study. This research has mostly been aimed to elucidate atherogenic consequences during and post-therapy. However, these effects are also relevant when one considers that many of the post-ADT patients will subsequently develop CRPC. Thus, any changes in cholesterol induced by reducing androgens may be significant for the progression and ultimately, for the recurrence of the disease itself.

The loss of testosterone resulting from ADT causes increases in obesity, specifically truncal fat deposition, while decreasing lean body mass and causing significant changes to the lipid profile (71,73). The changes seen in the lipid profiles of post-ADT subjects include an increase in total cholesterol, triglycerides, LDL-cholesterol and oxidized LDL even in the presence of statin therapy (73-75). Many of these changes are documented as early as three months after therapy initiation. Mixed results have been obtained for HDL-cholesterol levels. Some groups have found a decrease in HDL-cholesterol post-ADT, while others have found no significant change (71-74,76).

No studies to date have looked at potential correlation between lipoprotein changes post-ADT and progression to CRPC. However, some studies have looked at the effect that lipoproteins have on androgen-dependent versus castration-resistant cancer cell growth. It was found that LDL, as well as remnant lipoprotein particles, which are the hydrolysis products of very low density lipoproteins and chylomicrons, induce proliferation of castration-resistant PC-3 cells, but not androgen-dependent LNCaP cells (77). Interestingly, LDL and HDL have been found to stimulate androgen production in

steroidogenic tissues (78-81). The lipoprotein-induced proliferation likely reflects a need for lipid source for rapidly dividing cells. Since CRPC cells have been found to be steroidogenic it is possible that this finding may also support lipoprotein-stimulated androgen production. Thus the post-ADT changes may provide an environment for CaP recurrence and growth.

1.5 SOURCES OF CELLULAR CHOLESTEROL

Cells within the body, including tumor cells, can obtain cholesterol from *de novo* synthesis or from lipoproteins in the circulation. Once in the cell, cholesterol is stored as cholesteryl esters in lipid droplets, but can be metabolized when the need for cholesterol arises. Cholesterol homeostasis is a very complex network of pathways, transporters and enzymes (53). It has been proposed that cholesterol homeostasis enters into a state of dysregulation in cancer, demonstrated by the accumulation in tumors (55). Some recent discoveries by our group and many others have renewed interest in the study of cholesterol and its potential role in the progression to CRPC.

1.5.1 CHOLESTEROL SYNTHESIS

Cholesterol is synthesized from acetyl-CoA in the endoplasmic reticulum (ER) of all cells of the body through the multi-step mevalonate pathway. The rate-limiting step in this process is 3-hydroxy-3-methylglutaryl-Coenzyme A reductase (HMGCR) which converts 3-hydroxy-3-methyl-glutaryl-Coenzyme A into mevalonate (53,82). Cholesterol synthesis is controlled at the transcriptional level by sterol regulatory element binding protein (SREBP-2). SREBP-2 is found within the endoplasmic reticulum (ER) bound to

SCAP (SREBP cleavage activating protein). SCAP is, in turn, bound to another ER protein, INSIG, when sterol levels are normal within the cell thereby retaining the SREBP in the ER. In times of low cellular cholesterol levels and thus, cellular cholesterol need, SCAP and INSIG do not associate and SREBP can then move to the golgi apparatus. Golgi-associated proteases cleave SREBP from SCAP and release it into the cytosol whereby it moves to the nucleus and acts as a transcription factor. SREBP binds to the sterol response element of many target genes causing induction of HMGCR protein expression as well as many other factors, including influx transporters, to increase cholesterol levels within the cell (53). Once the level of cholesterol is restored the transcriptional factor is returned to the ER. This pathway also responds to androgens because their biomolecular structure is similar to their precursor, cholesterol (49).

Our group found that HMGCR activity (Figure 2A) was increased in *ex vivo* tumor samples in the progression to the castrate-resistant state in a LNCaP xenograft model (50,83). Many other groups have found increases in protein expression of HMGCR in the progression to CRPC (79,84-87), however, our group did not find a significant change in HMGCR protein expression between tumor stages in a LNCaP xenograft model (50). The transcriptional regulation of HMGCR via SREBP-2 in CRPC has been explored *in vitro* and in a LNCaP xenograft model. It was shown at the cellular level in PC-3 and DU145, both castration-resistant cell lines, that the presence of cholesterol no longer initiates down-regulation of this key transcriptional factor. Thus, the downstream effectors of SREBP-2 including HMGCR, are not down-regulated and thus cholesterol levels remain high. However, a normal response to sterols was seen in androgen-dependent LNCaP cells and non-carcinogenic prostatic epithelium (79,84-87). These findings were mirrored

in AD and CRPC cell lines and LNCaP xenograft tumor samples (49,88,89). These findings suggest an explanation for the increased levels of cholesterol in CRPC tissue specimens and consequently, have raised the possibility that dysregulation in cholesterol homeostasis may be linked closely to androgens (49,58,90).

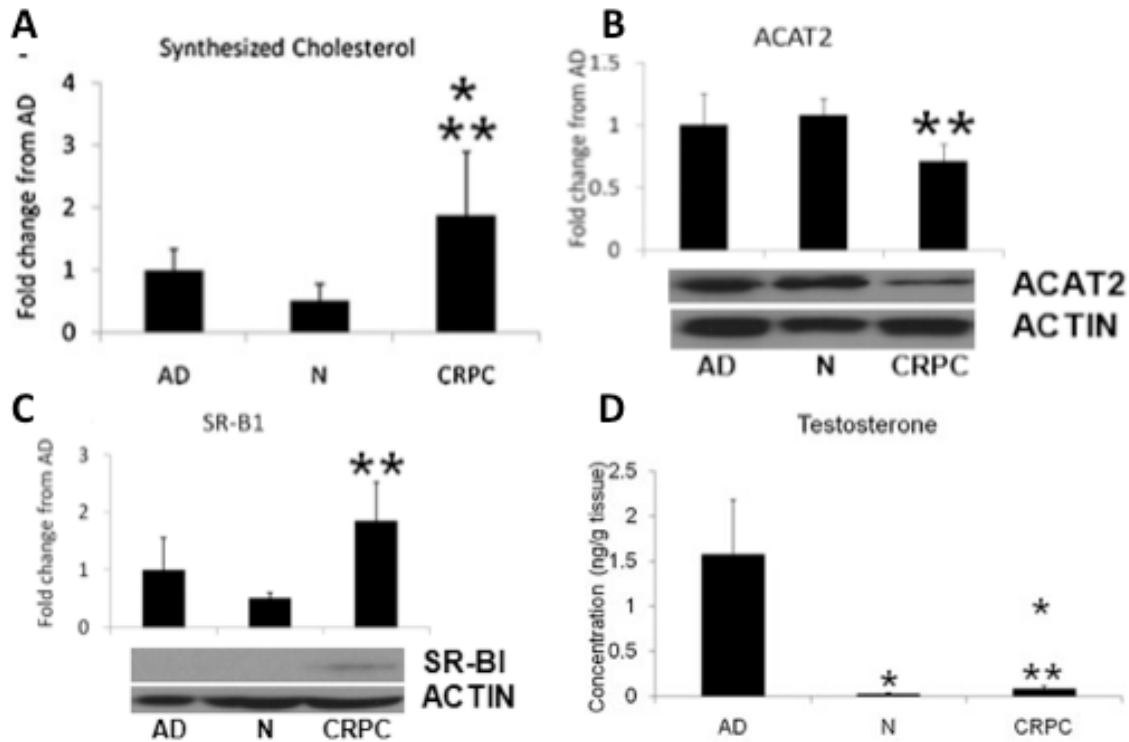


Figure 2A-D: LNCaP xenograft *ex vivo* cholesterol synthesis activity (A), ACAT2 (B) and SR-BI (C) protein expression and testosterone (D) concentrations in androgen-dependent (AD), nadir/castrate and castration-resistant (CRPC) tumour samples (adapted from (50)). *, **, $p < 0.05$ as compared to AD and Nadir, respectively.

1.5.2 METABOLISM OF INTRACELLULAR CHOLESTEROL

Cholesterol in its free form is toxic to the cell because it is a pro-apoptotic, thus it is quickly converted to the nontoxic storage form, cholesteryl esters (CE), after synthesis or

influx (53). This conversion from free cholesterol to CE is completed by acetyl coA:acyl transferase (ACAT) which adds a fatty acid to the hydroxyl group the third carbon of first hexane ring in the cholesterol moiety (82). ACAT exists as two isoforms in humans, ACAT-1 and ACAT-2. Both are integral membrane proteins of approximately 50kDa (91). In general, the ACAT enzymes are most active in times of cholesterol excess within cells (82). While ACAT-1 is thought to be ubiquitously expressed in the body, ACAT-2, is predominantly found in the brain and intestine (92,93). However, protein expression of both has been demonstrated in CaP (50,83).

When cholesterol levels are low or free cholesterol is required for cellular processes, hormone sensitive lipase (HSL), a neutral cholesteryl ester hydrolase hydrolyzes CE to free cholesterol (94). As its name suggests, HSL is regulated in part by hormone levels, but appears to also be controlled by cholesterol feedback mechanisms similar to HMGCR (95). Furthermore, it has been found in murine steroidogenic tissues that HSL selectively hydrolyzes CE from HDL to create androgens and this enzyme is present in the CRPC tumor cell (79,86,96).

Changes in the expression of ACAT-1, ACAT-2 and HSL have been demonstrated in CaP. Among the changes observed was a significant decrease in ACAT-2 expression from AD to the CRPC state in a LNCaP xenograft model (Figure 2B), as well as an increase in HSL from AD to nadir (50,96). These findings, paired with the fact that intracellular tumor testosterone levels also increased from nadir to CRPC in the same model, indirectly imply that the alterations in cholesterol processes, such as decreased

packaging of cholesterol to its storage form, are perhaps to provide substrate for *de novo* androgen synthesis (50).

1.5.3 CHOLESTEROL TRANSPORT-EFFLUX AND INFLUX

In addition to being synthesized and metabolized within the cell, cholesterol is fluxed in and out of the cell through the plasma membrane in a dynamic fashion (53). Since cholesterol exists in the circulation within lipoproteins it is transported to and from these lipoproteins at cell membranes (58). Lipoprotein profiles naturally change with age and obesity, two factors that have been correlated to CaP incidence, perhaps inferring provision of lipoprotein-derived cholesterol to cells also changes in CaP (59,65).

1.5.3.1 ATP-BINDING CASSETTE TRANSPORTER SUBFAMILY A1

When the cell has ample free cholesterol, the conversion to the storage form is activated. Additionally, efflux pathways are upregulated in order to rid the cell of the toxic molecule. The major cholesterol efflux transporters in cells are from the ATP-binding cassette transporter superfamily (ABCs). The major families involved in the efflux of cholesterol are the ABC-As and ABC-Gs, but most notably, ABC-A1. This is a large, 220 kDa protein has two six-helix transmembrane domains that are thought to form an aqueous pocket that translocates molecules to the cell surface (97,98). ABC-A1 is an important mediator in the first step of reverse cholesterol transport- the efflux of cellular cholesterol and phospholipids to membrane-bound apolipoproteins. It is found in many tissues of the body because of this important cholesterol efflux function, including CaP

and specifically, CRPC (50,99,100). Preliminary data suggest that ABC-A1 protein expression is increased in castration-resistant tumor cells when compared to an androgen-dependent counterpart, further implicating altered cholesterol regulation in CaP recurrence (50,100).

1.5.3.2 LOW-DENSITY LIPOPROTEIN RECEPTOR

Cholesterol in the circulation is predominantly found in lipoproteins and can be taken up by lipoprotein transporters into the cell. One of the major lipoprotein transporters involved in this influx of cholesterol is the low-density lipoprotein receptor (LDLrec). This transporter interacts with a number of different donor lipoproteins in order to take up cholesterol (101). LDLrec predominantly binds to apoB100 and apoE-containing lipoproteins, such as LDL, VLDL and chylomicrons (101). Lipoproteins bound to the LDLrec are then taken into cells via an endosomal pathway. This involves uptake of the entire lipoprotein particle into clathrin-coated endosomal compartment where acidic catabolism occurs and the lipid contents of the lipoprotein particles can then be used or metabolized by the cell into storage form (101). The receptors are recycled back to the cell surface in the endosome. LDLrec is controlled at the transcriptional level by SREBP-2, much like HMGCR and HSL. As described previously, SREBP-2-mediated cholesterol regulation appears to be dysfunctional in CRPC. These findings have stimulated some research exploring the relationship between the SREBP-2 dysregulation and its implication for LDLrec expression and activity. The few studies that have examined LDLrec in CRPC have found that the transporter is present in CRPC and is up-regulated, perhaps due to the lack of SREBP-2-mediated control (45,50,88,89).

1.5.3.3 SCAVENGER RECEPTOR CLASS B TYPE I

The second major cholesterol influx transporter is scavenger receptor class B type I (SR-BI), or CLA-1 (CD36 and LIMPII analogous-1) as it is sometimes called to in humans. This 82 kDa protein is a ubiquitous protein involved in reverse cholesterol transport (94,102), but it is more densely expressed in cells involved in cholesterol metabolism, such as the liver, and steroidogenic tissues (103). Morphologically, SR-BI has a horseshoe-like membrane topology with two transmembrane domains that serve to anchor a large extracellular domain (Figure 3) (103).

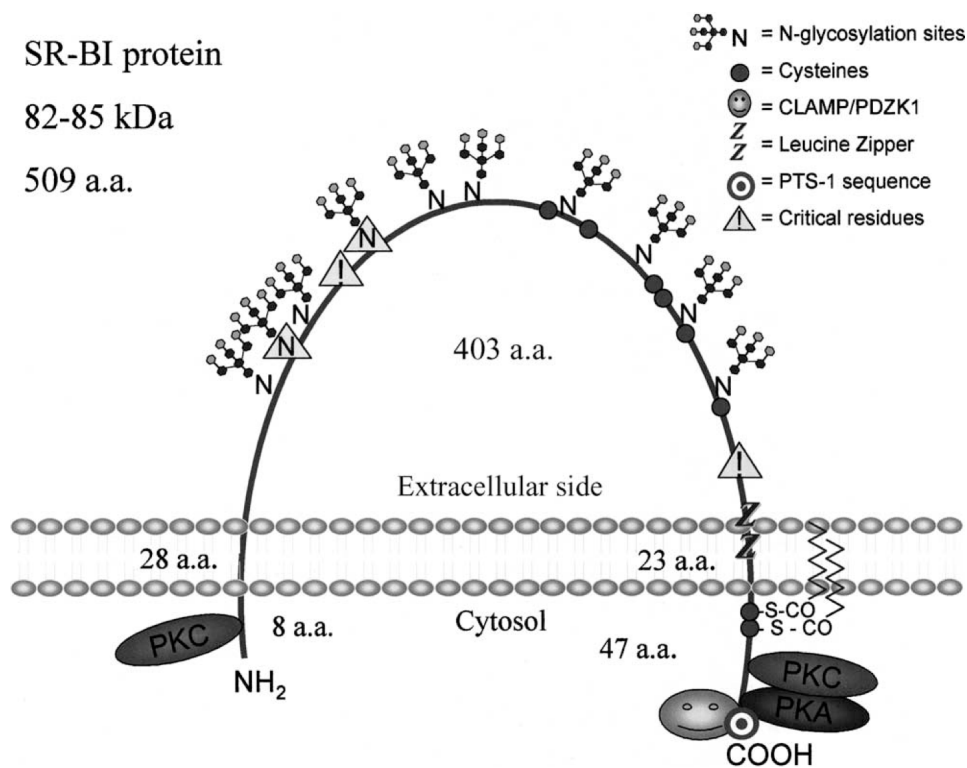


Figure 3: Plasma membrane topology of Scavenger Receptor Class B Type I (103).

SR-BI has become colloquially termed the ‘HDL transporter’ because it is one of the few receptors through which HDL-cholesterol can be taken into cells and because it has an apparent preference for the selective uptake of HDL-CE in steroidogenic and hepatic tissues of mice (94,103-107). However, there is some debate whether this holds true for human tissues, as rodent models predominantly rely on HDL, rather than LDL, which is the most abundant lipoprotein in humans (108,109). Furthermore, research of the last decade has suggested that SR-BI is also capable of bidirectional free cholesterol flux, as well as uptake of cholesteryl esters, triglycerides and phospholipids from LDL, VLDL and modified lipoproteins (94,103,110,111). The exact mechanism by which SR-BI takes in cholesterol from lipoproteins is not completely understood. However, the mechanism of selective HDL-CE uptake is thought to involve a collision-mediated transfer of only the CE content after the lipoprotein docks onto the receptor surface (105,112,113). The docking is thought to occur because of interaction with both the lipid and apoprotein of the lipoprotein (111,112,114). SR-BI is thought to be regulated in a feedback-type fashion by both androgens and cholesterol, although inversely, in that, decreased androgen levels and increased cholesterol curtail the expression of SR-BI (94,115).

The presence of SR-BI in CRPC has been confirmed by protein expression in PC-3 cells and in the CRPC tumors in a LNCaP xenograft model by our group and others (50,100,116,117). Furthermore, our group found that protein expression of SR-BI was significantly increased from nadir to CRPC in combination with a rebound in intratumoral testosterone concentrations (Figure 2C and D) (50). Interestingly, it has also

been discovered that males have significantly higher mRNA levels of *SCARB1*, the SR-BI gene (118-120). The natural predominance of *SCARB1* in males paired with the preliminary results our group have obtained in the LNCaP xenograft model provides more impetus to pursue an explanation for the potential role of SR-BI in changing androgen and cholesterol levels in the progression to CRPC.

1.6 CHOLESTEROL IN STEROIDOGENIC TISSUES

It has been demonstrated by many groups that *de novo* androgen synthesis is occurring intratumorally in CRPC cells, indicating that they have become steroidogenic. Our data indicate that cholesterol pathways are altered and this is perhaps to facilitate provision of the substrate, free cholesterol, to this intratumoral steroidogenesis. Other steroidogenic tissues in the body, namely the adrenals, have been studied extensively and have demonstrated some interesting preferences when it comes to cholesterol sources for androgen synthesis. Since CRPC tumours appear to be steroidogenic, they may have also adapted some of the same tendencies of the classical steroidogenic tissues of the body, such as the adrenals. Thereby these tissues may provide insight into the mechanism of CRPC androgen synthesis and perhaps the potential source of cholesterol.

Adrenal cells seem to preferentially rely on lipoprotein sources for cholesterol precursor, namely through SR-BI, rather than from *de novo* synthesis via HMGCR (79,86,114). This was demonstrated by the fact that LDLR-knockout mice; mice lacking the LDL receptor gene and therefore the receptor, had unaffected steroid production. This finding suggests that either synthesis of cholesterol or a different lipoprotein transporter was compensating for the loss of LDLrec-mediated cholesterol influx (86). In contrast,

SR-BI knockout mice have severely stunted steroidogenic capabilities (121). This decline in steroid production occurs despite a significant compensatory increase in HMGCR activity (114). This indicates that *de novo* synthesis of cholesterol is not able to compensate for the loss of cholesterol uptake via SR-BI. These studies suggest that steroidogenic tissues preferentially use HDL-CE from SR-BI-mediated influx for *de novo* androgen synthesis and perhaps, by inference, CRPC cells might have the same bias. This bias has also been demonstrated in breast cancer cells that are thought to possess a similar steroidogenic potential as their male counterpart, CaP (122,123). Also, adrenal cells over-expressing SR-BI have demonstrated induction of steroidogenesis and therefore SR-BI changes following castration may serve a similar function in CaP (124). Interestingly, the work completed to date by our group in CRPC complements the inferences made from steroidogenic tissues. Namely, SR-BI expression is statistically significantly increased upon progression to CRPC, paired with an unchanged HMGCR expression and an increased HMGCR activity (50). However, caution must be taken when attempting to translate murine findings to humans, particularly from a lipoprotein prospective as humans and rodents have different lipoprotein profiles.

1.7 NEW ANDROGEN RECEPTOR-SIGNALING THERAPIES

It has become very apparent with the research of the last few decades that the aggressive, complex and heterogeneous nature of castration-resistant CaP has made it a very challenging and thus far, impossible disease to treat effectively. The standard for treatment of CRPC has been administration of the chemotherapeutic, docitaxel in combination with prednisone (125). The recent focus in CRPC has been towards

identifying potential new therapeutic targets, as the therapies currently implemented—namely chemotherapy, achieve limited and often short-lived success. Considering that average survival of men with CRPC is less than 2 years, the need for more successful therapies is evident (126). The acknowledgment that the androgen receptor and androgen-response axis is still an integral part of CRPC has resulted in the development of a number of new therapies that are focused on this relationship between androgens and the androgen receptor at different points in the pathway. Such therapies include abiraterone acetate, an orally bioavailable specific CYP17A inhibitor, MDV3100, a small androgen receptor antagonist, and 17-AAG and STA-9090, inhibitors of heat shock protein-90, all of which are under development in a clinical setting (127-131).

Abiraterone acetate acts in a similar manner to ketoconazole, in that it is a cytochrome P450 inhibitor. However, it has greater specificity for CYP17A1 and displays more potent inhibition thereof. Abiraterone inhibits two key reactions in androgen biosynthesis via 17 α hydroxylase and 17,20 lyase preventing modification of pregnenolone and progesterone. In Phase II and III trials the drug elicited PSA decreases of more than 50% from baseline in 20% of chemotherapy-naïve patients and 36% of docetaxel-treated patients when treated with abiraterone acetate (132,133). Despite the success in lowering PSA, the side effects that have limited the utility of ketoconazole, primarily due to secondary mineralocorticoid excess are still present in patients taking abiraterone acetate. However, administration of eplerenone, a mineralocorticoid inhibitor, eliminated a large portion of these side effects including hypertension, hypokalemia and

edema (131,132). As a result, in April of 2011 abiraterone acetate or Zytiga™, received FDA approval for treatment of metastatic castration-resistant CaP.

MDV3100 is an orally administered AR inhibitor that is more potent than its AR antagonist predecessors, flutamide and bicalutamide, which have low affinity for the AR. MDV3100 has entered into multinational Phase III trials after 56% of chemotherapy-naïve patients experienced more than a 50% decrease in PSA levels (134). However, the initial success of this AR inhibitor is shadowed by the reversal of function of bicalutamide, from antagonist to agonist, seen in the presence of increased AR after longterm androgen withdrawal, such as in CRPC (135-138). This paradigm is thought to occur in part because these AR inhibitors bind to the ligand binding pocket of the receptor causing a subsequent change in the ligand binding domain. The change in the ligand binding domain induced by these antiandrogens, although effective at first, increases the rate of AR mutations, AR expression and cofactor expression thought to lead to the CRPC state and the paradoxical agonist effect of bicalutamide seen at this state (8,135,139,140). Although MDV3100 acts directly to block androgen binding and prevents translocation to the nucleus, it is possible that the same reversal of function may occur as seen with bicalutamide (134). Thus far, MDV3100 has not elicited significant side effects in subjects other than fatigue (134).

17-AAG is a benzoquinone ansamycin antibiotic that acts to inhibit the binding of heat shock protein-90 to the AR and subsequently disrupts AR stabilization. This drug underwent a two-stage Phase II trial in metastatic CRPC patients, but the study was

closed prematurely because PSA response was limited (130). Another small molecule heat shock protein-90 inhibitor, STA-9090 (ganetespib), is undergoing Phase II clinical trials with and without dutasteride, an SRD5A1 and 2 inhibitor. It is hoped that targeting multiple points in the AR-signaling pathway may improve the success of both drugs (141).

Although numerous novel therapeutics are being tested in clinical trials, this small selection was included to demonstrate the many potential points of intervention in the androgen receptor signaling pathway. In the last year a number of therapies not exclusively targeting the AR pathway have also had successful Phase III results. Sipeucel-T (Provenge®), an immunotherapy, and Cabazitaxel (Jevtana®), a chemotherapeutic agent, have both received FDA approval for the treatment of CRPC. While, alpharadin, a targeted α -radiotherapy and OGX-011 (Custersin), an anti-sense oligonucleotide targeting clusterin, have been given fast track designation and will likely receive approval as well. Although these recent approvals are promising, the exploration of novel targets must continue (142).

1.7.2 STATINS AS PROSTATE CANCER THERAPEUTICS

The exploration of cholesterol in CaP is not novel. In fact, considerable retrospective analyses have assessed statin use in CaP patients. Statins are a large class of drugs that are used extensively in cardiovascular disease because these drugs act to lower cholesterol levels by inhibiting HMGCR, the rate-limiting enzyme in cholesterol synthesis. Not only do statins cause decrease in total cholesterol, they also decrease LDL-

cholesterol and provide a modest increase in HDL-cholesterol (143). Interestingly, this reduction in plasma cholesterol and change in lipoprotein profile is accompanied by a reduction in PSA in non-cancer patients, which may indicate interruption in the normal steroidogenic processes in these men (66,144,145). In addition, these lipoprotein effects may be corrective for the changes induced post-ADT, namely increased total and LDL cholesterol, and thus statins could potentially be implemented to prevent progression to CRPC. Although no studies have looked specifically at statins in CRPC patients or the direct effects on tumor cholesterol, many studies have explored the potential of using statins as a preventative therapy. The results of epidemiologic studies assessing the association between statin use and incident CaP risk have been mixed (144,146). These mixed findings may be due to the heterogeneity of study protocols or may be as a result of statin-induced SRD5A2 expression. This enzyme catalyzes the conversion of testosterone to the potent metabolite, DHT (147). More recent studies have explored the specific association between statin use and more advanced CaP cases that have metastasized. These studies have found a reduction in the onset of the aggressive, late-stage disease state in statin users (66,144,148). The apparent benefit of statin use in the more advanced stages of cancer provides support for the importance of cholesterol but more research is necessary, particularly in a CRPC cohort.

A major obstacle of systemic treatments, such as statins is penetration and targeting of cancerous tissues. *In vitro* studies bypass this obstacle and a few have explored statin effects in CaP tumour cells. Interestingly, the inhibition of HMGCR by statins has a greater effect in androgen-dependent, LNCaP cells compared to castration-

resistant, PC-3 cells (89). Although both cell lines were responsive to changing levels of sterols, the LNCaP cells appeared to alter cholesterol synthesis to a greater extent than the PC-3, demonstrating that cholesterol dysregulation may be playing a role in the effectiveness of statins. Furthermore, some *in vitro* research has shown that statins, namely lovastatin, simvastatin and atorvastatin, cause growth inhibition in LNCaP cells, as well as in a few CRPC cell lines, but to a lesser extent (149). However, in a recent study exposing castration-resistant cells to statins combined with a COX-2 inhibitor, a potent anti-inflammatory agent, significant cell death was observed (150). These results did not examine effects on intracellular steroids, therefore it is difficult to determine if the impact on cells is elicited through attenuation of the steroid synthesis pathway rather than reflecting anti-proliferative or autophagic effects (151). However, the different responses observed between statin-treated androgen-dependent and castration-resistant cells warrants further study to properly assess the effect of statins or other cholesterol modulators on intratumoral steroidogenesis and the utility, thereof, as viable therapeutic options alone or in combination.

1.8 OBJECTIVE

The goal of the studies in my thesis was to determine the effect of knocking down the expression of SR-BI in two CaP cell lines, by examining different points of cellular regulation and proteins in the cholesterol and androgen-signaling pathways.

1.9 SIGNIFICANCE OF THE RESEARCH

The exploration of the physiological role of SR-BI in CaP may be important due to the findings presented above, specifically our finding in the LNCaP xenograft model that demonstrated an up-regulation of SR-BI expression in the progression from nadir to castration-resistance paired with an increased *ex vivo* cholesterol synthesis activity and rebound in testosterone production (50). In addition, the importance of cholesterol in rapidly dividing cancer cells has been a topic of investigation in connection with membrane integrity and lipid raft content, but few groups have explored the potential link to the intracellular supply of precursor for *de novo* steroidogenesis in the castration-resistant state. Therefore, it is hoped that determination of the effects of SR-BI down-regulation in CaP cells will help elucidate the importance of this influx transporter for the survival and growth of these cells.

1.10 HYPOTHESIS

Castration-resistant CaP cells (C4-2) rely on Scavenger Receptor Class B Type I as a major source of cholesterol, particularly for *de novo* androgen synthesis, compared to androgen-dependent LNCaP cells.

CHAPTER 2 AIMS

2.1 SPECIFIC AIMS

AIM 1:

To verify the LNCaP and C4-2 cell model via PSA response to androgens and characterize the basal expression of SR-BI in LNCaP and C4-2 cells.

AIM 2:

To determine the effect of silencing SR-BI expression on cell cytotoxicity and viability in LNCaP and C4-2 cells.

AIM 3:

To determine the effect of silencing SR-BI on cholesterol levels and compensatory cholesterol processes, namely cholesterol efflux (ABC-A1) and influx (LDLrec) transporter expression, cholesterol synthesis (HMGCR) and metabolism (ACAT-1, ACAT-2 and HSL).

AIM 4:

To determine the effect of silencing SR-BI on androgen production, PSA response and protein expression of steroidogenic acute regulatory protein (stAR) and the androgen receptor (AR).

2.2 RATIONALE

AIM 1:

It was discovered in an LNCaP xenograft model that SR-BI protein expression was increased in CRPC tumours as compared to AD and PSA nadir tumours post-castration. In addition, *ex vivo*, cholesterol synthesis was increased at CRPC, in concert with a decreased ACAT-2 expression (50). These findings, paired with a rebound in intratumoral testosterone concentrations in the same model at CRPC has led to the supposition that at the castration-resistant disease state, more cholesterol is required for synthesis of androgens. Furthermore, the SR-BI up-regulation paired with inferences from steroidogenic tissue preference for cholesterol influx via this transporter, have led to the proposal that SR-BI is up-regulated at CRPC as part of an adaptive response to the exposure to an androgen-deprived environment.

The androgen-sensitive LNCaP cell lines and its second generation castration-resistant subline, C4-2, were chosen as the experimental model because, despite their differences in androgen requirement, they have similar phenotypic features including PSA mRNA and protein and a mutated AR. The response to DHT treatment in both cell lines helped to determine if the cells were behaving as previous studies have predicted (43). The assessment of basal protein expression ascertained if the castrate environment the C4-2 cells were exposed to upon their derivation terminally altered these cells compared to the LNCaP cells with respect to cholesterol-related proteins and points in the androgen-signaling pathway. In addition, these measures served as a baseline for comparison to siRNA-induced changes in other Aim 3 and 4.

AIM 2:

Preliminary *in vitro* data in C4-2 and LNCaP cells completed in Aim 1 and the evidence from the xenograft model suggested that SR-BI was up-regulated to support cellular cholesterol need at the castration-resistant state (50). To determine if this influx transporter is physiologically important to the cells, the cytotoxicity and viability of cells with silenced SR-BI was examined.

AIM 3:

Cholesterol homeostasis is complex and has many points of regulation. Evidence suggests that cholesterol homeostasis becomes dysregulated in CRPC (49,54). To determine if silencing SR-BI affected this balance differentially in LNCaP compared to C4-2 the cholesterol levels were measured. As well the protein expression of other points of cholesterol regulation, including the other major influx transporter; LDLrec, the efflux transporter; ABC-A1, the rate-limiting enzyme in cholesterol synthesis; HMGCR and cholesterol metabolism enzymes; ACAT-1, ACAT-2 and HSL were assessed.

AIM 4:

Evidence suggests that cholesterol influx and cellular processing may be linked to *de novo* androgen synthesis within the cell, since increased testosterone production was associated with an increased SR-BI expression at CRPC (50). To determine if SR-BI silencing affected intracellular androgen synthesis, the expression of stAR; the

mitochondrial cholesterol shuttle and intracellular testosterone concentrations were assessed. The binding of androgens to the AR elicits PSA production. Analyses of AR expression and PSA secretion in LNCaP and C4-2 cells were performed to determine if SR-BI silencing elicited effects on downstream effectors in the androgen-androgen receptor signaling pathway.

CHAPTER 3 MATERIALS AND METHODS

3.1 MATERIALS AND REAGENTS

Poly-L-lysine (0.01% solution), cholesterol, Triton® X-100, dimethyl sulphoxide, phenylmethanesulfonyl fluoride, protease inhibitor cocktail, Trizma®-hydrochloride, Trizma® base, glycine, lyophilized bovine serum albumin, sodium dodecyl sulfate, ammonium persulfate, tetramethylethylenediamine, sodium hydroxide, sodium chloride, sodium deoxycholate, nonyl phenoxy polyethylene ethanol (NP-40) and ethylenediamine tetraacetic acid (Sigma-Aldrich, St. Louis, MO, USA), human high and low-density lipoproteins (Biovision Research Products, Mountain View CA, USA), acetic acid [$1\text{-}^{14}\text{C}$]- (American Radiolabeled Chemicals, Inc., Saint Louis, MO, USA), cholesterol [$1, 2\text{-}^3\text{H(N)}$]- (PerkinElmer Inc. Waltham, MA, USA). Scintillation fluid was purchased from MP Biomedicals (Solon OH, USA). RPMI-1640 without phenol red, Hank's balanced salt solution, 0.25% trypsin-EDTA, penicillin-streptomycin liquid, fetal bovine serum, charcoal-stripped fetal bovine serum, OptiMEM®, Lipofectamine RNAiMax®, Stealth RNAi® Negative Control Duplexes and Stealth RNAi® SCARB1 duplex oligonucleotides (HSS101571) were purchased from Invitrogen (Life Technologies, Invitrogen, Burlington, Ontario). Chloroform, ethyl acetate, hexanes, ethanol, methanol and isopropanol were purchased from Fisher Scientific (Waltham, MA, USA). SuperSubstrate® West Pico Solution was obtained from Thermo Scientific (Rockford IL, USA).

3.1.1 ANTIBODIES

The characteristics of the primary antibodies used for the western blotting procedures described in section 3.6, including target amino acid region, dilution, mammalian host and source company are detailed in Table 1. Goat polyclonal anti-rabbit

IgG, bovine polyclonal anti-goat IgG and donkey anti-mouse IgG all conjugated to horse radish peroxidase were used as secondary antibodies matched with the corresponding host of the primary antibodies (Novus Biologicals, Littleton, CO, USA and Santa Cruz Biotechnology Inc., Santa Cruz CA, USA).

Table 1: Antibody specifications used in western blotting techniques.

Antigen	Target	Host	Clonality	Dilution used	Source Company
Beta-actin	~C-term	goat	polyclonal	1:1000	Santa Cruz (sc-1616)
ABC-A1	~1100-1300	rabbit	polyclonal	1:500	Novus Biologicals (400-105)
ACAT-1	1-125	rabbit	polyclonal	1:1000	Santa Cruz (sc-20951)
ACAT-2	n/a	rabbit	polyclonal	1:1000	AbCam (ab37467)
AR	299-315	mouse	monoclonal	1:500	Santa Cruz (sc-7305)
HMGCR	827-840	rabbit	polyclonal	1:500	Upstate Biotechnology (07-572)
HSL	476-775	rabbit	polyclonal	1:1000	Santa Cruz (sc-25843)
LDLrec	499-511	rabbit	polyclonal	1:500	AbCam (ab30532)
SR-BI	496-509	rabbit	polyclonal	1:1000	AbCam (ab396)
stAR	1-285	rabbit	polyclonal	1:1000	Santa Cruz (sc-25806)

3.2 CELL CULTURE

The human CaP cell lines, LNCaP and C4-2, were generously provided by Dr. Paul Rennie from the Prostate Centre at Vancouver General Hospital. LNCaP cells were used between the passage numbers of 41-48. Both cell lines were maintained in phenol red-free RPMI-1640 media supplemented with 10% non heat-inactivated fetal bovine serum and 1% penicillin-streptomycin at 37°C in a humidified, 5% CO₂ environment.

3.3 PROTEIN QUANTIFICATION

In order to quantify the amount of protein in cell samples in experiments detailed below, the Dc Protein Assay (BioRad, Hercules CA, USA); a modified Lowry assay, was implemented. Cells from each experiment were washed with HBSS to remove dead cells and debris and were subsequently lysed using ice cold modified radio-immunoprecipitation assay (RIPA) buffer, supplemented with 1% protease inhibitor

cocktail and phenylmethanesulfonylfluoride (PMSF) which was added to culture plates containing cells. After an hour, the cells in RIPA were scraped and extracted from the surface of the plate and were placed in individual 1.5 mL microcentrifuge tubes. The eppendorfs were then centrifuged at 11,000 rpm for 20 minutes at 4 °C. The supernatant was removed from the solid pellet of cell debris and was used for protein quantification. Triplicate wells with 5 uL of cell lysate or the appropriate amount of BSA standard were added to a 96-well plate. 25 uL of Reagent A', a 50:1 solution of Reagent A (alkaline copper tartrate): Reagent S (mild detergent), was added to the wells followed by 200 uL of Reagent B (Folin reagent). Alkaline copper tartrate reacts with proteins in the samples and elicits a blue colour upon addition of the Folin reagent. The plate was mixed and allowed to sit for 15 minutes at which point the absorbance at 650 nm was measured using a Labsystems, Multiskan plate reader (Fisher Scientific, Waltham, MA, USA). The BSA standard curve was created by diluting a known amount of a 2 mg/mL BSA standard solution to the desired concentrations between 0-30 µg/mL. A sample BSA standard curve has been provided in Figure 4. Absorbance values obtained for cell samples were extrapolated from the equation of the regression line of the BSA standard curve. The amount of protein in 1 million LNCaP and C4-2 cells was measured to determine if relative amounts of protein in the two cell lines were comparable, as protein was used to normalize data between treatment groups (Appendix A).

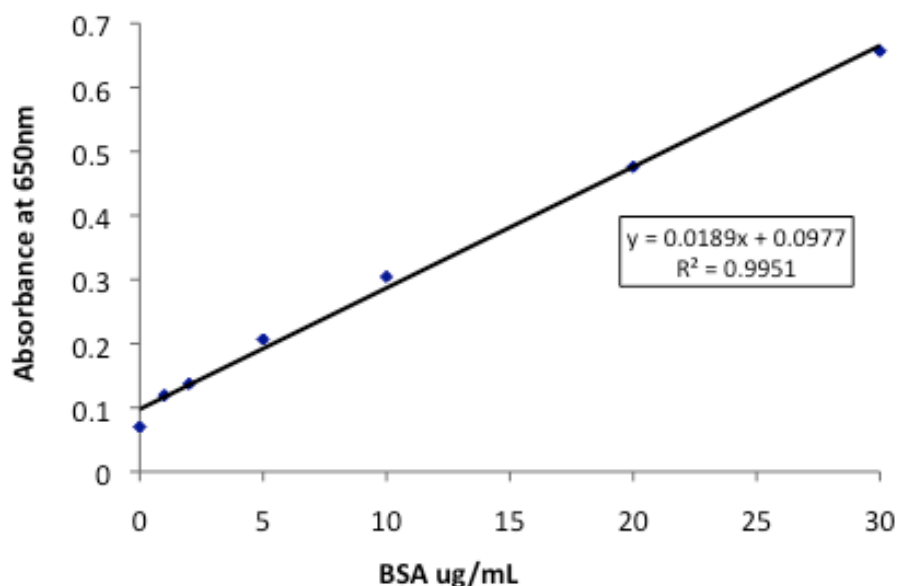


Figure 4: A typical BSA standard curve is shown. This standard curve plots absorbance at 650nm against known concentrations of BSA ($\mu\text{g/mL}$). The equation of the line is determined and sample protein concentrations are extrapolated by solving for x.

3.4. SIRNA TRANSFECTION PROTOCOL

Cells were seeded in RPMI-1640 with 5% FBS at a density of 7.5×10^4 in 6-well plates or 5×10^3 in 96-well (both are 7.5×10^3 cells/cm²) pre-treated with poly-L-lysine, a positively charged synthetic amino acid that promotes adherence. 24 hours after seeding, the media was changed to RPMI with 1% FBS and no antibiotics to optimize transfection. 10nM final concentration of Stealth RNAi duplexes targeting the SR-BI gene (HSS101571: AUAUCCGAACUUGUCCUUGAAGGG) and Low GC Negative Control Duplexes with 2.0×10^3 μM of Lipofectamine® RNAiMAX cationic lipid reagent diluted in OptiMEM® were combined in a sterile 1.5 mL microcentrifuge tube,

mixed gently and allowed to incubate at room temperature for 20 minutes. This incubation allows for the cationic lipids to surround the duplexes to facilitate diffusion across the plasma membrane of cells. This solution, either SR-BI siRNA (SRBI-KD) or negative control siRNA (NC), or OptiMEM® alone (Blank) was added to the antibiotic-free cell media and was left to incubate at 37°C for 5 hours (152). After 5 hours, the transfection media was removed carefully and replaced with 2 mL of antibiotic supplemented RPMI with 1% FBS. Viable cells and media samples for the experiments described below were then collected pre-transfection (day 0), 24 hours post-transfection (day 1), 72 hours post-transfection (day 3) and 144 hours post-transfection (day 6). The optimal siRNA concentration of 10 nM with 2.0 nM cationic lipid delivery solution was selected after performing a series of protein expression and cytotoxicity assays using the final concentrations of 1-50 nM siRNA combined with 1-5 µL (or 0.4-2.0 nM) of RNAiMax® lipid reagent. Appendix B demonstrates the results for the dose combinations of 1 nM or 10 nM siRNA with 2.5 µL (1.0 nM) or 5.0 µL (2.0 nM) cationic lipid reagent in both C4-2 and LNCaP cells. The combination of 10nM siRNA and 2.0 nM RNAiMax® elicited the greatest SR-BI protein silencing (Appendix B, Figure B: C-D) and least cytotoxicity (Appendix B, Figure B: A-B) and thereby, was chosen for use in all experiments.

Comparison of cytotoxicity between NC and SRBI-KD doses was also considered, as it is important that the delivery system itself is not eliciting non-specific toxicity. In addition, the optimal dose was assessed in cells using 5% charcoal-dextran stripped serum in RPMI-1640 instead of 1% FBS. The viability (see section 3.5.1 for protocol) of C4-2 and LNCaP cells subjected to 5% CSS are shown in Appendix C.

LNCaP cells displayed no growth after siRNA treatment, therefore 1% FBS was implemented for siRNA experiments.

3.5 CELL CYTOTOXICITY AND VIABILITY

Cells were plated in 96-well plates at a density of 5×10^3 cells per well 24 hours prior to transfection as detailed above. Treatments and controls were assigned triplicate wells in each plate. 50 μ L of medium was taken from above the cells at the described time points; day 0 and day 1, 3 and 6 post-transfection to use in the cytotoxicity experiments set up on a separate 96-well plate, while the remaining cells were washed carefully twice with HBSS and used for the viability assays.

3.5.1 LDH ASSAY

The lactate dehydrogenase (LDH) assay was used to assess cytotoxicity. The cytotoxicity of cells was measured based on the presence of lactate dehydrogenase (LDH) in the media which causes conversion of a tetrazolium salt into a red formazan product. The formazan product results in absorbance readings at 492 nm directly proportional to presence of LDH thereby giving an indication of the membrane integrity of cells. 50 μ L of LDH substrate was added to the 50 μ L of media removed from each sample well and placed in a separate 96-well plate. The plate was then covered to protect from light and was incubated for 30 minutes at which point the absorbance was read at 492 nm. A 100% death control was obtained as an absolute positive control by exposing untreated cells, seeded at the same density as treated cells, with 10 μ L of a 1% t-octylphenoxy-polyethoxyethanol (triton X-100) solution in HBSS for two hours. Triton X-100 is a non-

ionic surfactant that easily solubilizes membranes and therefore leads to necrosis and subsequent maximal LDH release into media. In addition, a positive LDH control provided by the kit was used to confirm the reaction was taking place. A background reading was obtained by measuring absorbance of media alone, in addition to a volume-corrected media control with 10uL of the triton X-100 solution to control for dilution effects in the 100% death group.

3.5.2 MTS ASSAY

Cell viability was assessed using the CellTiter 96® AQueous One Solution Cell Proliferation or MTS assay. This assay measures metabolically active cells since NADH and NADPH are produced via mitochondrial respiration, a process indicative of living cells. This NADH or NADPH can reduce a tetrazolium compound (3-(4,5-dimethylthiazol-2-yl)-5-(3-carboxymethoxyphenyl)-2-(4-sulfophenyl)-2H-tetrazolium), thereby producing a formazan product that elicits a colorimetric reading proportional to its quantity at 492 nm. Therefore the absorbance reading obtained is proportional to the number of living cells. Cells remaining in the plates were washed and 50 µL of a 2:3 solution of MTS reagent with 1% FBS RPMI media was added carefully to the cells (83,153). The plate was then covered with aluminum foil to protect from light and was incubated at 37 °C for 3 hours. After 3 hours, absorbance readings at 492 nm were taken using a plate reader. A background reading was obtained for the MTS and media solution. Average absorbance values were calculated from the replicates of the treatment and control cells.

3.5.2.1 LIPOPROTEIN QUANTIFICATION

Commercial human HDL and LDL were diluted in serum-free RPMI and were subsequently passed through a 22 μm filter in order to remove any large impurities.

Doses of lipoprotein in serum free RPMI were determined by assessing the protein content in the diluted samples using the protein assay described previously.

Concentrations of HDL from 0-50 $\mu\text{g/mL}$ based on protein content and 0-31.3 $\mu\text{g/mL}$ of LDL were tested for effects on viability using the MTS assay described above in C4-2 and LNCaP cells without siRNA treatment (Appendix D). Cells were plated at 7.5×10^3 cells/ cm^2 in 24-well plates. 24 hours after plating, media containing the desired doses of lipoproteins were added to triplicate wells. The viability was assessed 24 hours later and was compared to un-treated controls. 10 $\mu\text{g/mL}$ HDL was chosen as the optimal dose to use for further viability experiments presented in Aim 2 because it was the dose that elicited the maximal effect on viability of both cell lines (Appendix D, Figure A and B). 6.25 $\mu\text{g/mL}$ LDL was chosen for further because none of the LDL doses elicited increased viability (Appendix D, Figure C and D). The optimal lipoprotein doses were added to siRNA experiments (seen in section 4.2) immediately after transfection and therefore, 24 hours prior to cell viability assessment.

3.6 WESTERN BLOTTING

Cell samples taken at day 0 and day 1, 3 and 6 post-transfection, as described in section 3.4, were lysed in modified RIPA and the supernatant of each sample was collected as described in section 3.3. Equivalent aliquots of protein (15 µg protein per lane), determined by BioRad Dc protein assay, were loaded onto 7%, 10% or 4-15% SDS-PAGE gels. Lower percentage and gradient gels were used for separation of large proteins (> 200 kD). Gel electrophoresis was run for an hour at a constant voltage of 100V in Mini Transwell Protean system. Gels were removed from the cassettes, rinsed in distilled water and were subsequently transferred onto nitrocellulose membranes. The transfer process was 90 minutes at constant voltage of 100V using 1X Towbin's transfer buffer (154). After transfer, membranes were blocked with 3:1 blocking buffer (3:1, 3% milk: 3% BSA) or 3% BSA alone for 1-2 hours, followed by treatment with primary antibodies overnight in the respective blocking buffers at 4°C. The next day, primary antibodies were removed and blots were washed 3 times for 6 minutes with 1% TBS-0.1% Tween. Blots were then treated with the respective secondary antibodies diluted in 1% TBS-0.1% Tween for two hours. Blots were washed an additional 3 times with 1% TBS-0.1% Tween and were then treated with SuperSubstrate® West Pico Solution at 1mL per 1 cm² of membrane. After 5 minutes, the chemiluminescent reagent was poured off and blots were developed using an Epi-Chemi II Gel Documentation system. Band density was analyzed using Labworks densitometric analysis program. The protein band of interest was normalized to the β-actin band (loading control) in the same well. All basal protein expression values in LNCaP and C4-2 cells are expressed as the normalized band density for each protein relative to the LNCaP cell line (fold change from LNCaP),

so as to present them in the same figure. All protein expression data completed in the siRNA experiments is presented as fold change in actin-normalized band density of a treatment group (SRBI-KD or NC) from the pre-transfection (day 0) control in the respective cell line.

3.7 CHOLESTEROL ANALYSES

Cell lysates from siRNA experiments in LNCaP and C4-2 cells were extracted as described in section 3.4 at day 0 and day 1, 3 and 6 post-transfection. Cell lysates prior to centrifugation, as described in section 3.3, were used to reflect a whole cell cholesterol fraction. All subsequent analyses of cholesterol parameters using these lysates were corrected for protein levels in each sample.

3.7.1 CHOLESTEROL QUANTIFICATION

Whole cell lysates from LNCaP and C4-2 pre-transfection and day 1, day 3 and day 6 post-transfection were collected using cold modified RIPA buffer as described above. Cholesterol content of whole cell lysates was analyzed using an Amplex® Red Cholesterol assay (Invitrogen). Samples were diluted in 1X reaction buffer from 1:5 (day 0 and day 1) to 1:50 (day 3 and day 6) and 50 µL of each of these samples and cholesterol standards, 0-8 µg/ml, were added in triplicate to a 96-well plate. Hydrogen peroxide was used a positive control for the reaction. 300 µM Amplex® Red solution was created by combining Amplex Red stock solution, horseradish peroxidase, cholesterol oxidase and cholesterol esterase with 1X reaction buffer (as provided in the kit). 50 µL of this solution

was added to each of the triplicate well of standard and sample. A separate Amplex® Red solution without esterase was created in order to determine cholesteryl esters (esterase-free values subtracted from esterase values). The plate was covered with aluminum foil and incubated for 30 minutes at 37 °C. Fluorescence readings were obtained on a fluorescent plate reader at an excitation wavelength of 530nm and an emission wavelength of 590 nm. Total cholesterol values were extrapolated from the standard curve (Figure 5) and were expressed as cholesterol concentration per µg of protein in each sample. In addition, the area under the cholesterol-time curve (AUC) created in each experiment, was determined using GraphPad Prism software. This program determines AUC using the trapezoidal method.

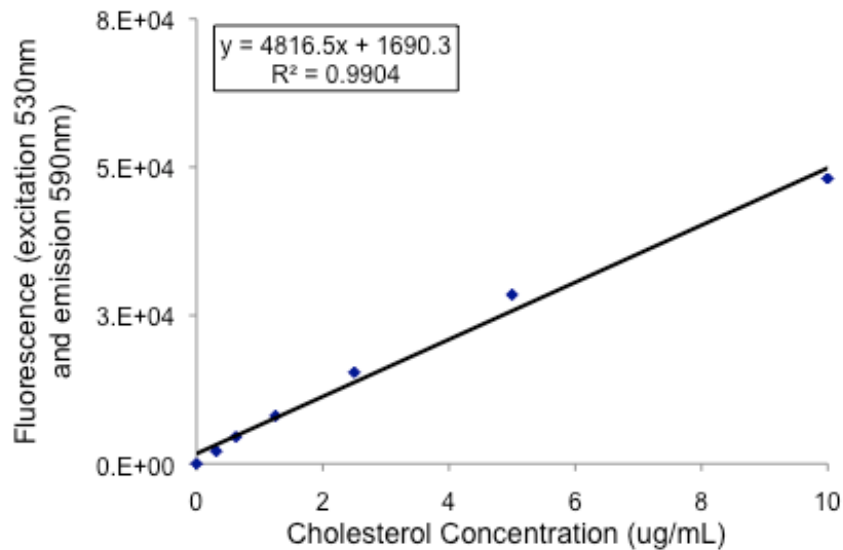


Figure 5: A typical Amplex® Red cholesterol assay standard curve is shown. This standard curve plots fluorescence (excitation of 530 nm and emission of 590 nm) of known concentrations of cholesterol (µg/mL). The equation of the line is determined and sample cholesterol concentrations are determined by solving for x.

3.7.2 CHOLESTEROL SYNTHESIS (HMGCR ACTIVITY) ASSAY

Cells were grown with a similar silencing protocol as described in section 3.4 in 6-well plates. At day 0 and day 6 the cell media was removed from the plates. Cells were washed carefully with HBSS and 500 μ L of 1% FBS RPMI with .5 μ Ci of 14 C-acetic acid was added to the wells for 3 hours. Cells were washed 3 times with HBSS following incubation with radioactive acetate. 500 μ L of distilled water was added to each well and cells were scraped carefully from the surface. Cells and water were extracted from the wells and were pipetted into the bottle of a glass tube. A 1:1000 solution of 3 H-cholesterol in 100% ethanol was prepared and vortexed. 10 μ L of this 1 μ Ci/mL solution was added to the tubes containing cells as a lipid recovery control.

3.7.2.1 LIPID EXTRACTION

The lipid content of these cell samples were then extracted using the Bligh Dyer lipid extraction method (155). 3.75 mL of 2:1 chloroform:methanol was added to the glass tubes containing cells and 3 H-cholesterol. Tubes were then vortexed for 5 minutes. 1.25 mL of chloroform and 1.25 mL distilled water were then added sequentially to the tubes, followed each by 1 minute of vortexing. The tubes were then centrifuged at 425 g for 2 minutes at which point the upper layer was discarded and the lower layer was transferred to a clean glass tube. The samples were then evaporated using nitrogen and reconstituted in 100 μ L of chloroform.

3.7.2.2 THIN LAYER CHROMATOGRAPHY

Samples resuspended in chloroform were dotted onto a silica gel plate, 1 inch from the bottom edge. Samples were run alongside a cold cholesterol control (10 mg/mL)

and 10 μL of the ^3H [1,2]-cholesterol in ethanol. Samples were placed in a covered glass TLC chamber with 200 mL of a 9:1 solution of hexanes and ethyl acetate, respectively. This solution served as the mobile phase and facilitated separation of lipids in the samples on the silica gel plate (50). After 2-3 hours of runtime, the plate was exposed to iodine crystals that cause lipid spots to appear yellow-orange on the plate. Similar sized pieces of silica plate were cut for each sample at the same point as the cold cholesterol control and were placed in 6 mL of scintillation fluid. Disintegrations per minute for ^{14}C and ^3H were assessed using a beta counter. Values of for synthesis for the treatment and control groups were obtained by dividing ^{14}C dpm by ^3H dpm and then values were normalized to protein content in a given sample.

3.8 TESTOSTERONE ASSAY

Cell lysates and media samples from above LNCaP and C4-2 cells at day 0, day 1, 3 and 6 post-transfection (section 3.4) were collected for testosterone analysis using a testosterone ELISA (R&D Systems, Minneapolis MN, USA). Samples were diluted in calibrator diluent provided in the kit; 1:2 for media samples, day 0 and day 1 samples, and 1:10 for day 3 and day 6 samples. Dilutions were completed in order to obtain values within the working range of .041 ng/mL to 10 ng/mL of testosterone but were adjusted post-assay. The mean minimum detectable dose for this assay was 0.03 ng/mL. Primary antibody solution was added to a 96-well plate and allowed to incubate for an hour prior to addition of 50 μL of sample and testosterone standards in duplicate. Testosterone conjugate was then added to the wells and the plate was then incubated for 3 hours at room temperature on a horizontal orbital microplate shaker at 500 ± 50 rpm. All the wells

were then aspirated and washed 4 times prior to the addition of substrate solution and were incubated for 30 minutes at room temperature protected from light. Stop solution (a diluted acid) was then added to terminate the reaction and the plate was measured at 450 nm with a wavelength correction at 540 nm to account for imperfections in the plate. Mean readings for the samples and standards were calculated and the non-specific binding (wells with calibrator diluent) optical density was subtracted from each. A standard curve was created using a four-parametric logistical regression model equation (Fig. 6) and testosterone concentrations were extrapolated from the following equation:

$$y = \min + \frac{\max - \min}{1 + 10^{(\log EC_{50} - x)Hillslope}}$$

Values extrapolated from the curve were corrected for protein in a given sample.

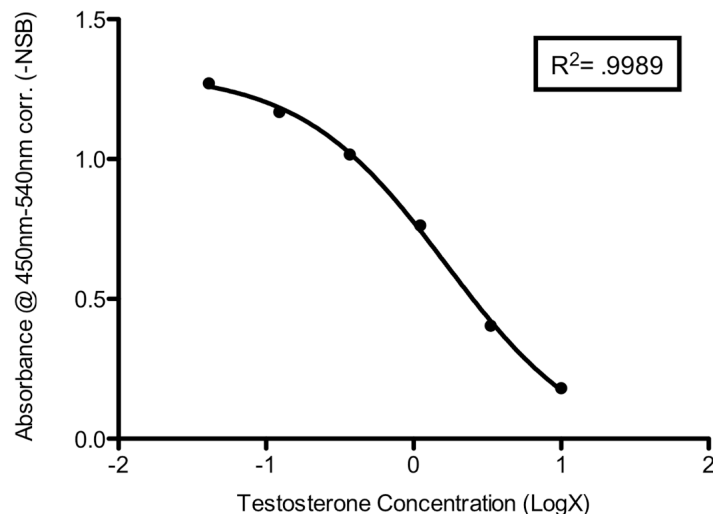


Figure 6: A typical testosterone standard curve is shown. This standard curve plots absorbance (450 nm-540 nm) corrected for non-specific binding (NSB) against known log-transformed testosterone concentrations. The equation of the sigmoidal line is determined using 4-parametric linear regression model.

3.9 PROSTATE SPECIFIC ANTIGEN ASSAY

A prostate specific antigen enzyme linked immunosorbant assay was used to analyze PSA and was purchased from ClinPro Intl. (Union City, CA, USA). Cell media fractions from each time point (day 0 - day 6) and treatment group (NC and SRBI-KD) were analyzed based on the manufacturers protocol (83). Media samples were diluted in serum-free RPMI at 1:10 for day 0 and day 1 samples and 1:50 for day 3 and day 6 samples in order to stay within the standard curve. 50 μ L of diluted media samples and standards (0 ng/mL-120 ng/mL) were added in triplicate to antibody-coated wells along with 50 μ L of zero buffer (as provided in the kit) and incubated at room temperature for an hour. The plate was washed thoroughly and treated with 100 μ L of an enzyme conjugate reagent for an hour. After another washing, 100 μ L of TMB reagent was added and absorbance at 450 nm was measured using a Labsystems, Multiskan plate reader (Fisher Scientific, Waltham, MA, USA). PSA concentration in the samples was extrapolated from the standard curve created from known concentration samples provided in the kit. These values were subsequently normalized to the protein content in the respective samples. A sample PSA standard curve is shown in Figure 7.

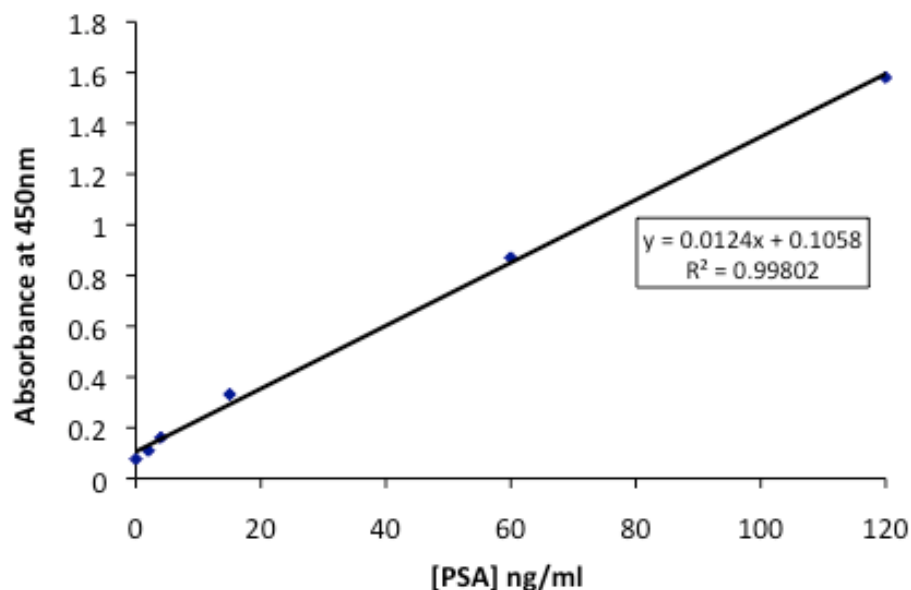


Figure 7: A typical PSA standard curve is shown. This standard curve plots absorbance at 450nm against known concentrations of PSA (ng/mL) as provided. The equation of the line is determined and sample PSA concentrations are determined by solving for x.

3.9.1 BASAL PSA AND RESPONSE TO DHT

LNCaP and C4-2 cells were seeded at 1.0×10^5 cells per well in a 6-well plate in 10% FBS RPMI. After 24 hours the media was replaced with 5% CSS RPMI for 2 days at which point media was changed to either 10nM dihydrotestosterone in 2 mL 5% CSS RPMI or 2 mL of 5% CSS RPMI alone. The media was collected 72 hours later and was analyzed using the above assay protocol. Cells were washed twice with HBSS and protein content was analyzed for normalization in the respective cell samples. The data using this specific protocol is described in section 4.1.1.

3.10 STATISTICAL ANALYSES

The statistical analyses on all data were performed using GraphPad Prism software. Student's t-tests were used to determine differences between NC and SRBI-KD at each time point. A one-way analysis of variance was used to analyze the basal protein expression in LNCaP and C4-2 cells in Figure 9 and a two-way analysis of variance was used to determine differences in the PSA response in LNCaP and C4-2 cells +/- DHT seen in Figure 8. These statistical analyses were followed up with a Tukey post-hoc analysis. All data are shown as mean +/- standard error of the mean. Means of the data sets were considered to be statistically significantly different if $p < 0.05$. Differences between the NC group and untreated control (Blanks) were assessed for each experiment, at each time point and were not found to be statistically different. Therefore, NC was used as a comparison to SRBI-KD for the results presented, rather than the Blank.

CHAPTER 4 RESULTS

4.1 AIM 1 EXPERIMENTS

4.1.1 PSA SECRETION IN THE PRESENCE AND ABSENCE OF DHT

The androgen-sensitive CaP cell line, LNCaP, and the castration-resistant lineage-derived cell line, C4-2, were chosen as the experimental model. Both cell lines were treated with 10 nM DHT and the resulting prostate-specific antigen (PSA) response was analyzed, as described in section 3.9.1. In the absence of DHT treatment (-DHT) it was found that C4-2 cells had a significantly higher basal PSA level as compared to the LNCaP cells (Figure 8). C4-2 cells secreted approximately 53.3 ng/mL per ug of protein, while the LNCaP cells secreted 12.9 ng/mL per ug protein, an approximate 4-fold difference. Upon treatment with 10nM DHT (+DHT), C4-2 cells secreted approximately 110.9 ng/mL per ug protein, while LNCaP cells secreted 41.1 ng/mL per ug protein. Despite the difference in basal PSA levels, both cell lines responded with a significant increase in PSA from the respective untreated group as can be seen in Figure 8.

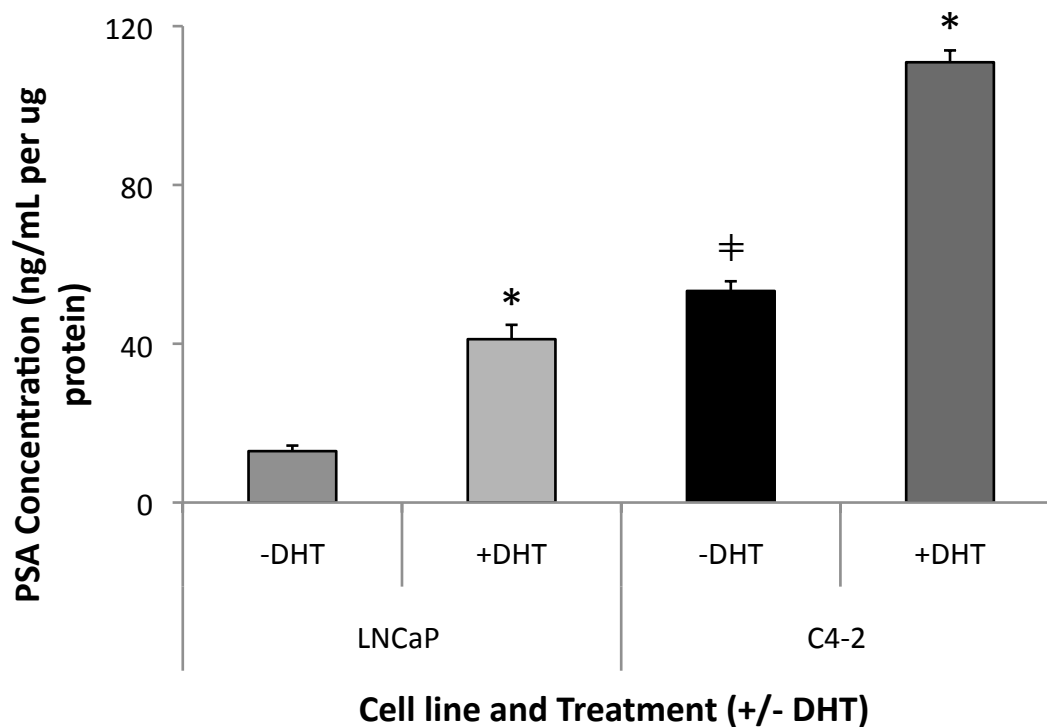


Figure 8: PSA secretion (ng/mL) per ug of protein in LNCaP and C4-2 cells untreated (-DHT) and treated (+DHT) with 10nM DHT in 5% CSS for 72 hours. Columns, mean (n=6 for LNCaP and n=12 for C4-2); bars, +/-SD. *, p<.05, -DHT vs +DHT of each group, #, p<.05, -DHT LNCaP vs -DHT C4-2.

4.1.2 BASAL PROTEIN EXPRESSION

Basal protein expression in C4-2 and LNCaP cells as derived from Western blot analyses is demonstrated in Figure 9. These expression levels were evaluated in pre-transfection cell samples (day 0) of the two CaP cell lines. LNCaP and C4-2 protein expression levels were statistically compared to each other using a one-way ANOVA. All proteins examined, with the exception of SR-BI and HSL (see Figure 10) did not have significantly different expression levels in LNCaP and C4-2 cells, although LDLrec and stAR demonstrated an increasing pattern.

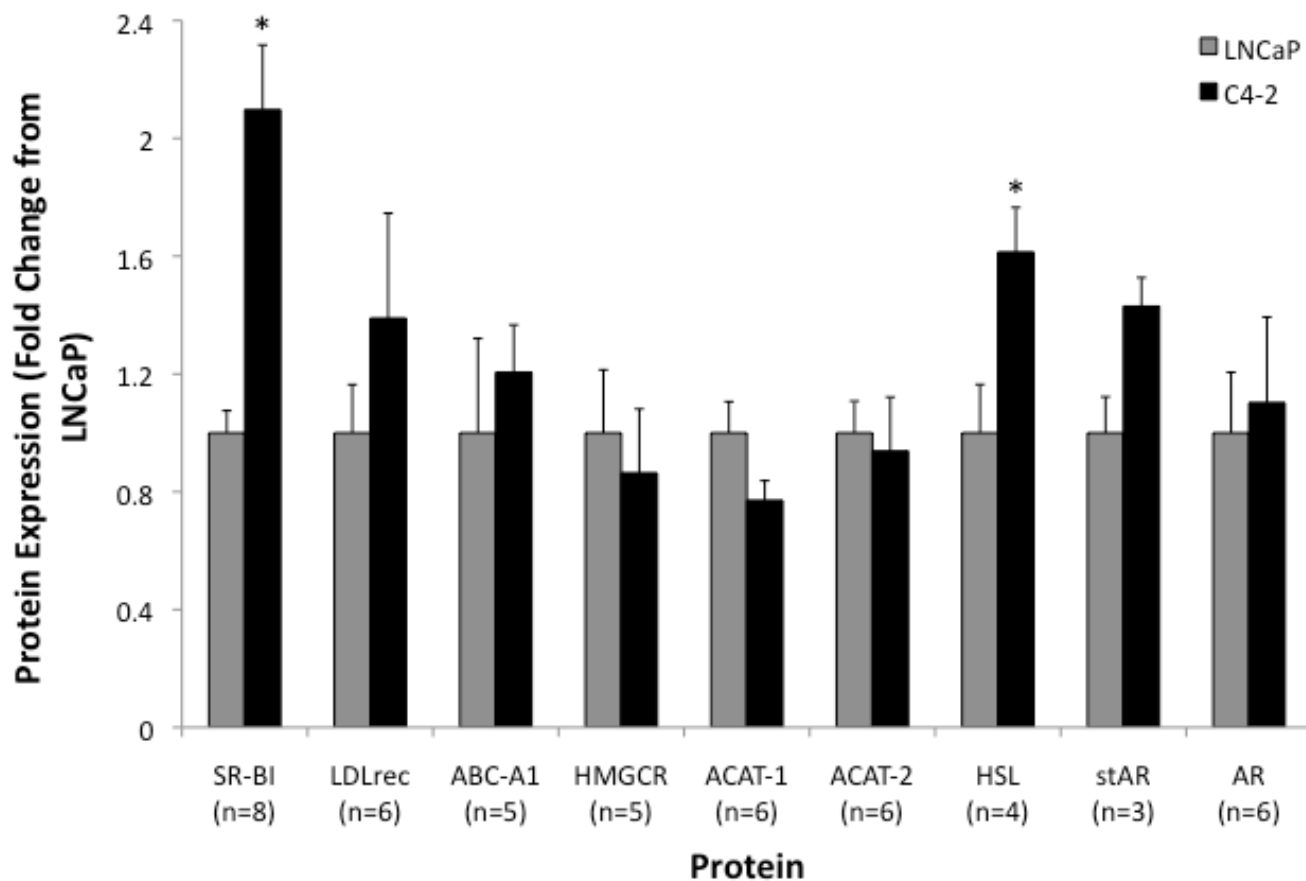


Figure 9: Basal protein expression derived from Western blots of proteins involved in cholesterol influx (SR-BI, LDLrec), efflux (ABC-A1), synthesis (HMGCR), metabolism (ACAT-1, ACAT-2 and HSL), transport into mitochondria (stAR) and the androgen receptor (AR) in LNCaP (grey) and C4-2 cells (black). All values are shown normalized to expression in LNCaP cells. Columns, mean (n is specified below the respective proteins); bars, +/-SEM. *, $p < .05$, LNCaP vs C4-2.

4.1.2.2 BASAL SR-BI AND HSL EXPRESSION

The protein expression of SR-BI (Fig. 10A) and HSL (Fig. 10C) was found to be significantly higher in C4-2 cells than LNCaP cells in the basal condition (as taken from Figure 9). HSL expression has approximately 1.6 fold higher and SR-BI expression was approximately 2.1 fold higher in C4-2 cells as compared to LNCaP cells. Figure 10B and 10D show representative blots of the expression of SR-BI, HSL and the corresponding actin bands in both cell types.

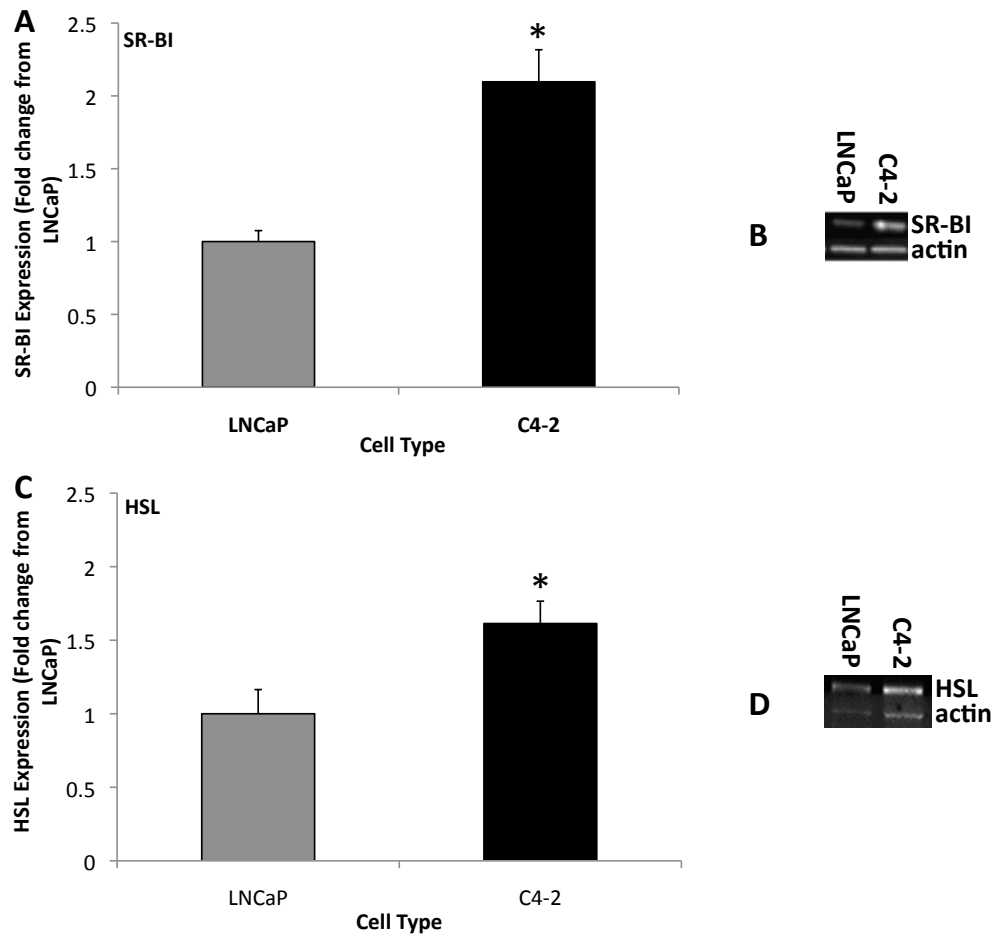


Figure 10A-D: Basal protein expression of SR-BI (A) and HSL (C) in LNCaP and C4-2 cells normalized to expression in LNCaP cells. Representative blots of each protein are shown for SR-BI (B) and HSL (D) with the respective actin bands. Columns, mean (n=8 for SR-BI and n=4 for HSL); bars, +/-SEM. *, p<.05.

4.2 AIM 2 EXPERIMENTS

4.2.1 SIRNA-INDUCED SILENCING OF SR-BI

The protein expression of SR-BI in LNCaP and C4-2 cells treated with the optimal dose of 10 nM SR-BI siRNA (SRBI-KD) or negative control (NC) siRNA with 2.0 nM Lipofectamine RNAiMAX was examined in order to determine if the knockdown resulted in >80% reduction in protein expression. Protein samples at day 0 and day 1, 3, and 6 post-transfection were analyzed by western blot to determine the degree of SR-BI silencing obtained. All values are expressed as fold change from day 0 values for the respective cell type. As can be seen in Figure 11A and 11B, the protein expression of SR-BI in C4-2 and LNCaP cells, respectively, was decreased by greater than 80% by day 3 and to >90% by day 6. These results confirmed that the protocol utilized was providing persistent and significant knockdown of SR-BI expression in both cell types.

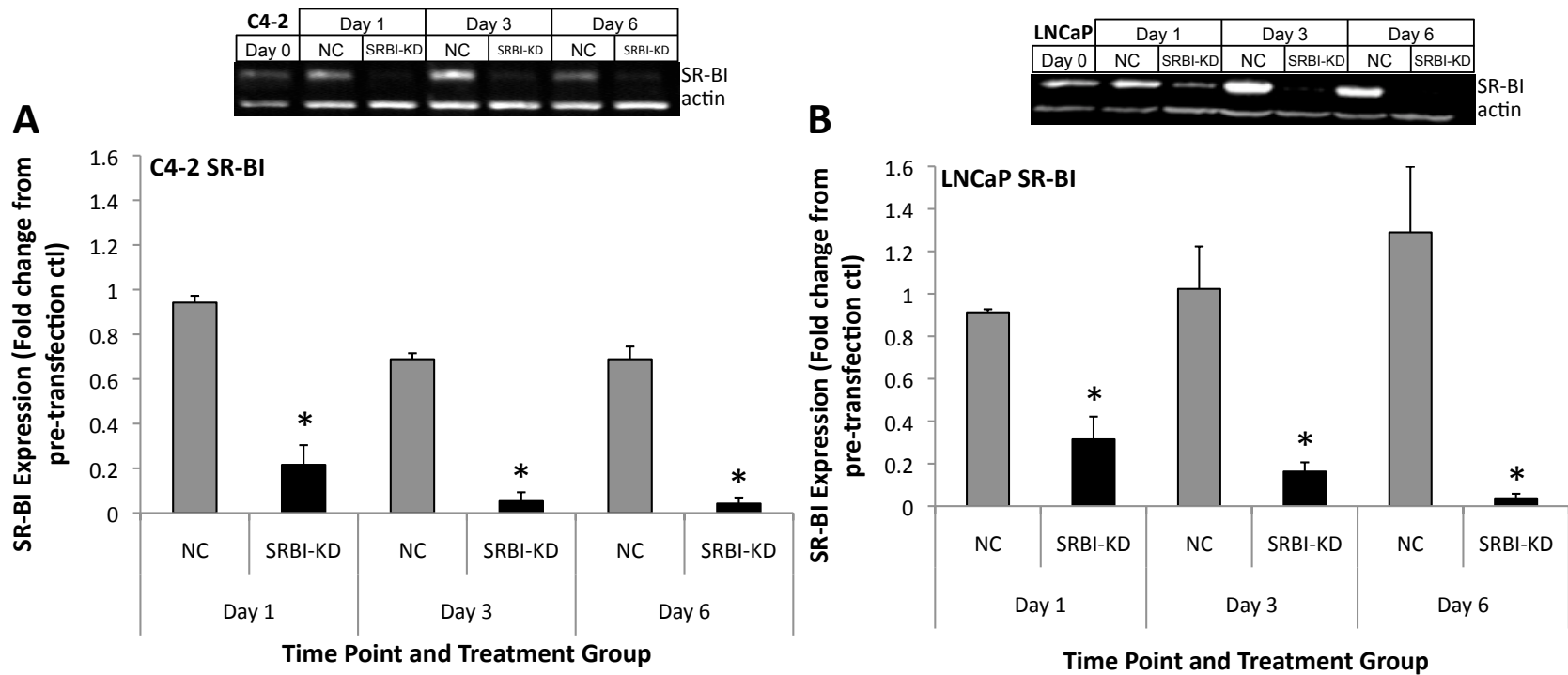


Figure 11A-B: Silencing of SR-BI protein expression in C4-2 (A) and LNCaP (B) cells at Day 1, 3 and 6 post-transfection with negative control (NC) and SR-BI (SRBI-KD) siRNA. Data is shown as the fold change in SR-BI expression from the expression in a pre-transfection control for each cell type. NC was not significantly different than Blank (not shown). Inset diagrams demonstrate representative blots analyzed in each cell type. Columns, mean (n=6); bars, +/-SEM. *, p<.05, NC versus SRBI-KD.

4.2.2 CYTOTOXICITY OF SR-BI SILENCED CELLS

The cytotoxicity of C4-2 and LNCaP cells post-transfection with negative control (NC) or SR-BI (SRBI-KD) siRNA was assessed to determine if there was any RNAi-related effects or cytotoxic effects specific to SR-BI silencing. Values are expressed as a percent of the 100% cytotoxicity control and were normalized to the cytotoxicity observed at day 0 in each cell type. The means of the cytotoxicity measured at each day in the SRBI-KD group were compared to the NC counterpart at that particular time point. The treatment groups were not significantly different in either C4-2 cells (Figure 12A) or LNCaP cells (Figure 12B). However, these data display a trend toward greater cytotoxicity in the SRBI-KD cells, particularly in the C4-2 cells and may be found to be significantly different if the power was improved.

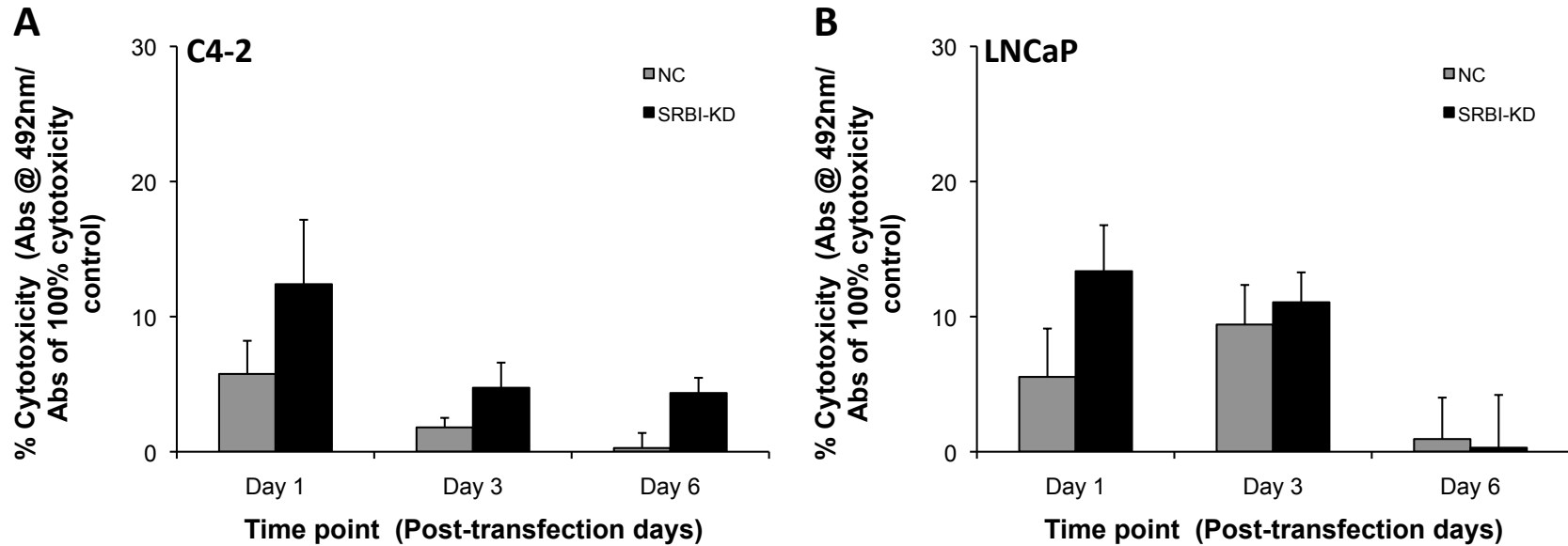


Figure 12A-B: Cell cytotoxicity is demonstrated as % cytotoxicity based on a 100% cytotoxic control, representing the amount of LDH in the media of C4-2 (A) and LNCaP (B) cells treated with SR-BI siRNA (SRBI-KD, black bars) and a negative control siRNA (NC, grey bars) at Day 1, 3 and 6 post-transfection. Values are controlled for day 0 cytotoxicity. Columns, mean (n=5); bars, +/-SEM.

4.2.3 CELL VIABILITY OF SR-BI SILENCED CELLS

The viability of cells treated with SR-BI (SRBI-KD) and negative control (NC) siRNA was assessed over the 6-day siRNA protocol discussed in section 3.4. The viability of each treatment group, SRBI-KD or NC, was expressed as fold change from the pre-transfection control that has been considered 1.0. The viability of C4-2 cells treated with siRNA is shown in Figure 13A, while LNCaP data is shown in Figure 13B. In C4-2 cells at day 3 and day 6 the SRBI-KD cells have significantly lower viability than the NC cells on the same day by approximately 28% and 22%, respectively (Fig. 13A). SR-BI silencing seems to have affected LNCaP cell viability as well, but groups were not significantly different due to the large variability observed. In order to indirectly demonstrate that SR-BI activity was reduced along with the protein silencing, cells were treated with 10 $\mu\text{g/mL}$ of HDL based on protein content and the resultant viability was analyzed (Figure 13C & D). Although other lipoproteins interact with SR-BI, HDL is thought to be its major substrate and does not interact with other influx transporters, such as LDL receptor (94,103). HDL was added to cells immediately following transfection and cell viability was assessed 24 hours later. NC C4-2 cells treated with HDL (NC+HDL, Fig. 13C) had significantly increased cell viability compared to the untreated NC cells, while the SRBI-KD C4-2 cells treated with HDL (SRBI-KD+HDL, Fig.13C) were not different from the untreated SRBI-KD cells. The same trend was seen in the LNCaP cells (Fig. 13D), but the difference was not significant. These data indicate that SR-BI activity was likely reduced in SRBI-KD cells because providing substrate did not correct for the reduction in viability. LDL addition did not have significant effect on the growth of either cell line (Appendix E).

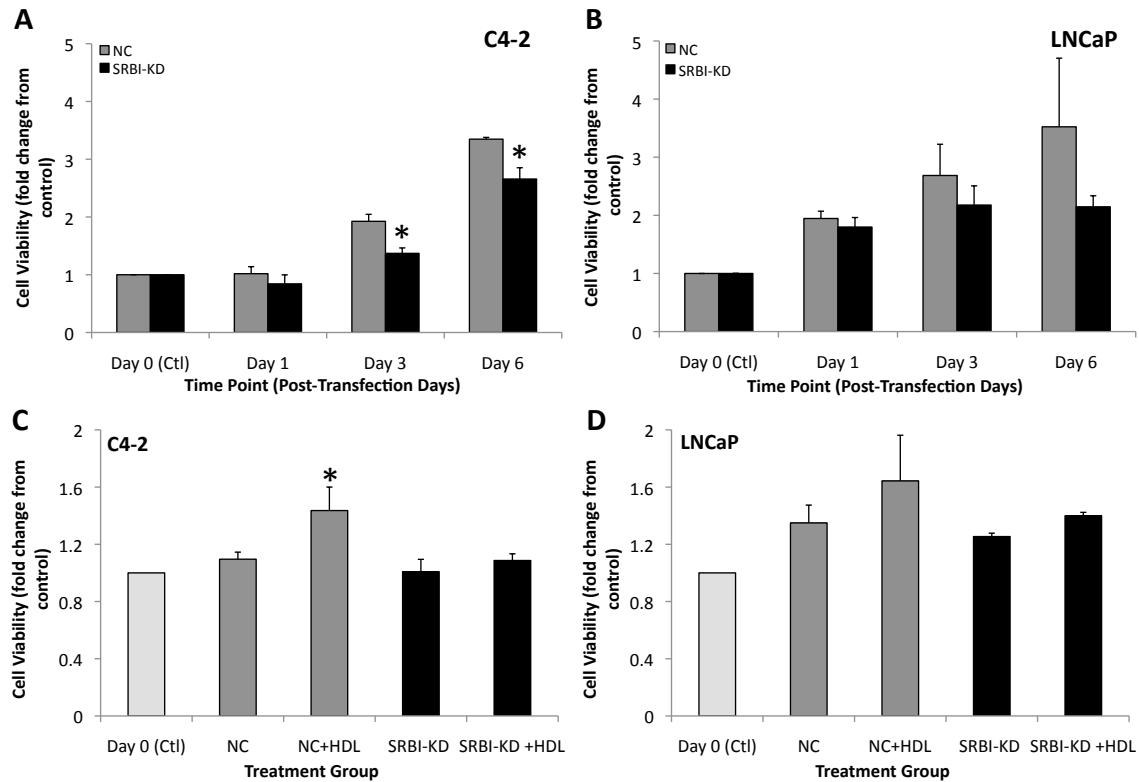


Figure 13A-D: Cell viability is demonstrated as fold change in viability from the pre-transfection (Day 0) control in C4-2 (A) and LNCaP (B) cells treated with SR-BI siRNA (SRBI-KD, black columns), a negative control siRNA (NC, grey columns) at Day 1, 3 and 6 post-transfection. C&D: Measures were taken 24hrs after the addition of 10ug/mL HDL (+HDL) which was added immediately post-transfection on Day 0 to NC (grey columns) and SRBI-KD (black columns) cells. Columns, mean (n=6 for A/B, n=3 for C/D); bars, +/-SEM. *, p<.05, SRBI-KD vs NC (A/B) and NC+HDL vs NC (C).

4.3 AIM 3 EXPERIMENTS

4.3.1 CELLULAR CHOLESTEROL IN SR-BI SILENCED CELLS

Total cellular cholesterol levels were measured pre-transfection (day 0) and at day 1, 3, and 6 post-transfection in viable cells treated with SR-BI (SRBI-KD) or negative control (NC) siRNA. No statistically significant differences were observed in total cholesterol levels between SRBI-KD and NC-treated groups in either C4-2 (Figure 14A)

or LNCaP (Figure 14B) whole cell samples. It appears that the LNCaP cholesterol levels have a different trend at day 6 as compared to that of the C4-2 cellular cholesterol levels, but the areas under these concentration curves, 48.52 ± 4.18 and 61.38 ± 16.92 $\mu\text{g}\cdot\text{day}/\mu\text{L}$, respectively, were not statistically significantly different. Figure 14C and 14D depict the free cholesterol and cholesteryl ester concentrations in C4-2 and LNCaP whole cell samples, respectively. No changes were observed in either of these parameters. Intracellular cholesterol concentrations were also assessed using the dissolved fraction of RIPA lysates from each cell type and time point to determine if a membrane-free sample would demonstrate changes in cholesterol levels. No differences were seen between the NC and SRBI-KD groups in these samples, similar to the results for whole cell lysates (Appendix F).

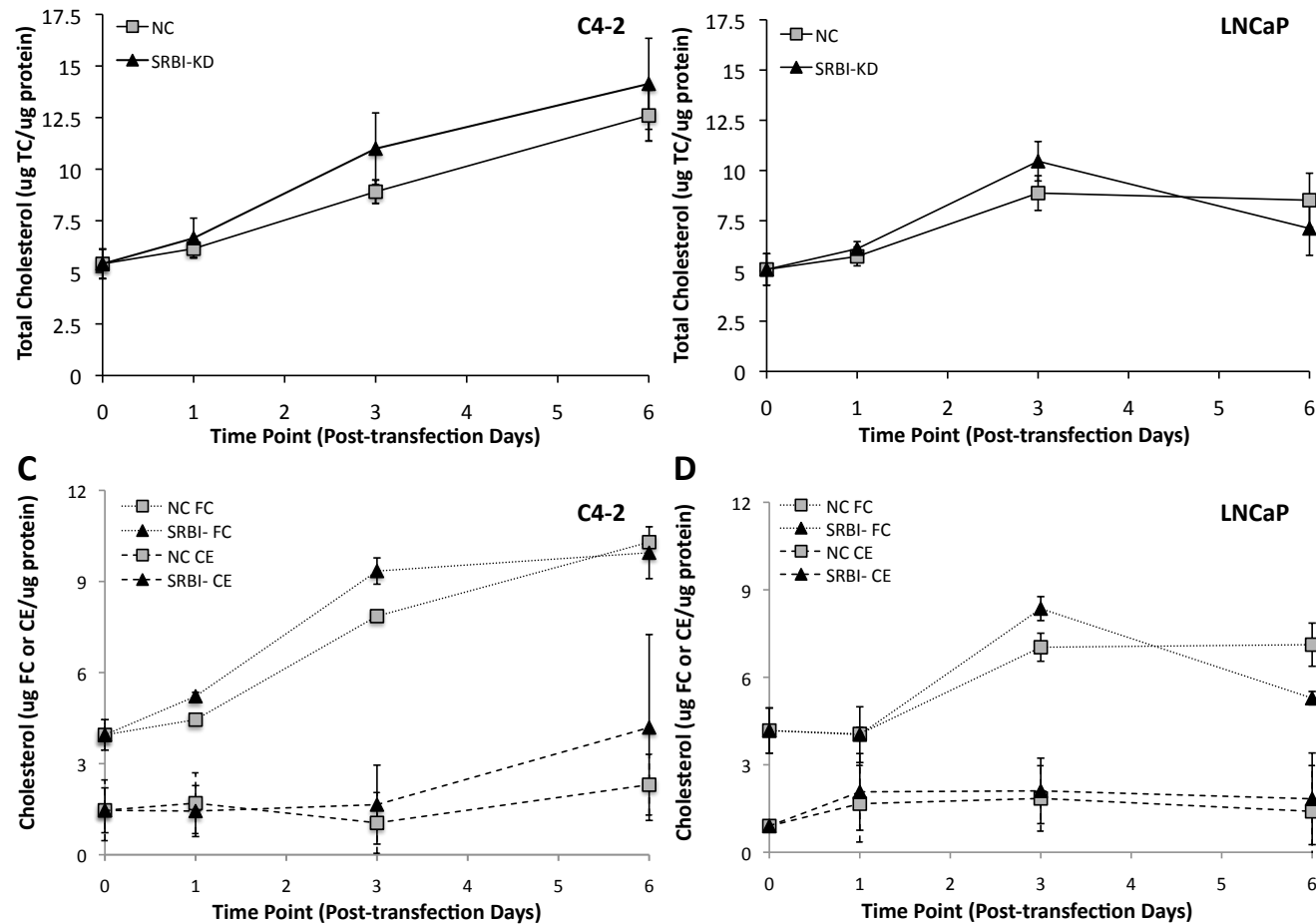


Figure 14A-D: Total cholesterol is shown as μg cholesterol per μg protein in whole cell lysates of C4-2 (A) and LNCaP (B) cells treated with SR-BI siRNA (SRBI-KD, black triangles) and negative control (NC, grey boxes) siRNA at Day 0 (pre-transfection) and Day 1, 3 and 6 post-transfection. Free cholesterol (FC, dotted lines) and cholesteryl ester (CE, broken lines) concentration (μg FC or CE/ μg of protein) is shown in C4-2 (C) and LNCaP (D) cells. Curve, mean ($n=5$); error bars, \pm -SEM.

4.3.2 PROTEIN EXPRESSION IN SR-BI SILENCED CELLS

4.3.2.1 INFLUX AND EFFLUX TRANSPORTERS

The lack of differences in cholesterol levels despite the significant down-regulation of SR-BI raised the question of potential compensatory measures in other major cholesterol transporters. The LDL receptor is another major provider of exogenous cholesterol to the cell via influx from lipoprotein sources. The protein expression of the LDL receptor was assessed over the 6-day SR-BI silencing period in both cell lines and is shown in Figure 15A and B in C4-2 and LNCaP cells, respectively. All values are expressed as fold change from day 0 values for the respective cell type. No significant differences were observed between SRBI-KD and NC groups. Similarly, the protein expression of the major cholesterol efflux transporter, ABC-A1 was determined (Figure 15C & D). Although it appears that ABC-A1 expression was decreased in the SR-BI silenced cells at day 3 and day 6 in C4-2 cells and at day 6 in LNCaP cells, the differences were not statistically significant.

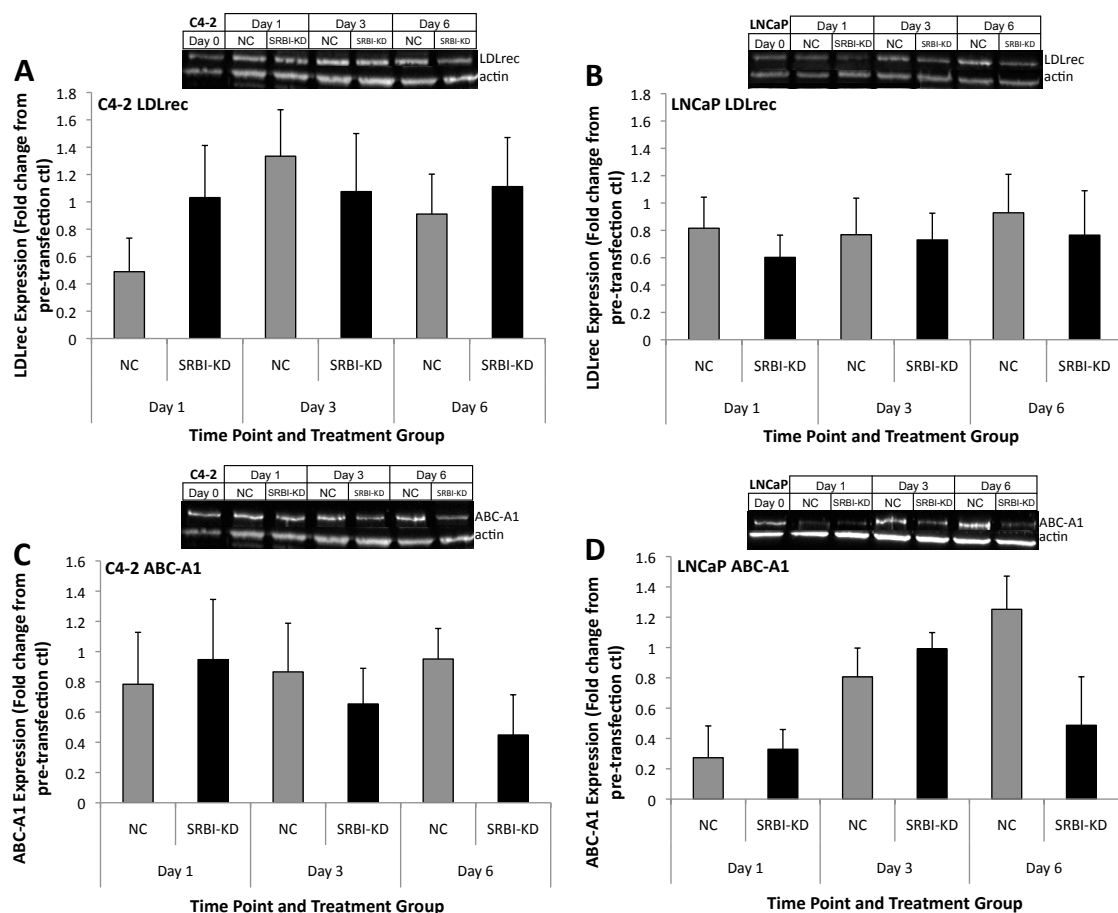


Figure 15A-D: Expression of LDLrec in C4-2 (A) and LNCaP (B) cells at Day 1, 3 and 6 post-transfection with negative control (NC) and SR-BI (SRBI-KD) siRNA. Expression of ABC-A1 is shown in C4-2 (C) and LNCaP (D) cells. Data is shown as the fold change in LDLrec and ABC-A1 expression from the respective protein expression in a pre-transfection control for each cell type. Inset diagrams demonstrate representative blots analyzed in each cell type. Columns, mean (n=6 for LDLrec and n=5 for ABC-A1); bars, +/-SEM.

4.3.2.2. CHOLESTEROL METABOLISM ENZYMES

The possible effect of silencing SR-BI on the metabolic processing of cholesterol, namely the process of storing cholesterol as cholesteryl esters via ACAT-1 and ACAT-2 and the release of free cholesterol from cholesteryl ester stores via HSL was assessed by

examining the protein expression of these enzymes. All values are expressed as fold change from day 0 values for the respective cell type. ACAT-1 and ACAT-2 protein levels did not change significantly in C4-2 cells (Fig. 16A and C) or in LNCaP cells (Fig. 16B and D) treated with SR-BI siRNA as compared to the respective negative controls. However, Figure 16E demonstrates that HSL expression was significantly increased by ~30% in SRBI-KD cells at day 3 compared to the day 3 NC counterpart in C4-2 cells. SR-BI silencing did not elicit any significant changes in the expression of HSL in LNCaP cells at any time point (Figure 16F).

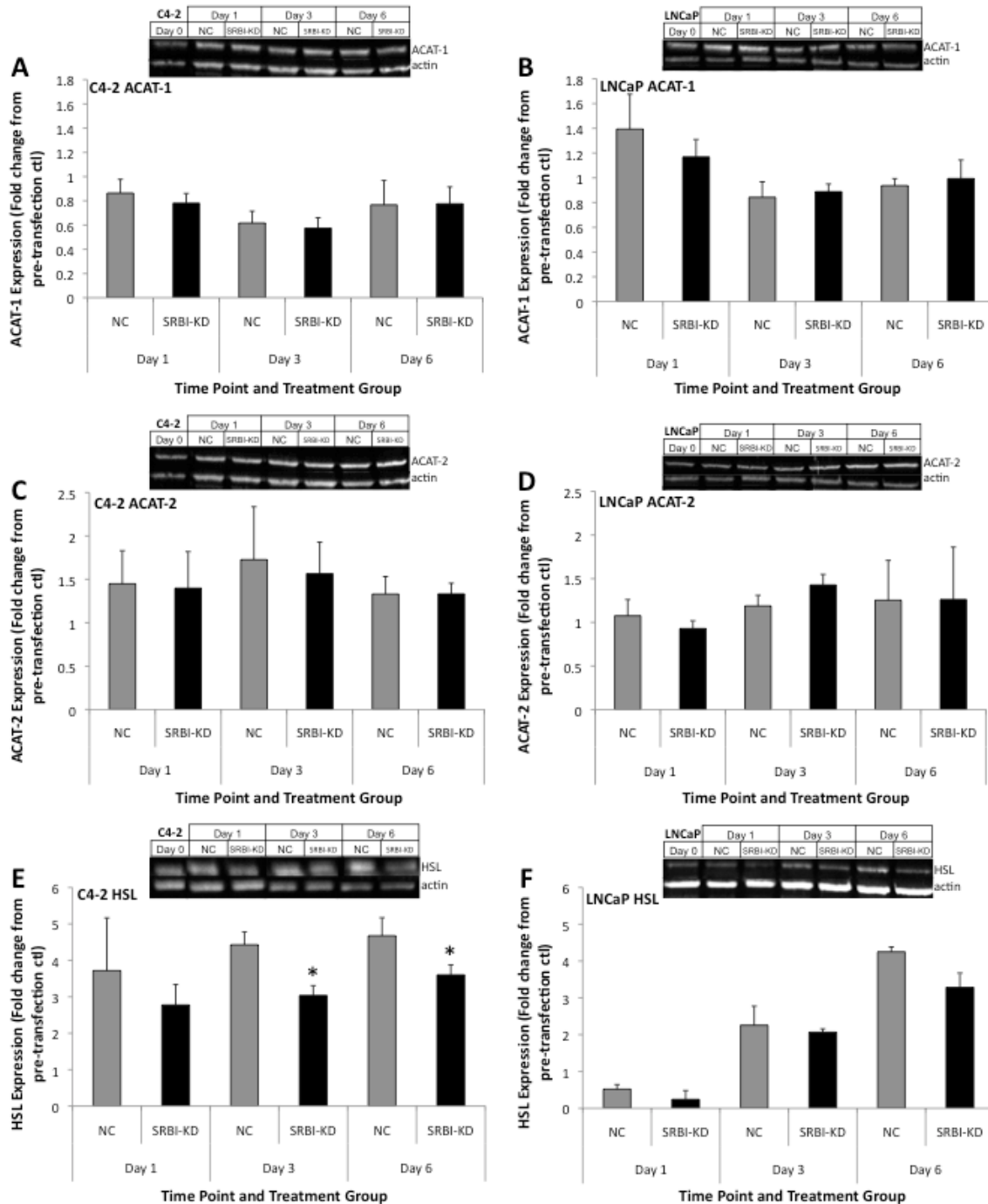


Figure 16A-F: Expression of ACAT-1 and ACAT-2 in C4-2 (A,C) and LNCaP (B,D) cells at Day 1, 3 and 6 post-transfection with negative control (NC) and SR-BI (SRBI-KD) siRNA. Expression of HSL is shown in C4-2 (E) and LNCaP (F) cells. Data is shown as the fold change in ACAT-1, ACAT-2 and HSL expression from the respective protein expression in a pre-transfection control for each cell type. Inset diagrams demonstrate representative blots analyzed in each cell type. Columns, mean (n=6; ACAT-1/2 and n=4; HSL); bars, +/-SEM. *, p<.05. NC versus SRBI-KD.

4.3.2.3 CHOLESTEROL SYNTHESIS- HMGCR EXPRESSION

Protein expression of HMG CoA reductase (HMGCR), the enzyme responsible for the rate-limiting step in intracellular *de novo* cholesterol synthesis, was examined to determine if SR-BI silencing would elicit compensatory changes. All values are expressed as fold change from day 0 values for the respective cell type. HMGCR protein expression, although displaying a decreasing tendency in the SRBI-KD group at all days and in both cell types, was not statistically different from the respective NC groups (Figure 17A and B).

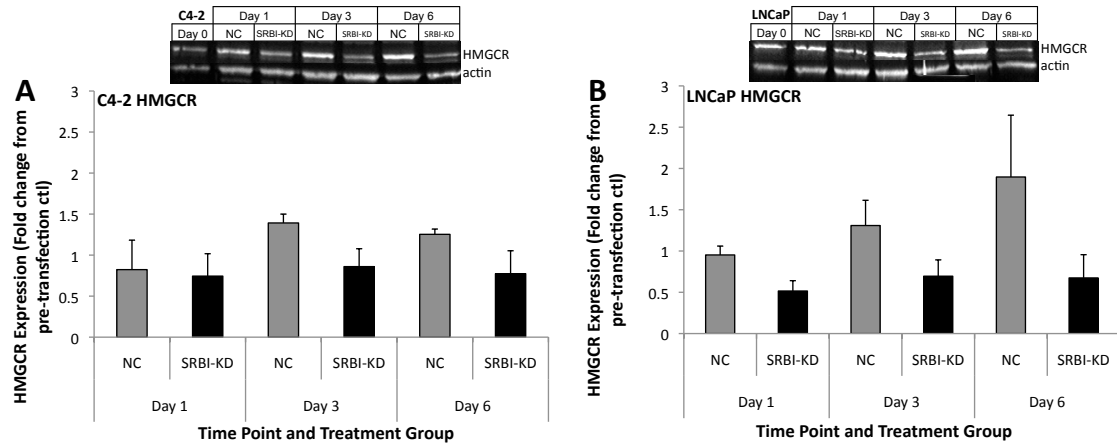


Figure 17A-B: Expression of HMGCR in C4-2 (A) and LNCaP (B) cells at Day 1, 3 and 6 post-transfection with negative control (NC) and SR-BI (SRBI-KD) siRNA. Data is shown as the fold change in HMGCR expression from the expression in a pre-transfection control for each cell type. Inset diagrams demonstrate representative blots analyzed in each cell type. Columns, mean (n=5); bars, +/-SEM.

4.3.3 CHOLESTEROL SYNTHESIS ACTIVITY

The activity of HMGCR was also assessed due to its complex processing in the cell and therefore, potentially confounding representation in protein expression (Fig. 17). Scintillation readings of cholesterol on the silica gel plate, as confirmed by the position of

a cold cholesterol sample, were taken for both SRBI-KD and NC cells at day 0 and day 6. These measures reflected incorporation of the radiolabelled precursor, ^{14}C -acetate, into cholesterol. The values obtained were then normalized to the amount of protein within the given sample. Data are expressed as ^{14}C dpm incorporated into cholesterol divided by ^3H dpm control counts per μg protein in the sample. As can be seen in Figure 18, the HMGCR activity is significantly higher basally in C4-2 cells, as compared to LNCaP cells. There is no difference in the activity observed in LNCaP SRBI-KD and NC cells at day 6, while the C4-2 SRBI-KD cells have a significantly higher cholesterol synthesis activity, a difference of approximately 2 fold, at day 6 than the NC counterpart cells at the same time point. The HMGCR activity was also analyzed at day 3 post-transfection in C4-2 cells and can be seen in Appendix G.

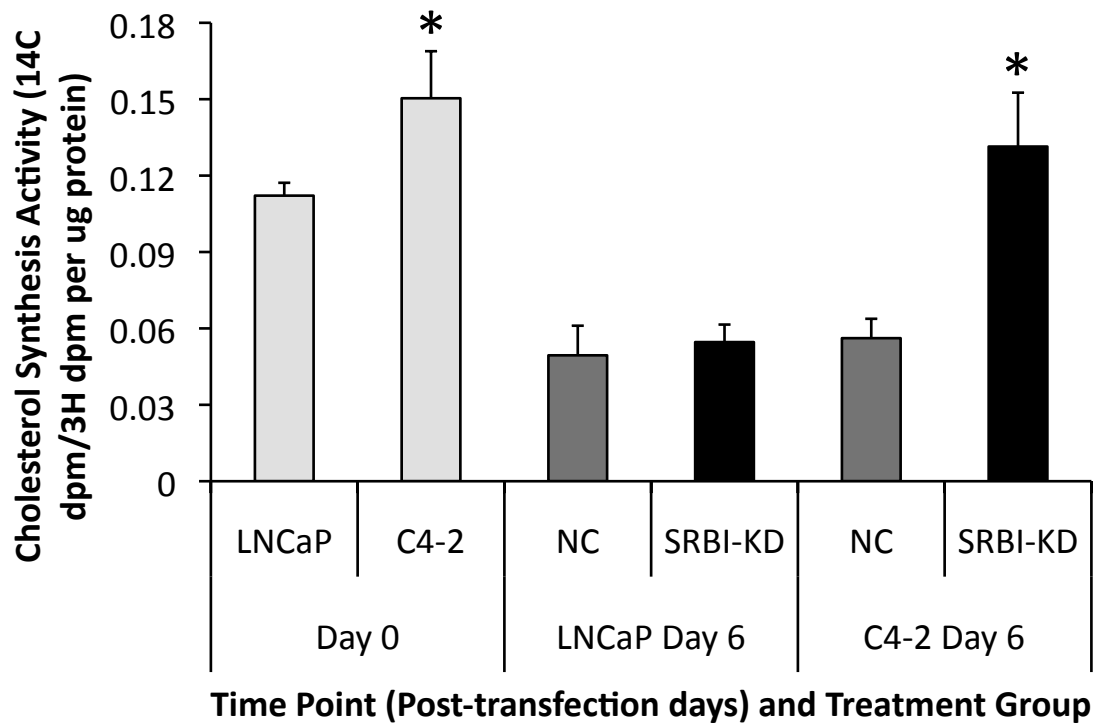


Figure 18: Cholesterol synthesis was measured by following the incorporation of ^{14}C -acetate into cellular cholesterol as measured by scintillation counting after separation by thin layer chromatography in C4-2 and LNCaP cells at Day 0 (white columns) and Day 6 post-transfection with negative control siRNA (NC, grey columns) and SR-BI siRNA (SRBI-KD, black columns). All values are corrected by ^3H -cholesterol control counts (dpm) and by ug of protein in a given sample. Columns, mean (n=3); bars, +/- SEM. *, $p < .05$ Day 6 NC vs Day 6 SRBI-KD.

4.4 AIM 4 EXPERIMENTS

4.4.1 PSA SECRETION IN SR-BI SILENCED CELLS

The prostate specific antigen secretion of LNCaP and C4-2 cells at day 0, as well as at day 1, 3, and 6 post-transfection of cells with SR-BI siRNA and NC siRNA was quantified in the supernatant. The amount of PSA is expressed as concentration (ng/mL) and was then normalized to the amount of protein (ug) in the cell samples from the respective wells of the analyzed supernatant. The PSA secretion in the SR-BI-KD

treatment group of both C4-2 and LNCaP cells was significantly lower than that of the respective negative control group (Fig. 19). At day 6 in C4-2 cells the SR-BI-KD cells had secreted 111.7 ± 27.5 ng/mL per ug protein as compared to 243 ± 37.6 ng/mL per ug protein secreted by the NC cells. LNCaP SR-BI-KD cells secreted 70.4 ± 23.6 ng/mL per ug protein versus 165.6 ± 28.4 ng/mL per ug protein in the NC cells. This represents a reduction of approximately 55% and 58% in the C4-2 and LNCaP cells, respectively.

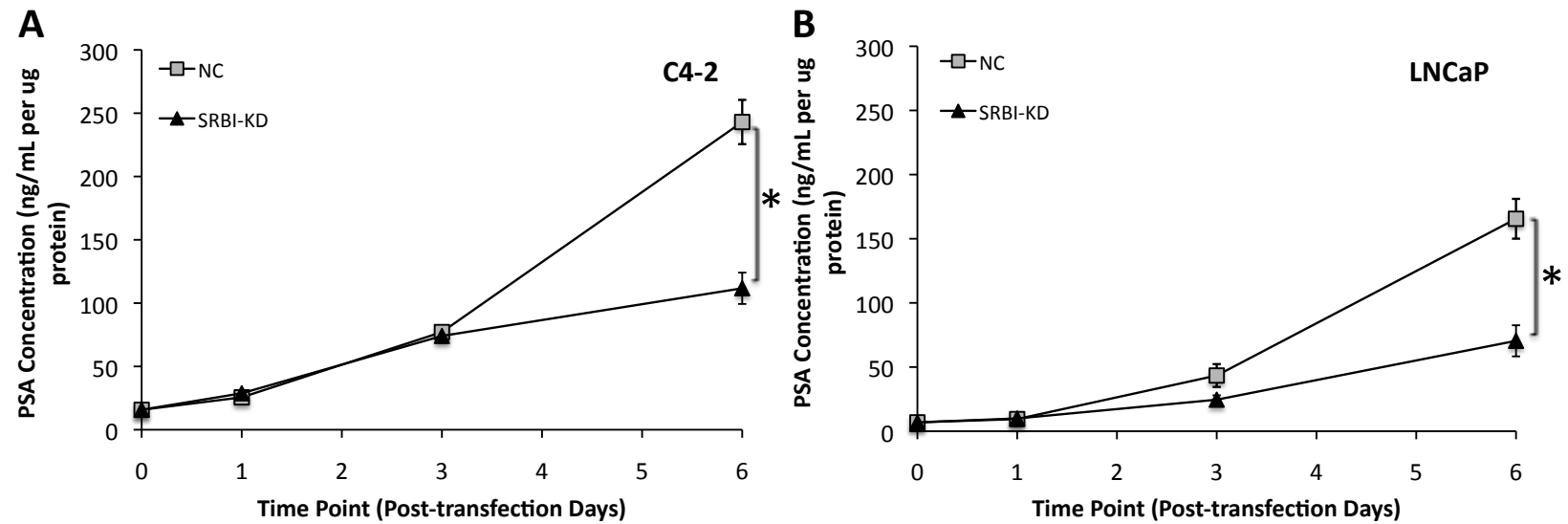


Figure 19A-B: PSA secretion is demonstrated as concentration in the media of C4-2 (A) and LNCaP (B) cells treated with SR-BI siRNA (SRBI-KD, black triangles), a negative control siRNA (NC, grey squares) at Day 0 (pre-transfection) and Day 1, 3 and 6 post-transfection. Values were adjusted for the amount of protein in the respective samples. Curve, mean (n=5); bars, +/-SEM. *, $p < .05$ Day 6 NC versus Day 6 SRBI-KD.

4.4.2 INTRACELLULAR TESTOSTERONE IN SR-BI SILENCED CELLS

Testosterone was measured in media and cell lysates at day 0 (pre-transfection), day 1, 3 and 6 post-transfection. All values obtained in the media samples were below the detection limit of the ELISA (0.03 ng/mL) and were therefore not quantifiable and were consequently not included. Intracellular testosterone levels, as taken from the supernatant of cell samples lysed with modified RIPA buffer, are shown in Figure 20. The amount of testosterone is shown as concentration (ng/mL) per μg of protein in the respective sample. Testosterone levels were not significantly different between SRBI-KD and NC groups in the LNCaP cells (Fig. 20B). However, the SRBI-KD group in the C4-2 cells at day 3 had significantly higher (~35%) intracellular testosterone concentration as compared to the NC group (Fig. 20A).

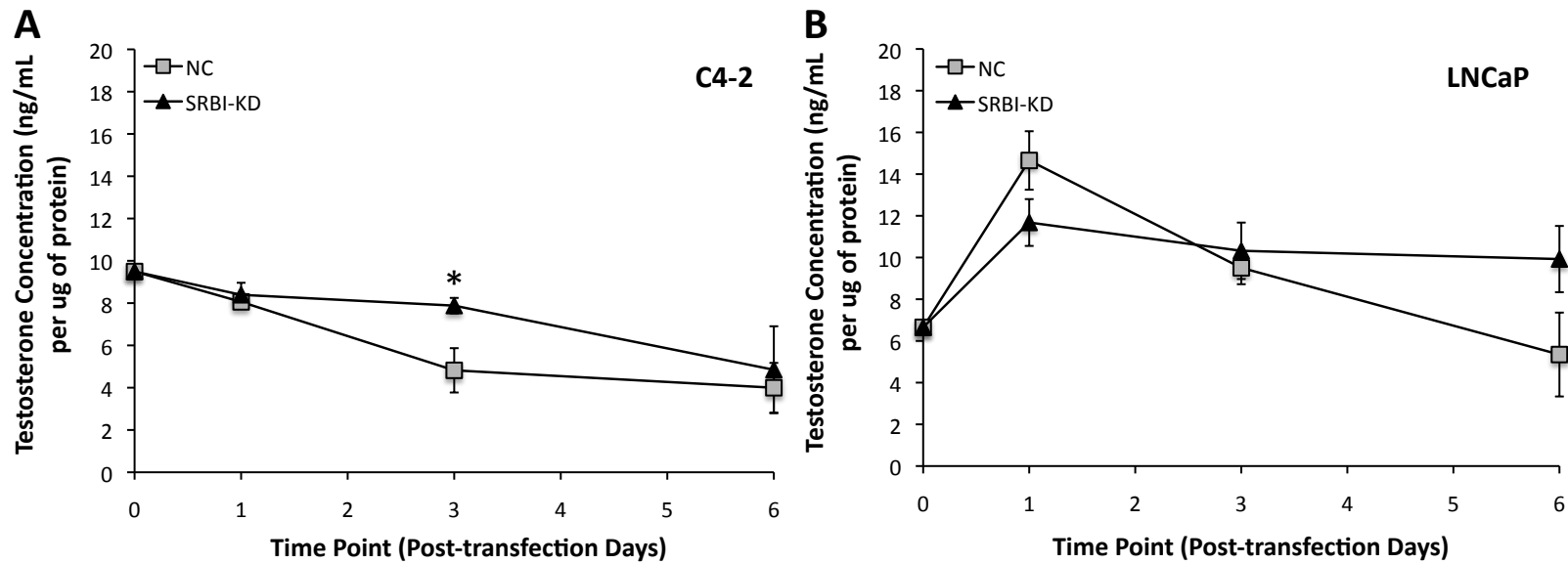


Figure 20A-B: Intracellular testosterone concentration (ng/mL) is shown in C4-2 (A) and LNCaP (B) cells treated with SRBI siRNA (SRBI-KD, black triangles) and a negative control siRNA (NC, grey squares) at Day 0 (pre-transfection) and Day 1, 3 and 6 post-transfection. Values were adjusted for the amount of protein (μ g) in the respective samples. Curve, mean (n=5); bars, \pm SEM. *, $p < .05$ Day 3 NC versus Day 3 SRBI-KD.

4.4.3 STAR AND AR PROTEIN EXPRESSION IN SR-BI SILENCED CELLS

In order for cholesterol to be synthesized into androgens it must first be brought from the cellular compartment into the mitochondrial matrix. This step is completed by stAR. AR is the receptor that binds to androgens in the cytosol in order to elicit a number of effects, including PSA production. It was thought that the expression of these proteins may change in response to SR-BI down-regulation and subsequently reflect changes in the intracellular steroid production pathways. However, no differences were seen between the NC and SRBI-KD groups in either cell type indicating that silencing SR-BI does not effect the protein expression of stAR (Fig. 21A and B) or AR (Figure 21C and D). All values are expressed as fold change from day 0 values for the respective cell type.

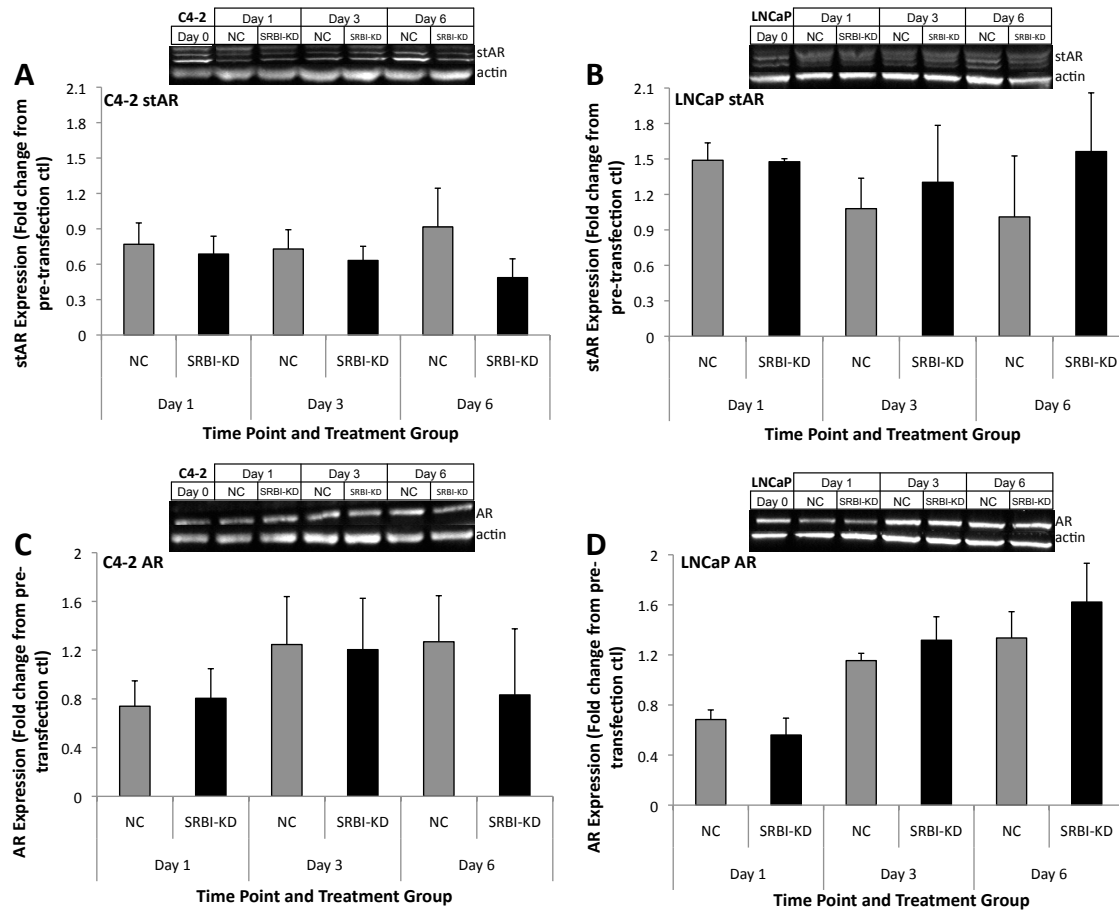


Figure 21A-D: Expression of stAR in C4-2 (A) and LNCaP (B) cells at Day 1, 3 and 6 post-transfection with negative control (NC) and SR-BI (SRBI-KD) siRNA. Expression of AR is shown in C4-2 (C) and LNCaP (D) cells. Data is shown as the fold change of stAR and AR expression from the respective protein expression in a pre-transfection control for each cell type. Inset diagrams demonstrate representative blots analyzed in each cell type. Columns, mean (n=3 for stAR and n=6 for AR); bars, +/-SEM.

CHAPTER 5 DISCUSSION

5.1 BASAL SR-BI IN LNCAP AND C4-2

Inevitably, disseminated CaP treated with hormone therapy will recur in a more aggressive castration-resistant form in the low exogenous androgen environment. Many lines of evidence support the importance of the androgen-AR signaling pathway in the castration-resistant state, including intracellular *de novo* synthesis of androgens from cholesterol. One source of cholesterol to the cell is SR-BI, a cholesterol influx transporter. SR-BI has been shown to be important for provision of cholesterol to the steroidogenic pathway in the adrenal tissues of rodents. In addition, perturbation of SR-BI expression in humanized murine models elicits stunted steroid production, a deficit unchanged by compensatory increases in cholesterol synthesis (79,86,114). In addition, our group found that SR-BI expression was increased in an LNCaP xenograft model upon progression to castration-resistance (50). Therefore, the current study investigated the role of SR-BI as a potential source of precursor to *de novo* androgen synthesis (Fig. 22). Cholesterol homeostasis is complex, therefore four major points in cellular cholesterol regulation- efflux, influx, metabolism and synthesis, were examined in connection with the androgen AR-signaling pathway (Fig. 22).

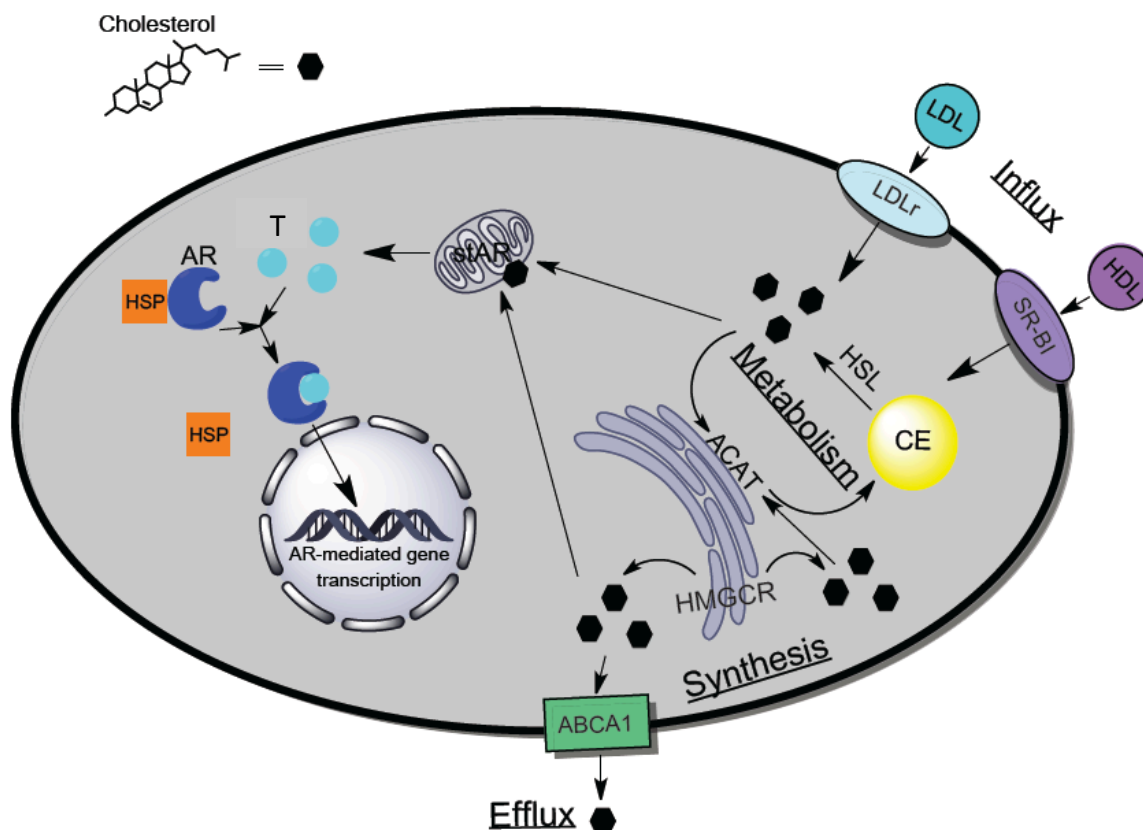


Figure 22: Diagram of cellular cholesterol (●) pathways- synthesis, metabolism, influx and efflux. Cholesterol moves to mitochondria where stAR initiates androgen synthesis by shuttling cholesterol into the intermitochondrial space. Androgens (T) bind to the AR and cause gene transcription (Adapted from (156)).

To determine if SR-BI has a significant physiological role in CaP, particularly in different forms of the disease, LNCaP and C4-2 cells were selected as the model. In the absence of DHT treatment it was found that C4-2 cells had a significantly higher basal PSA level as compared to the LNCaP, confirming the findings of many other groups that C4-2 cells have a basally active AR and thus a higher basal PSA than LNCaP cells (43,157,158). DHT treatment caused a significant increase in PSA secretion in both cell types as can be seen in Figure 8. The mutated AR present in both the LNCaP and C4-2 cells responds to androgens in a similar manner as the wild type receptor, but it has less

binding specificity due to changes in the binding pocket (34) making it promiscuous. This promiscuity is present in approximately 10% of recurrent CaP facilitates AR activation via binding of a number of substrates in addition to androgens, including progesterone and cortisol (159,160).

The basal protein expression of major proteins in the cholesterol and the androgen receptor-signaling pathway were assessed. Interestingly, it was demonstrated herein that basal expression of SR-BI was two-fold higher in the C4-2 cells than the LNCaP cells (Fig. 10), while the LDLrec, although displaying a similar pattern was not statistically significantly different (Fig. 9). These findings are in agreement with the up-regulation of SR-BI observed at castration-resistance in the LNCaP xenograft model mentioned previously (50). Selective uptake of cholesteryl ester from HDL via SR-BI has been tightly linked to HSL expression near the surface of the cell (95). This co-expression is thought to serve cellular cholesterol needs by hydrolyzing incoming CEs into free cholesterol for use in cellular processes. Interestingly, this relationship is demonstrated herein, in that HSL, in concert with SR-BI, was significantly up-regulated basally in C4-2 cells as compared to LNCaP cells (Fig. 10). These findings suggest that castration-resistant cells may adapt to the exogenously low androgen environment in which they were derived by increasing cholesterol influx to supply cellular needs, including provision of precursor to *de novo* androgen synthesis (43,50). In addition, it is possible that the elevated SR-BI and HSL may reflect induction by the basal intracellular androgen concentrations, since androgens cause an increase in the expression of these proteins, an inverse response to that elicited by cholesterol (94,112,115,161,162). Basal

testosterone concentrations were found to be approximately 30% higher in C4-2 cells than the LNCaP cells as demonstrated by the day 0 values in Figure 20. Although this difference was not statistically significantly different it may have been sufficient to cause induction of SR-BI and HSL expression and may partially explain their up-regulation in C4-2 cells.

It was expected that the basal AR expression in C4-2 cells would be significantly higher than in the LNCaP cells, a finding demonstrated in C4-2 cells and a number of other sublines of LNCaP (34). The findings herein indicate this trend was present, however, the difference was not significant due to high variability in the expression levels obtained (Fig. 9). Although this finding was unexpected, the higher basal PSA seen in the C4-2 cells suggests that AR activity is higher and perhaps the technique used to extract the AR is the problem. As discussed previously, the AR moves to the nucleus upon androgen binding and it is possible that a more efficient nuclear protein extraction procedure would reflect the different AR protein levels found by other groups.

5.2 SR-BI SILENCING AFFECTS CELL VIABILITY

Silencing target protein synthesis with RNA interference is emerging as a new modality for the treatment of cancer (163-165). Down-regulation of SR-BI expression using this method caused a significant reduction in the viability of C4-2 cells, but not in LNCaP cells despite a tendency toward the same effect (Fig.13A and B). This finding supports the aforementioned hypothesis that castration-resistant cells have a greater reliance on this transporter. The observed reduction in viability is thought to be due to the loss of SR-BI and not the transfection process, as all values are compared to cells

transfected with negative control siRNA and no significant toxicity was observed (Fig. 12). A similar SR-BI silencing procedure was implemented in human granulosa luteal cells and the cell viability was not affected, further implicating a cell specific effect of SR-BI modulation (166). Addition of HDL, a SR-BI substrate, increased the viability of negative control cells as has been seen by other groups, but did not abrogate the reduced viability of the SRBI-KD cells (Fig. 13C and D) (77,167). This result supports the hypothesis that the functional loss of SR-BI, and therefore a source of cholesterol, is responsible for the observed attenuation in viability, as well as potential signal transduction effects as discussed in section 5.5.

Cell cytotoxicity was not found to be significantly different, despite a trend towards greater toxicity in the SRBI-KD groups compared to NC groups, especially one day after the transfection (Fig. 12). This may indicate an initial insult to the membrane integrity due to the physical loss of SR-BI from the membrane structure, but it is difficult to be certain. The fact that the cytotoxicity data do not complement the viability data may indicate that maintenance of membrane integrity does not necessarily correlate directly with metabolic activity (168). Since a direct apoptotic marker was not measured, it is difficult to infer programmed cell death over necrosis based on the data obtained. However, the minimal cytotoxicity in conjunction with significant viability changes in SR-BI-KD versus NC cells indicates intracellular processes are likely affected to a greater extent after day 1.

5.3 SR-BI SILENCING AFFECTS CHOLESTEROL SYNTHESIS

It was expected that the SR-BI silencing effects on cell viability were due to the

loss of cholesterol influx, the main function of this transporter. However, it was found that the cholesterol levels were unchanged between treatment groups (Fig. 14). The lack of change in cellular cholesterol indicates that perhaps the other cholesterol pathways were able to compensate for the loss of SR-BI-mediated influx and maintain cholesterol levels. Thus, it was expected that other major players in the complex network of cholesterol homeostasis, namely other influx transporters, efflux, synthesis and metabolism, would be altered as a result of the reduction in SR-BI (Fig. 22).

Intuitively, it was assumed that reducing influx of cholesterol via SR-BI would cause an increased influx through the LDL receptor, the other major lipoprotein influx transporter, and decreased efflux via ABC-A1; a shift that would potentially be reflected by a change in protein expression. However, there were no significant changes observed in either the LDL receptor or ABC-A1 between the treatment groups, despite decreased expression in ABC-A1 in the SRBI-KD group (Fig. 15). Thus, it seems that the unchanged cholesterol levels in spite of the decrease in SR-BI could not be explicitly explained by changes in the efflux and influx transporters. Therefore, HMGCR, the rate-limiting enzyme in *de novo* synthesis of cholesterol was examined.

Cholesterol is an essential molecule in all cells and therefore its homeostasis is tightly regulated (53,82). However, a major cholesterol regulator, SREBP-2, has been shown to be dysfunctional in castration-resistant cancer cells. This finding was supported by an increased *ex vivo* HMGCR activity observed by our group upon progression to castration-resistance in a LNCaP xenograft model (45,50,88,89). HMGCR, the rate-

limiting step in the mevalonate pathway, is controlled at the transcriptional level by SREBP-2 (101). The higher basal cholesterol synthesis activity in C4-2 cells as compared to the LNCaP cells observed in this study may reflect this dysfunction, but SREBP-2 was not quantified therefore this is only speculation. HMGCR protein expression increases have been seen in the progression to CRPC (79,84-87). In the current study, the significant increase in activity seen at day 6 in the C4-2 cells with knocked down SR-BI (Fig. 18) was not mirrored by an increase in the HMGCR protein expression (Fig. 17). The lack of correlation between protein expression and activity of HMGCR may be a reflection of acute versus chronic regulation of the enzyme. While long-term regulation of HMGCR should be reflected in protein levels, acute alterations are better represented by the enzyme activity which is increased via phosphorylation by AMP-activated kinase (169,170). The increase in cholesterol synthesis in C4-2 SRBI-KD compared to NC cells 6 days after transfection indicates a need to perhaps compensate for the loss of cholesterol influx from SR-BI, resulting in the unchanged cholesterol levels that were observed (Fig. 18). Since this compensatory increase in synthesis was observed in parallel with decreased viability and unchanged cholesterol levels, it is possible that the increased synthesis was not only supplying membrane creation and proliferative requirements of the cell, but perhaps other cellular processes, such as the hypothesized androgen synthesis. The LNCaP cells did not display a similar increase in cholesterol synthesis in the SRBI-KD group at day 6 as compared to the NC cells. However, the total cholesterol in the LNCaP SRBI-KD at day 6 was lower than the NC group. Although this difference was not significant, the decreased cholesterol corresponds to the lack of compensatory up-regulation in cholesterol synthesis observed in the LNCaP cells.

The effect of SR-BI silencing on cholesterol metabolism was also explored. Cells with adequate intracellular cholesterol will store it as cholesteryl esters in lipid droplets, a process facilitated by ACAT-1 and ACAT-2 (Fig. 22). Alternatively, in times of cellular cholesterol requirement, HSL hydrolyzes the CE stores or incoming CEs at the cell surface to create free cholesterol for use by the cell (Fig. 22). Although no significant changes in the expression of either ACAT isoform were observed (Fig. 16A-D), HSL expression was significantly altered in the C4-2 cells. At day 3 and day 6, the SRBI-KD cells had significantly decreased HSL expression as compared to the NC group in C4-2 cells (Fig. 16E and F). A similar pattern was seen in the LNCaP cells at day 6 but was not statistically different. This finding is contrary to the premise that cholesterol need would be greater in response to reduced influx of cholesterol via SR-BI and thereby, HSL would have been expected to be up-regulated. However, the cholesterol levels in the cell did not change as a result of SR-BI silencing. Also, as mentioned, HSL expression has been linked to SR-BI expression and therefore SR-BI silencing may impact HSL expression due to their co-expressive tendencies (95). It is also possible, as hypothesized, that the loss of SR-BI caused a decrease in *de novo* androgen synthesis within these cells and consequently caused an attenuated hormone-induced expression of HSL.

5.4 SR-BI SILENCING-INDUCED EFFECTS ON PSA

SR-BI down-regulation had an impact on cell viability, cholesterol synthesis and the hormone-regulated enzyme, HSL, within the cells. Therefore, it was critical to determine if the effects would permeate to more terminal effectors such as the expression of stAR and AR and the levels of intracellular testosterone and PSA secretion. A major

link between cellular cholesterol and the androgen-androgen receptor signaling pathway is the transport of cholesterol into the mitochondria for potential biosynthetic creation of androgens; a process facilitated by stAR (Fig. 22) (16). No significant change in the expression of stAR was induced by SR-BI silencing, despite seemingly decreased stAR expression in the SRBI-KD groups in the C4-2 cells and increased stAR expression in the same group in LNCaP cells beyond day 3 (Fig. 21A and B).

After stAR shuttles cholesterol into the inner mitochondrial space it can be converted into androgens, one of which is testosterone. Intracellular testosterone concentrations were measured in order to reflect changes in androgen synthesis within the cell. Since the media did not contain detectable amounts of testosterone ($<.03\text{ng/mL}$) it was thought that any testosterone changes observed would be a reflection of intracellular processes rather than exogenous changes to the cell media environment. Intracellular testosterone concentrations were not affected by SR-BI silencing, with the exception of the SRBI-KD groups at day 3 in the C4-2 cells, which was significantly higher than the respective NC group (Fig 20). Although the testosterone levels in the both cell types decreased over time, the LNCaP cells had a spike in levels at day 1 in both treatment groups. Presumably, the passive diffusion of the minimal androgens present in the media would be equivalent in both cell types, therefore, this spike in testosterone likely reflects intracellular events, such as metabolism. As mentioned in the introduction, the mRNA and protein expression of steroid-5- α -reductase-1 (SRD5A1); the enzyme responsible for conversion of testosterone to DHT, are increased in CRPC (29,171). Therefore, if this is true in comparison between LNCaP and C4-2 cells, it is possible that DHT analysis or

SRD5A1 expression would give a more complete explanation of the testosterone differences observed.

Androgens, including testosterone, can bind to the AR and subsequently exert a number of transcriptional effects. AR expression was not significantly different between treatment groups in either cell line. However, the AR protein levels in the LNCaP cells, regardless of treatment group, appeared to increase with the time exposed to the steroid-depleted environment, with the exception of levels at day 1 (Fig. 21C and D) (136). AR expression is regulated in part by androgens. Although testosterone was the only androgen measured, its concentration appeared to decrease over time, which is in opposition to the increased AR expression observed in the LNCaP cells. These data are counter-intuitive, as it is commonly known that, not only is the AR stabilized by the presence of androgens, but also, androgens decrease transcription of AR mRNA (172,173). In addition, the half-life of the AR in LNCaP cells in the absence of androgens is approximately 3 hours in comparison to 7 hours in C4-2 cells. However, it has been found that the AR in LNCaP cells in the absence of androgens was predominantly detected in the cytoplasm, versus a nuclear translocation in a castration-resistant cell line (34). Therefore, it is possible that the technique used to lyse the cells may not fully extract nuclear protein. Therefore the observed expression reflected only the cytosolic fraction of AR and thereby, over-estimated the whole-cell AR expression. For future studies it may be important to determine the nuclear and cytosolic expression using an antibody directed to the C-terminal end of the AR. Alternatively, the spike in testosterone levels seen at day 1 in the LNCaP cells may have induced AR expression, a change that

manifested at day 3 and day 6.

A downstream indicator of androgenic regulation and AR activity commonly used as a clinical marker in CaP is prostate specific antigen (PSA) (23). As mentioned, androgens bind to the AR and this complex then translocates to the nucleus where it exerts a number of transcriptional programs, including PSA production (10,22). It has been debated whether PSA secretion in cell models directly translates to cell viability, however, PSA is a good indicator of the androgen-signaling pathway (174). PSA secretion in both the LNCaP and C4-2 SRBI-KD cells was significantly decreased, by 58% and 55%, compared to the NC groups, respectively (Fig. 19). This indicates that perturbation of SR-BI expression may impact AR activity. However, the protein expression of the AR did not significantly change in the SRBI-KD cells as compared to the NC cells in either cell line (Fig. 21C and D), possibly indicating that another mechanism may be contributing to the observed decrease in PSA.

5.5 SR-BI MEDIATED SIGNAL TRANSDUCTION

In addition to the transcriptional effects mentioned above, the AR may also exert non-transcriptional effects via interaction with other signaling cascades, specifically cross-reaction with mitogenic kinases (175-177). Signaling pathways that have been connected to AR activation appear to be particularly concentrated in lipid rafts (178,179). So too, it has been demonstrated that modulation of cholesterol content in the plasma membrane and consequently lipid raft functionality, reduced growth and PSA production by decreasing activity of the AR, an effect that was linked to suppression of Akt activation (180,181). Lipid raft and plasma membrane cholesterol content can be altered

by statins, as has been demonstrated in CaP, but also by SR-BI modulation (180,182,183). The lack of concrete changes in cellular cholesterol, testosterone and other downstream androgen-regulated proteins in the current study suggested that silencing SR-BI in CaP cells may be interrupting other pathways in addition to cholesterol influx. Interestingly, SR-BI has also been implicated in MAPK/ERK and PI3K/Akt signaling pathways whereby HDL, and not LDL, binding to SR-BI induces activation of PI3K, Akt and ERK (184-186). These findings may help explain the induction in CaP cell viability that was observed with the addition of HDL, but not LDL (Fig. 13C-D, Appendix E). Although there are many theories with regard to the specific role of SR-BI in signal transduction pathways, it appears that it may be due to the activation of Src (187). Src is a non-receptor tyrosine kinase that impacts downstream cellular events, including cell division and survival pathways, via PI3K phosphorylation (Fig. 23, adapted from (188)). Src activity is thought to be induced directly by SR-BI-mediated binding to HDL.

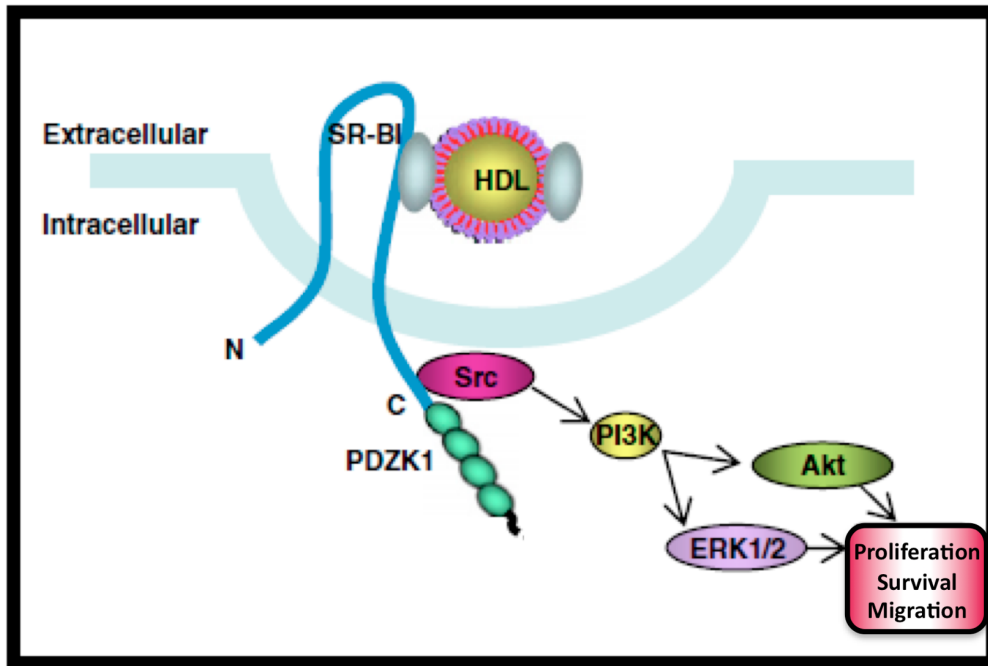


Figure 23: A depiction of one possible SR-BI-mediated effect on cell signaling pathways. Src is activated by SR-BI thereby eliciting downstream phosphorylation and consequent activation of ERK1/2 and Akt which then induce cellular events (adapted from (188)).

Furthermore, a reduction in cell signaling has been connected to the loss of SR-BI. Knockdown of SR-BI using siRNA and inhibition of SR-BI using an antibody resulted in decreased phosphorylation of Akt in fibroblasts and activation of Ras in Chinese hamster ovary cells, respectively (189,190). Although the effects of HDL and SR-BI-mediated signal transduction have not received much attention in CaP thus far, the observations herein that silencing SR-BI causes a reduction in cell viability and that HDL addition to NC cells improves cell viability are in agreement with the findings from other cell models discussed above. Thus, the knockdown of SR-BI may not only have reduced cholesterol influx but may have also affected cell signaling, which contributed to the decreased cell viability and PSA secretion observed. Future studies are required to determine the specific mechanisms underlying the SR-BI silencing-induced effects seen in C4-2 and

LNCaP cells.

5.6 LIMITATIONS OF CURRENT RESEARCH AND FUTURE STUDIES

The data suggest that silencing a cholesterol influx transporter has an effect on the PSA secretion of CaP cells. However, these findings were not reflected in testosterone levels, perhaps because changes occurred in one of the other androgens. Future studies examining multiple intracellular hormones including DHT, DHEA and progesterone using mass spectrometry may provide a more complete explanation of the aforementioned effects of SR-BI knockdown in CaP cells. This would be of particular importance if future work is completed using cell lines with the T877A mutated AR because it can interact with multiple androgens and androgen precursors.

Cholesterol homeostasis is complex; therefore, it may be important to assess gene expression in addition to protein and activity in future studies, so as to create a more complete profile of changes that occur. In addition, it was speculated that survival or anti-apoptotic pathways might have been affected by SR-BI silencing. Future studies should directly analyze apoptosis in the form of a TUNEL or PARP cleavage assay, in addition to phosphorylation of Akt and ERK, to determine if signal transduction pathways are affected.

It was found that cholesterol synthesis, via increased HMGCR activity, was a major compensatory measure initiated in C4-2 cells when SR-BI was silenced. In future studies it will be important to examine the effects of inhibiting cholesterol synthesis alone and in

concert with SR-BI silencing to determine if the effects are amplified. This may be of particular interest due to the prevalence of statin use in CaP patients.

Humans have a predominance of LDL in our circulation, as compared to rodents, which are predominantly HDL mammals. To determine if the LDL receptor has a more important role than SR-BI for provision of cholesterol, similar studies down-regulating the LDL receptor should be completed. Also, the effects on parameters, such as viability, PSA production and cholesterol concentration should be measured in response to lipoprotein treatment, as these data were not collected in the current work. In addition, cellular fractionation and subsequent cholesterol analysis may aid in determining fraction-specific effects on cholesterol.

The RNAi protocol that was used to complete all studies in this project involved a single dose of siRNA. Although this method produced persistent down-regulation of SR-BI protein expression, it may be important to investigate use of a multiple dosing procedure. A preliminary attempt at a dual-dosing SR-BI siRNA protocol and the subsequent effect on PSA and cell viability is shown in Appendix H. Should this work continue, it may be more appropriate to use this method. In addition, Kreiger *et al.* at Massachusetts Institute of Technology have developed a selective SR-BI inhibitor, called block lipid transport (BLT) (191). It may be useful to repeat the siRNA experiments using this inhibitor to determine if the same effects are observed, as an inhibitor would likely not change membrane morphology to the extent of siRNA. In addition, the specific impact on the activity of SR-BI and the mRNA expression should be examined, as

neither parameter was directly measured in the current project.

An examination of cholesterol pathways in other cell lines, such as PC-3 and VCaP, which have an absence of the AR and a wild-type AR, respectively, may provide further understanding of the link between cholesterol and the androgen-signaling pathway. Also, exploration of SR-BI in human tumour samples may help determine if the findings in a homogenous cell environment will have merit in the heterogeneous tissues.

5.7 CONCLUSIONS

In conclusion, it seems that silencing the expression of SR-BI in C4-2 cells reduces viability of these cells to a greater extent than LNCaP cells, a result that was complemented by a significantly decreased PSA secretion. This may reflect a greater reliance on the SR-BI transporter by C4-2 cells, an inference complemented by the finding that there was more SR-BI expressed basally in this cell type. These data provide support for the initial hypothesis. However, the PSA data in LNCaP cells suggest that, they too, were influenced by SR-BI down-regulation. Unfortunately, the lack of changes in cellular cholesterol concentrations and intracellular testosterone levels make it difficult to conclude that the growth effect is explicitly due to a lack of cholesterol provision to the *de novo* androgen synthesis pathway. However, the increase in cholesterol synthesis in the SR-BI silenced C4-2 cells indicates there is a need for compensatory supply of cholesterol to offset the attenuated influx. Furthermore, the addition of HDL, a substrate for SR-BI and known inducer of CaP cell growth, was not able to increase viability in SR-BI knockdown cells. These findings suggest that the loss of an SR-BI-mediated

mechanism; cholesterol influx or cell signaling, has affected not only compensatory cholesterol pathways, but also cell viability and downstream PSA secretion. This indicates that there may be a link between cholesterol influx and androgen-AR signaling. However, further exploration is necessary to determine if the observed effects were mediated by the loss of precursor for *de novo* androgen synthesis.

5.8 SIGNIFICANCE OF FINDINGS

The findings suggest that SR-BI silencing perturbs viability, PSA secretion and cholesterol synthesis of CaP cells, in particular the castration-resistant cell line, C4-2. Although further elucidation of the specific mechanism whereby SR-BI elicits these effects, it is possible that inhibiting the supply of cholesterol for *de novo* androgen synthesis or other cell needs, may be a novel point of therapeutic intervention alone or perhaps in combination with another therapy. There are very few treatments available for CRPC and even fewer that are effective. Therefore, exploration of any potential targets, such as cholesterol influx may be important for understanding the mechanisms of disease progression and the development of future therapies.

REFERENCES

1. Jemal A, Siegel R, Ward E, Hao Y, Xu J, Thun MJ. Cancer statistics, 2009. *CA Cancer J Clin* 2009;59(4):225-249.
2. Prostate Cancer Statistics, Canadian Cancer Society. 2009. Available from: <http://www.cancer.ca/canada-wide/about%20cancer/cancer%20statistics/stats%20at%20a%20glance/prostate%20cancer.aspx>
3. Prostate Cancer Statistics, Canadian Cancer Society. 2011. Available from: http://www.cancer.ca/Canada-wide/About%20cancer/Cancer%20statistics/Stats%20at%20a%20glance/Prostate%20cancer.aspx?sc_lang=en
4. Marrett LD, De P, Airia P, Dryer D. Cancer in Canada in 2008. *CMAJ* 2008;179(11):1163-1170.
5. Hsing AW, Chokkalingam AP. Prostate cancer epidemiology. *Front Biosci* 2006;11:1388-1413.
6. Feldman BJ, Feldman D. The development of androgen-independent prostate cancer. *Nat Rev Cancer* 2001;1(1):34-45.
7. Goldenberg SL, Gleave ME, Taylor D, Bruchovsky N. Clinical Experience with Intermittent Androgen Suppression in Prostate Cancer: Minimum of 3 Years' Follow-Up. *Mol Urol* 1999;3(3):287-292.
8. Schroder FH. Progress in understanding androgen-independent prostate cancer (AIPC): a review of potential endocrine-mediated mechanisms. *Eur Urol* 2008;53(6):1129-1137.
9. Greene DR, Fitzpatrick JM, Scardino PT. Anatomy of the prostate and distribution of early prostate cancer. *Semin Surg Oncol* 1995;11(1):9-22.
10. Srinivasan G, Campbell E, Bashirelahi N. Androgen, estrogen, and progesterone receptors in normal and aging prostates. *Microsc Res Tech* 1995;30(4):293-304.
11. Huggins C, Hodges CV. Studies on prostatic cancer. I. The effect of castration, of estrogen and of androgen injection on serum phosphatases in metastatic carcinoma of the prostate. 1941. *J Urol* 2002;167(2 Pt 2):948-951; discussion 952.

12. Locke JA, Nelson CC, Adomat HH, Hendy SC, Gleave ME, Guns ES. Steroidogenesis inhibitors alter but do not eliminate androgen synthesis mechanisms during progression to castration-resistance in LNCaP prostate xenografts. *J Steroid Biochem Mol Biol* 2009;115(3-5):126-136.
13. Miller WL, Auchus RJ. The molecular biology, biochemistry, and physiology of human steroidogenesis and its disorders. *Endocr Rev*;32(1):81-151.
14. Bartsch W, Klein H, Schiemann U, Bauer HW, Voigt KD. Enzymes of androgen formation and degradation in the human prostate. *Ann N Y Acad Sci* 1990;595:53-66.
15. Hales DB, Allen JA, Shankara T, Janus P, Buck S, Diemer T, Hales KH. Mitochondrial function in Leydig cell steroidogenesis. *Ann N Y Acad Sci* 2005;1061:120-134.
16. Miller WL. Steroidogenic acute regulatory protein (StAR), a novel mitochondrial cholesterol transporter. *Biochim Biophys Acta* 2007;1771(6):663-676.
17. Manna PR, Dyson MT, Stocco DM. Regulation of the steroidogenic acute regulatory protein gene expression: present and future perspectives. *Mol Hum Reprod* 2009;15(6):321-333.
18. Payne AH, Hales DB. Overview of steroidogenic enzymes in the pathway from cholesterol to active steroid hormones. *Endocr Rev* 2004;25(6):947-970.
19. Miller WL. Molecular biology of steroid hormone synthesis. *Endocr Rev* 1988;9(3):295-318.
20. Wright AS, Douglas RC, Thomas LN, Lazier CB, Rittmaster RS. Androgen-induced regrowth in the castrated rat ventral prostate: role of 5alpha-reductase. *Endocrinology* 1999;140(10):4509-4515.
21. Edwards J, Bartlett JM. The androgen receptor and signal-transduction pathways in hormone-refractory prostate cancer. Part 2: Androgen-receptor cofactors and bypass pathways. *BJU Int* 2005;95(9):1327-1335.
22. Rennie PS, Bruchovsky N, Goldenberg SL. Relationship of androgen receptors to the growth and regression of the prostate. *Am J Clin Oncol* 1988;11 Suppl 2:S13-17.
23. Kuriyama M. Prostate-specific antigen in prostate cancer. *Int J Biol Markers* 1986;1(2):67-76.

24. Schally AV, Andersen RN, Lipscomb HS, Long JM, Guillemin R. Evidence for the existence of two corticotrophin-releasing factors, alpha and beta. *Nature* 1960;188:192-193.
25. Thompson IM. Flare Associated with LHRH-Agonist Therapy. *Rev Urol* 2001;3 Suppl 3:S10-14.
26. Klotz L. Maximal androgen blockade for advanced prostate cancer. *Best Pract Res Clin Endocrinol Metab* 2008;22(2):331-340.
27. Mostaghel EA, Nelson PS. Intracrine androgen metabolism in prostate cancer progression: mechanisms of castration resistance and therapeutic implications. *Best Pract Res Clin Endocrinol Metab* 2008;22(2):243-258.
28. Montgomery RB, Mostaghel EA, Vessella R, Hess DL, Kalhorn TF, Higano CS, True LD, Nelson PS. Maintenance of intratumoral androgens in metastatic prostate cancer: a mechanism for castration-resistant tumor growth. *Cancer Res* 2008;68(11):4447-4454.
29. Locke JA, Guns ES, Lubik AA, Adomat HH, Hendy SC, Wood CA, Ettinger SL, Gleave ME, Nelson CC. Androgen levels increase by intratumoral de novo steroidogenesis during progression of castration-resistant prostate cancer. *Cancer Res* 2008;68(15):6407-6415.
30. Wako K, Kawasaki T, Yamana K, Suzuki K, Jiang S, Umezu H, Nishiyama T, Takahashi K, Hamakubo T, Kodama T, Naito M. Expression of androgen receptor through androgen-converting enzymes is associated with biological aggressiveness in prostate cancer. *J Clin Pathol* 2008;61(4):448-454.
31. Ryan CJ, Smith A, Lal P, Satagopan J, Reuter V, Scardino P, Gerald W, Scher HI. Persistent prostate-specific antigen expression after neoadjuvant androgen depletion: an early predictor of relapse or incomplete androgen suppression. *Urology* 2006;68(4):834-839.
32. Shiraishi S, Lee PW, Leung A, Goh VH, Swerdloff RS, Wang C. Simultaneous measurement of serum testosterone and dihydrotestosterone by liquid chromatography-tandem mass spectrometry. *Clin Chem* 2008;54(11):1855-1863.
33. So A, Gleave M, Hurtado-Col A, Nelson C. Mechanisms of the development of androgen independence in prostate cancer. *World J Urol* 2005;23(1):1-9.

34. Gregory CW, Johnson RT, Jr., Mohler JL, French FS, Wilson EM. Androgen receptor stabilization in recurrent prostate cancer is associated with hypersensitivity to low androgen. *Cancer Res* 2001;61(7):2892-2898.
35. Chen CD, Welsbie DS, Tran C, Baek SH, Chen R, Vessella R, Rosenfeld MG, Sawyers CL. Molecular determinants of resistance to antiandrogen therapy. *Nat Med* 2004;10(1):33-39.
36. van Weerden WM, van Steenbrugge GJ, van Kreuningen A, Moerings EP, De Jong FH, Schroder FH. Effects of low testosterone levels and of adrenal androgens on growth of prostate tumor models in nude mice. *J Steroid Biochem Mol Biol* 1990;37(6):903-907.
37. Mohler JL, Gregory CW, Ford OH, 3rd, Kim D, Weaver CM, Petrusz P, Wilson EM, French FS. The androgen axis in recurrent prostate cancer. *Clin Cancer Res* 2004;10(2):440-448.
38. Snoek R, Cheng H, Margiotti K, Wafa LA, Wong CA, Wong EC, Fazli L, Nelson CC, Gleave ME, Rennie PS. In vivo knockdown of the androgen receptor results in growth inhibition and regression of well-established, castration-resistant prostate tumors. *Clin Cancer Res* 2009;15(1):39-47.
39. Hofland J, van Weerden WM, Dits NF, Steenbergen J, van Leenders GJ, Jenster G, Schroder FH, de Jong FH. Evidence of limited contributions for intratumoral steroidogenesis in prostate cancer. *Cancer Res* 2010;70(3):1256-1264.
40. Stanbrough M, Bubley GJ, Ross K, Golub TR, Rubin MA, Penning TM, Febbo PG, Balk SP. Increased expression of genes converting adrenal androgens to testosterone in androgen-independent prostate cancer. *Cancer Res* 2006;66(5):2815-2825.
41. Seftel AD, Spirnak JP, Resnick MI. Hormonal therapy for advanced prostatic carcinoma. *J Surg Oncol Suppl* 1989;1:14-20.
42. Bhanalaph T, Varkarakis MJ, Murphy GP. Current status of bilateral adrenalectomy or advanced prostatic carcinoma. *Ann Surg* 1974;179(1):17-23.
43. Wu HC, Hsieh JT, Gleave ME, Brown NM, Pathak S, Chung LW. Derivation of androgen-independent human LNCaP prostatic cancer cell sublines: role of bone stromal cells. *Int J Cancer* 1994;57(3):406-412.
44. Chung LW. The role of stromal-epithelial interaction in normal and malignant growth. *Cancer Surv* 1995;23:33-42.

45. Waltering KK, Helenius MA, Sahu B, Manni V, Linja MJ, Janne OA, Visakorpi T. Increased expression of androgen receptor sensitizes prostate cancer cells to low levels of androgens. *Cancer Res* 2009;69(20):8141-8149.
46. Kaighn ME, Narayan KS, Ohnuki Y, Lechner JF, Jones LW. Establishment and characterization of a human prostatic carcinoma cell line (PC-3). *Invest Urol* 1979;17(1):16-23.
47. Mickey DD, Stone KR, Wunderli H, Mickey GH, Vollmer RT, Paulson DF. Heterotransplantation of a human prostatic adenocarcinoma cell line in nude mice. *Cancer Res* 1977;37(11):4049-4058.
48. Sato N, Gleave ME, Bruchovsky N, Rennie PS, Beraldi E, Sullivan LD. A metastatic and androgen-sensitive human prostate cancer model using intraprostatic inoculation of LNCaP cells in SCID mice. *Cancer Res* 1997;57(8):1584-1589.
49. Ettinger SL, Sobel R, Whitmore TG, Akbari M, Bradley DR, Gleave ME, Nelson CC. Dysregulation of sterol response element-binding proteins and downstream effectors in prostate cancer during progression to androgen independence. *Cancer Res* 2004;64(6):2212-2221.
50. Leon CG, Locke JA, Adomat HH, Ettinger SL, Twiddy AL, Neumann RD, Nelson CC, Guns ES, Wasan KM. Alterations in cholesterol regulation contribute to the production of intratumoral androgens during progression to castration-resistant prostate cancer in a mouse xenograft model. *Prostate* 2010;70(4):390-400.
51. Connolly JM, Coleman M, Rose DP. Effects of dietary fatty acids on DU145 human prostate cancer cell growth in athymic nude mice. *Nutr Cancer* 1997;29(2):114-119.
52. Wang Y, Corr JG, Thaler HT, Tao Y, Fair WR, Heston WD. Decreased growth of established human prostate LNCaP tumors in nude mice fed a low-fat diet. *J Natl Cancer Inst* 1995;87(19):1456-1462.
53. Ikonen E. Cellular cholesterol trafficking and compartmentalization. *Nat Rev Mol Cell Biol* 2008;9(2):125-138.
54. Hager MH, Solomon KR, Freeman MR. The role of cholesterol in prostate cancer. *Curr Opin Clin Nutr Metab Care* 2006;9(4):379-385.
55. Swyer G. The cholesterol content of normal and enlarged prostates. *Cancer Res* 1942;2:372-375.

56. Di Vizio D, Solomon KR, Freeman MR. Cholesterol and cholesterol-rich membranes in prostate cancer: an update. *Tumori* 2008;94(5):633-639.
57. Freeman MR, Solomon KR. Cholesterol and prostate cancer. *J Cell Biochem* 2004;91(1):54-69.
58. Jonas A. Biochemistry of Lipids, Lipoproteins and Membranes, 4th edition. In: Vance DE, Vance JE, editors: Elsevier; 2002. p 484-490.
59. Grosman H, Fabre B, Mesch V, Lopez MA, Schreier L, Mazza O, Berg G. Lipoproteins, sex hormones and inflammatory markers in association with prostate cancer. *Aging Male* 2009;13(2):87-92.
60. Laukkanen JA, Laaksonen DE, Niskanen L, Pukkala E, Hakkarainen A, Salonen JT. Metabolic syndrome and the risk of prostate cancer in Finnish men: a population-based study. *Cancer Epidemiol Biomarkers Prev* 2004;13(10):1646-1650.
61. Hsing AW, Gao YT, Chua S, Jr., Deng J, Stanczyk FZ. Insulin resistance and prostate cancer risk. *J Natl Cancer Inst* 2003;95(1):67-71.
62. Hsing AW, Devesa SS. Trends and patterns of prostate cancer: what do they suggest? *Epidemiol Rev* 2001;23(1):3-13.
63. Kolonel LN, Yoshizawa CN, Hankin JH. Diet and prostatic cancer: a case-control study in Hawaii. *Am J Epidemiol* 1988;127(5):999-1012.
64. Mettlin C, Selenskas S, Natarajan N, Huben R. Beta-carotene and animal fats and their relationship to prostate cancer risk. A case-control study. *Cancer* 1989;64(3):605-612.
65. Gronberg H. Prostate cancer epidemiology. *Lancet* 2003;361(9360):859-864.
66. Mondul AM, Clipp SL, Helzlsouer KJ, Platz EA. Association between plasma total cholesterol concentration and incident prostate cancer in the CLUE II cohort. *Cancer Causes Control* 2009;21(1):61-68.
67. Williams RR, Sorlie PD, Feinleib M, McNamara PM, Kannel WB, Dawber TR. Cancer incidence by levels of cholesterol. *JAMA* 1981;245(3):247-252.
68. Chyou PH, Nomura AM, Stemmermann GN, Kato I. Prospective study of serum cholesterol and site-specific cancers. *J Clin Epidemiol* 1992;45(3):287-292.

69. Hiatt RA, Fireman BH. Serum cholesterol and the incidence of cancer in a large cohort. *J Chronic Dis* 1986;39(11):861-870.
70. Fiorenza AM, Branchi A, Cardena A, Molgora M, Rovellini A, Sommariva D. Serum cholesterol levels in patients with cancer. Relationship with nutritional status. *Int J Clin Lab Res* 1996;26(1):37-42.
71. Derby CA, Zilber S, Brambilla D, Morales KH, McKinlay JB. Body mass index, waist circumference and waist to hip ratio and change in sex steroid hormones: the Massachusetts Male Ageing Study. *Clin Endocrinol (Oxf)* 2006;65(1):125-131.
72. Traish AM, Abdou R, Kypreos KE. Androgen deficiency and atherosclerosis: The lipid link. *Vascul Pharmacol* 2009;51(5-6):303-313.
73. Yannucci J, Manola J, Garnick MB, Bhat G, Bubley GJ. The effect of androgen deprivation therapy on fasting serum lipid and glucose parameters. *J Urol* 2006;176(2):520-525.
74. Usui S, Suzuki K, Yamanaka H, Nakano T, Nakajima K, Hara Y, Okazaki M. Estrogen treatment of prostate cancer increases triglycerides in lipoproteins as demonstrated by HPLC and immunoseparation techniques. *Clin Chim Acta* 2002;317(1-2):133-143.
75. Mohamedali HZ, Breunis H, Timilshina N, Alibhai SM. Changes in blood glucose and cholesterol levels due to androgen deprivation therapy in men with non-metastatic prostate cancer. *Can Urol Assoc J*;5(1):28-32.
76. Ahn J, Lim U, Weinstein SJ, Schatzkin A, Hayes RB, Virtamo J, Albanes D. Prediagnostic total and high-density lipoprotein cholesterol and risk of cancer. *Cancer Epidemiol Biomarkers Prev* 2009;18(11):2814-2821.
77. Sekine Y, Koike H, Nakano T, Nakajima K, Takahashi S, Suzuki K. Remnant lipoproteins induced proliferation of human prostate cancer cell, PC-3 but not LNCaP, via low density lipoprotein receptor. *Cancer Epidemiol* 2009;33(1):16-23.
78. Parinaud J, Perret B, Ribbes H, Chap H, Pontonnier G, Douste-Blazy L. High density lipoprotein and low density lipoprotein utilization by human granulosa cells for progesterone synthesis in serum-free culture: respective contributions of free and esterified cholesterol. *J Clin Endocrinol Metab* 1987;64(3):409-417.

79. Azhar S, Reaven E. Scavenger receptor class BI and selective cholesteryl ester uptake: partners in the regulation of steroidogenesis. *Mol Cell Endocrinol* 2002;195(1-2):1-26.
80. Enk L, Crona N, Hillensjo T. High- and low-density lipoproteins stimulate progesterone production in cultured human granulosa cells. *Hum Reprod* 1987;2(4):291-295.
81. Richardson MC, Davies DW, Watson RH, Dunsford ML, Inman CB, Masson GM. Cultured human granulosa cells as a model for corpus luteum function: relative roles of gonadotrophin and low density lipoprotein studied under defined culture conditions. *Hum Reprod* 1992;7(1):12-18.
82. Chang TY, Chang CC, Ohgami N, Yamauchi Y. Cholesterol sensing, trafficking, and esterification. *Annu Rev Cell Dev Biol* 2006;22:129-157.
83. Locke JA, Wasan KM, Nelson CC, Guns ES, Leon CG. Androgen-mediated cholesterol metabolism in LNCaP and PC-3 cell lines is regulated through two different isoforms of acyl-coenzyme A:Cholesterol Acyltransferase (ACAT). *Prostate* 2008;68(1):20-33.
84. Holzbeierlein J, Lal P, LaTulippe E, Smith A, Satagopan J, Zhang L, Ryan C, Smith S, Scher H, Scardino P, Reuter V, Gerald WL. Gene expression analysis of human prostate carcinoma during hormonal therapy identifies androgen-responsive genes and mechanisms of therapy resistance. *Am J Pathol* 2004;164(1):217-227.
85. Swinnen JV, Heemers H, van de Sande T, de Schrijver E, Brusselmans K, Heyns W, Verhoeven G. Androgens, lipogenesis and prostate cancer. *J Steroid Biochem Mol Biol* 2004;92(4):273-279.
86. Kraemer FB, Shen WJ, Patel S, Osuga J, Ishibashi S, Azhar S. The LDL receptor is not necessary for acute adrenal steroidogenesis in mouse adrenocortical cells. *Am J Physiol Endocrinol Metab* 2007;292(2):E408-412.
87. Lee MY, Moon JS, Park SW, Koh YK, Ahn YH, Kim KS. KLF5 enhances SREBP-1 action in androgen-dependent induction of fatty acid synthase in prostate cancer cells. *Biochem J* 2009;417(1):313-322.
88. Chen Y, Hughes-Fulford M. Human prostate cancer cells lack feedback regulation of low-density lipoprotein receptor and its regulator, SREBP2. *Int J Cancer* 2001;91(1):41-45.

89. Krycer JR, Kristiana I, Brown AJ. Cholesterol homeostasis in two commonly used human prostate cancer cell-lines, LNCaP and PC-3. *PLoS One* 2009;4(12):e8496.
90. Solomon KR, Freeman MR. Do the cholesterol-lowering properties of statins affect cancer risk? *Trends Endocrinol Metab* 2008;19(4):113-121.
91. Chang TY, Li BL, Chang CC, Urano Y. Acyl-coenzyme A:cholesterol acyltransferases. *Am J Physiol Endocrinol Metab* 2009;297(1):E1-9.
92. Accad M, Smith SJ, Newland DL, Sanan DA, King LE, Jr., Linton MF, Fazio S, Farese RV, Jr. Massive xanthomatosis and altered composition of atherosclerotic lesions in hyperlipidemic mice lacking acyl CoA:cholesterol acyltransferase 1. *J Clin Invest* 2000;105(6):711-719.
93. Repa JJ, Buhman KK, Farese RV, Jr., Dietschy JM, Turley SD. ACAT2 deficiency limits cholesterol absorption in the cholesterol-fed mouse: impact on hepatic cholesterol homeostasis. *Hepatology* 2004;40(5):1088-1097.
94. Connelly MA. SR-BI-mediated HDL cholesteryl ester delivery in the adrenal gland. *Mol Cell Endocrinol* 2009;300(1-2):83-88.
95. Kraemer FB, Shen WJ, Harada K, Patel S, Osuga J, Ishibashi S, Azhar S. Hormone-sensitive lipase is required for high-density lipoprotein cholesteryl ester-supported adrenal steroidogenesis. *Mol Endocrinol* 2004;18(3):549-557.
96. Locke JA, Guns ES, Lehman ML, Ettinger S, Zoubeidi A, Lubik A, Margiotti K, Fazli L, Adomat H, Wasan KM, Gleave ME, Nelson CC. Arachidonic acid activation of intratumoral steroid synthesis during prostate cancer progression to castration resistance. *Prostate* 2009;70(3):239-251.
97. Klappe K, Hummel I, Hoekstra D, Kok JW. Lipid dependence of ABC transporter localization and function. *Chem Phys Lipids* 2009;161(2):57-64.
98. Oram JF, Lawn RM. ABCA1. The gatekeeper for eliminating excess tissue cholesterol. *J Lipid Res* 2001;42(8):1173-1179.
99. Fukuchi J, Hiipakka RA, Kokontis JM, Hsu S, Ko AL, Fitzgerald ML, Liao S. Androgenic suppression of ATP-binding cassette transporter A1 expression in LNCaP human prostate cancer cells. *Cancer Res* 2004;64(21):7682-7685.

100. Ni J, Pang ST, Yeh S. Differential retention of alpha-vitamin E is correlated with its transporter gene expression and growth inhibition efficacy in prostate cancer cells. *Prostate* 2007;67(5):463-471.
101. Brown MS, Goldstein JL. A receptor-mediated pathway for cholesterol homeostasis. *Science* 1986;232(4746):34-47.
102. Calvo D, Vega MA. Identification, primary structure, and distribution of CLA-1, a novel member of the CD36/LIMPII gene family. *J Biol Chem* 1993;268(25):18929-18935.
103. Rhainds D, Brissette L. The role of scavenger receptor class B type I (SR-BI) in lipid trafficking. defining the rules for lipid traders. *Int J Biochem Cell Biol* 2004;36(1):39-77.
104. Saddar S, Mineo C, Shaul PW. Signaling by the high-affinity HDL receptor scavenger receptor B type I. *Arterioscler Thromb Vasc Biol* 2010;30(2):144-150.
105. Krieger M. Charting the fate of the "good cholesterol": identification and characterization of the high-density lipoprotein receptor SR-BI. *Annu Rev Biochem* 1999;68:523-558.
106. Reaven E, Lua Y, Nomoto A, Temel R, Williams DL, van der Westhuyzen DR, Azhar S. The selective pathway and a high-density lipoprotein receptor (SR-BI) in ovarian granulosa cells of the mouse. *Biochim Biophys Acta* 1999;1436(3):565-576.
107. Zimetti F, Weibel GK, Duong M, Rothblat GH. Measurement of cholesterol bidirectional flux between cells and lipoproteins. *J Lipid Res* 2006;47(3):605-613.
108. Dietschy JM, Turley SD. Control of cholesterol turnover in the mouse. *J Biol Chem* 2002;277(6):3801-3804.
109. Galman C, Angelin B, Rudling M. Prolonged stimulation of the adrenals by corticotropin suppresses hepatic low-density lipoprotein and high-density lipoprotein receptors and increases plasma cholesterol. *Endocrinology* 2002;143(5):1809-1816.
110. Connelly MA, Williams DL. SR-BI and HDL cholesteryl ester metabolism. *Endocr Res* 2004;30(4):697-703.

111. Trigatti BL, Krieger M, Rigotti A. Influence of the HDL receptor SR-BI on lipoprotein metabolism and atherosclerosis. *Arterioscler Thromb Vasc Biol* 2003;23(10):1732-1738.
112. Rhainds D, Bourgeois P, Bourret G, Huard K, Falstraalt L, Brissette L. Localization and regulation of SR-BI in membrane rafts of HepG2 cells. *J Cell Sci* 2004;117(Pt 15):3095-3105.
113. Gu X, Kozarsky K, Krieger M. Scavenger receptor class B, type I-mediated [3H]cholesterol efflux to high and low density lipoproteins is dependent on lipoprotein binding to the receptor. *J Biol Chem* 2000;275(39):29993-30001.
114. Plump AS, Erickson SK, Weng W, Partin JS, Breslow JL, Williams DL. Apolipoprotein A-I is required for cholesteryl ester accumulation in steroidogenic cells and for normal adrenal steroid production. *J Clin Invest* 1996;97(11):2660-2671.
115. Hersberger M, von Eckardstein A. Low high-density lipoprotein cholesterol: physiological background, clinical importance and drug treatment. *Drugs* 2003;63(18):1907-1945.
116. McConathy WJ, Nair MP, Paranjape S, Mooberry L, Lacko AG. Evaluation of synthetic/reconstituted high-density lipoproteins as delivery vehicles for paclitaxel. *Anticancer Drugs* 2008;19(2):183-188.
117. Mooberry LK, Nair M, Paranjape S, McConathy WJ, Lacko AG. Receptor mediated uptake of paclitaxel from a synthetic high density lipoprotein nanocarrier. *J Drug Target* 2009;18(1):53-58.
118. Lopez D, McLean MP. Estrogen regulation of the scavenger receptor class B gene: Anti-atherogenic or steroidogenic, is there a priority? *Mol Cell Endocrinol* 2006;247(1-2):22-33.
119. Chiba-Falek O, Nichols M, Suchindran S, Guyton J, Ginsburg GS, Barrett-Connor E, McCarthy JJ. Impact of gene variants on sex-specific regulation of human Scavenger receptor class B type 1 (SR-BI) expression in liver and association with lipid levels in a population-based study. *BMC Med Genet* 2010;11:9.
120. Bush TL, Fried LP, Barrett-Connor E. Cholesterol, lipoproteins, and coronary heart disease in women. *Clin Chem* 1988;34(8B):B60-70.

121. Hoekstra M, Ye D, Hildebrand RB, Zhao Y, Lammers B, Stitzinger M, Kuiper J, Van Berkel TJ, Van Eck M. Scavenger receptor class B type I-mediated uptake of serum cholesterol is essential for optimal adrenal glucocorticoid production. *J Lipid Res* 2009;50(6):1039-1046.
122. Pussinen PJ, Karten B, Wintersperger A, Reicher H, McLean M, Malle E, Sattler W. The human breast carcinoma cell line HBL-100 acquires exogenous cholesterol from high-density lipoprotein via CLA-1 (CD-36 and LIMPII analogous 1)-mediated selective cholesteryl ester uptake. *Biochem J* 2000;349(Pt 2):559-566.
123. Risbridger GP, Davis ID, Birrell SN, Tilley WD. Breast and prostate cancer: more similar than different. *Nat Rev Cancer* 2010;10(3):205-212.
124. Reaven E, Nomoto A, Cortez Y, Azhar S. Consequences of over-expression of rat Scavenger Receptor, SR-BI, in an adrenal cell model. *Nutr Metab (Lond)* 2006;3:43.
125. Tannock IF, de Wit R, Berry WR, Horti J, Pluzanska A, Chi KN, Oudard S, Theodore C, James ND, Turesson I, Rosenthal MA, Eisenberger MA. Docetaxel plus prednisone or mitoxantrone plus prednisone for advanced prostate cancer. *N Engl J Med* 2004;351(15):1502-1512.
126. Cho D, Di Blasio CJ, Rhee AC, Kattan MW. Prognostic factors for survival in patients with hormone-refractory prostate cancer (HRPC) after initial androgen deprivation therapy (ADT). *Urol Oncol* 2003;21(4):282-291.
127. Lattouf JB, Srinivasan R, Pinto PA, Linehan WM, Neckers L. Mechanisms of disease: the role of heat-shock protein 90 in genitourinary malignancy. *Nat Clin Pract Urol* 2006;3(11):590-601.
128. Mostaghel EA, Geng L, Holcomb I, Coleman IM, Lucas J, True LD, Nelson PS. Variability in the androgen response of prostate epithelium to 5alpha-reductase inhibition: implications for prostate cancer chemoprevention. *Cancer Res* 2010;70(4):1286-1295.
129. Taichman RS, Loberg RD, Mehra R, Pienta KJ. The evolving biology and treatment of prostate cancer. *J Clin Invest* 2007;117(9):2351-2361.
130. Heath EI, Hillman DW, Vaishampayan U, Sheng S, Sarkar F, Harper F, Gaskins M, Pitot HC, Tan W, Ivy SP, Pili R, Carducci MA, Erlichman C, Liu G. A phase II trial of 17-allylamino-17-demethoxygeldanamycin in patients with hormone-refractory metastatic prostate cancer. *Clin Cancer Res* 2008;14(23):7940-7946.

131. Attard G, Reid AH, Yap TA, Raynaud F, Dowsett M, Settatre S, Barrett M, Parker C, Martins V, Folkerd E, Clark J, Cooper CS, Kaye SB, Dearnaley D, Lee G, de Bono JS. Phase I clinical trial of a selective inhibitor of CYP17, abiraterone acetate, confirms that castration-resistant prostate cancer commonly remains hormone driven. *J Clin Oncol* 2008;26(28):4563-4571.
132. Reid AH, Attard G, Danila DC, Oommen NB, Olmos D, Fong PC, Molife LR, Hunt J, Messiou C, Parker C, Dearnaley D, Swennenhuis JF, Terstappen LW, Lee G, Kheoh T, Molina A, Ryan CJ, Small E, Scher HI, de Bono JS. Significant and sustained antitumor activity in post-docetaxel, castration-resistant prostate cancer with the CYP17 inhibitor abiraterone acetate. *J Clin Oncol*;28(9):1489-1495.
133. Danila DC, Morris MJ, de Bono JS, Ryan CJ, Denmeade SR, Smith MR, Taplin ME, Bubley GJ, Kheoh T, Haqq C, Molina A, Anand A, Koscuiskza M, Larson SM, Schwartz LH, Fleisher M, Scher HI. Phase II multicenter study of abiraterone acetate plus prednisone therapy in patients with docetaxel-treated castration-resistant prostate cancer. *J Clin Oncol*;28(9):1496-1501.
134. Scher HI, Beer TM, Higano CS, Anand A, Taplin ME, Efstathiou E, Rathkopf D, Shelkey J, Yu EY, Alumkal J, Hung D, Hirmand M, Seely L, Morris MJ, Danila DC, Humm J, Larson S, Fleisher M, Sawyers CL. Antitumour activity of MDV3100 in castration-resistant prostate cancer: a phase 1-2 study. *Lancet*;375(9724):1437-1446.
135. Culig Z, Comuzzi B, Steiner H, Bartsch G, Hobisch A. Expression and function of androgen receptor coactivators in prostate cancer. *J Steroid Biochem Mol Biol* 2004;92(4):265-271.
136. Culig Z, Hoffmann J, Erdel M, Eder IE, Hobisch A, Hittmair A, Bartsch G, Utermann G, Schneider MR, Parczyk K, Klocker H. Switch from antagonist to agonist of the androgen receptor bicalutamide is associated with prostate tumour progression in a new model system. *Br J Cancer* 1999;81(2):242-251.
137. Culig Z, Klocker H, Bartsch G, Hobisch A. Androgen receptor mutations in carcinoma of the prostate: significance for endocrine therapy. *Am J Pharmacogenomics* 2001;1(4):241-249.
138. Hobisch A, Hoffmann J, Lambrinidis L, Eder IE, Bartsch G, Klocker H, Culig Z. Antagonist/agonist balance of the nonsteroidal antiandrogen bicalutamide (Casodex) in a new prostate cancer model. *Urol Int* 2000;65(2):73-79.
139. Taplin ME, Bubley GJ, Ko YJ, Small EJ, Upton M, Rajeshkumar B, Balk SP. Selection for androgen receptor mutations in prostate cancers treated with androgen antagonist. *Cancer Res* 1999;59(11):2511-2515.

140. Taplin ME, Rajeshkumar B, Halabi S, Werner CP, Woda BA, Picus J, Stadler W, Hayes DF, Kantoff PW, Vogelzang NJ, Small EJ. Androgen receptor mutations in androgen-independent prostate cancer: Cancer and Leukemia Group B Study 9663. *J Clin Oncol* 2003;21(14):2673-2678.
141. Proia DA, Foley KP, Korbut T, Sang J, Smith D, Bates RC, Liu Y, Rosenberg AF, Zhou D, Koya K, Barsoum J, Blackman RK. Multifaceted intervention by the Hsp90 inhibitor ganetespib (STA-9090) in cancer cells with activated JAK/STAT signaling. *PLoS One*;6(4):e18552.
142. Yap TA, Zivi A, Omlin A, de Bono JS. The changing therapeutic landscape of castration-resistant prostate cancer. *Nat Rev Clin Oncol*;8(10):597-610.
143. Gotto AM, Jr. Management of dyslipidemia. *Am J Med* 2002;112 Suppl 8A:10S-18S.
144. Murtola TJ, Visakorpi T, Lahtela J, Syvala H, Tammela T. Statins and prostate cancer prevention: where we are now, and future directions. *Nat Clin Pract Urol* 2008;5(7):376-387.
145. Mener DJ, Cambio A, Stoddard DG, Martin BA, Palapattu GS. The impact of HMG-CoA reductase therapy on serum PSA. *Prostate* 2009;70(6):608-615.
146. Graaf MR, Beiderbeck AB, Egberts AC, Richel DJ, Guchelaar HJ. The risk of cancer in users of statins. *J Clin Oncol* 2004;22(12):2388-2394.
147. Seo YK, Zhu B, Jeon TI, Osborne TF. Regulation of steroid 5-alpha reductase type 2 (Srd5a2) by sterol regulatory element binding proteins and statin. *Exp Cell Res* 2009;315(18):3133-3139.
148. Platz EA, Till C, Goodman PJ, Parnes HL, Figg WD, Albanes D, Neuhaus ML, Klein EA, Thompson IM, Jr., Kristal AR. Men with low serum cholesterol have a lower risk of high-grade prostate cancer in the placebo arm of the prostate cancer prevention trial. *Cancer Epidemiol Biomarkers Prev* 2009;18(11):2807-2813.
149. Hoque A, Chen H, Xu XC. Statin induces apoptosis and cell growth arrest in prostate cancer cells. *Cancer Epidemiol Biomarkers Prev* 2008;17(1):88-94.
150. Zheng X, Cui XX, Avila GE, Huang MT, Liu Y, Patel J, Kong AN, Paulino R, Shih WJ, Lin Y, Rabson AB, Reddy BS, Conney AH. Atorvastatin and celecoxib inhibit prostate PC-3 tumors in immunodeficient mice. *Clin Cancer Res* 2007;13(18 Pt 1):5480-5487.

151. Parikh A, Childress C, Deitrick K, Lin Q, Rukstalis D, Yang W. Statin-induced autophagy by inhibition of geranylgeranyl biosynthesis in prostate cancer PC3 cells. *Prostate*;70(9):971-981.
152. Zhao M, Yang H, Jiang X, Zhou W, Zhu B, Zeng Y, Yao K, Ren C. Lipofectamine RNAiMAX: an efficient siRNA transfection reagent in human embryonic stem cells. *Mol Biotechnol* 2008;40(1):19-26.
153. Sachs-Barrable K, Thamboo A, Lee SD, Wasan KM. Lipid excipients Peceol and Gelucire 44/14 decrease P-glycoprotein mediated efflux of rhodamine 123 partially due to modifying P-glycoprotein protein expression within Caco-2 cells. *J Pharm Pharm Sci* 2007;10(3):319-331.
154. Towbin H, Staehelin T, Gordon J. Electrophoretic transfer of proteins from polyacrylamide gels to nitrocellulose sheets: procedure and some applications. *Proc Natl Acad Sci U S A* 1979;76(9):4350-4354.
155. Bligh EG, Dyer WJ. A rapid method of total lipid extraction and purification. *Can J Biochem Physiol* 1959;37(8):911-917.
156. Twiddy AL, Leon CG, Wasan KM. Cholesterol as a potential target for castration-resistant prostate cancer. *Pharm Res*;28(3):423-437.
157. Thalmann GN, Sikes RA, Chang SM, Johnston DA, von Eschenbach AC, Chung LW. Suramin-induced decrease in prostate-specific antigen expression with no effect on tumor growth in the LNCaP model of human prostate cancer. *J Natl Cancer Inst* 1996;88(12):794-801.
158. Sherwood ER, Berg LA, Mitchell NJ, McNeal JE, Kozlowski JM, Lee C. Differential cytokeratin expression in normal, hyperplastic and malignant epithelial cells from human prostate. *J Urol* 1990;143(1):167-171.
159. Zhao XY, Malloy PJ, Krishnan AV, Swami S, Navone NM, Peehl DM, Feldman D. Glucocorticoids can promote androgen-independent growth of prostate cancer cells through a mutated androgen receptor. *Nat Med* 2000;6(6):703-706.
160. Wang C, Young WJ, Chang C. Isolation and characterization of the androgen receptor mutants with divergent transcriptional activity in response to hydroxyflutamide. *Endocrine* 2000;12(1):69-76.
161. Langer C, Gansz B, Goepfert C, Engel T, Uehara Y, von Dehn G, Jansen H, Assmann G, von Eckardstein A. Testosterone up-regulates scavenger receptor BI

- and stimulates cholesterol efflux from macrophages. *Biochem Biophys Res Commun* 2002;296(5):1051-1057.
162. Langfort J, Jagsz S, Dobrzyn P, Brzezinska Z, Klapcinska B, Galbo H, Gorski J. Testosterone affects hormone-sensitive lipase (HSL) activity and lipid metabolism in the left ventricle. *Biochem Biophys Res Commun*;399(4):670-676.
 163. Pal A, Ahmad A, Khan S, Sakabe I, Zhang C, Kasid UN, Ahmad I. Systemic delivery of RafsiRNA using cationic cardiolipin liposomes silences Raf-1 expression and inhibits tumor growth in xenograft model of human prostate cancer. *Int J Oncol* 2005;26(4):1087-1091.
 164. Aleku M, Schulz P, Keil O, Santel A, Schaeper U, Dieckhoff B, Janke O, Endruschat J, Durieux B, Roder N, Loffler K, Lange C, Fechtner M, Mopert K, Fisch G, Dames S, Arnold W, Jochims K, Giese K, Wiedenmann B, Scholz A, Kaufmann J. Atu027, a liposomal small interfering RNA formulation targeting protein kinase N3, inhibits cancer progression. *Cancer Res* 2008;68(23):9788-9798.
 165. Bisanz K, Yu J, Edlund M, Spohn B, Hung MC, Chung LW, Hsieh CL. Targeting ECM-integrin interaction with liposome-encapsulated small interfering RNAs inhibits the growth of human prostate cancer in a bone xenograft imaging model. *Mol Ther* 2005;12(4):634-643.
 166. Kolmakova A, Wang J, Brogan R, Chaffin C, Rodriguez A. Deficiency of scavenger receptor class B type I negatively affects progesterone secretion in human granulosa cells. *Endocrinology*;151(11):5519-5527.
 167. Sekine Y, Demosky SJ, Stonik JA, Furuya Y, Koike H, Suzuki K, Remaley AT. High-density lipoprotein induces proliferation and migration of human prostate androgen-independent cancer cells by an ABCA1-dependent mechanism. *Mol Cancer Res*;8(9):1284-1294.
 168. Weyermann J, Lochmann D, Zimmer A. A practical note on the use of cytotoxicity assays. *Int J Pharm* 2005;288(2):369-376.
 169. Brown MS, Goldstein JL, Dietschy JM. Active and inactive forms of 3-hydroxy-3-methylglutaryl coenzyme A reductase in the liver of the rat. Comparison with the rate of cholesterol synthesis in different physiological states. *J Biol Chem* 1979;254(12):5144-5149.
 170. Hardie DG. Minireview: the AMP-activated protein kinase cascade: the key sensor of cellular energy status. *Endocrinology* 2003;144(12):5179-5183.

171. Mostaghel EA, Page ST, Lin DW, Fazli L, Coleman IM, True LD, Knudsen B, Hess DL, Nelson CC, Matsumoto AM, Bremner WJ, Gleave ME, Nelson PS. Intraprostatic androgens and androgen-regulated gene expression persist after testosterone suppression: therapeutic implications for castration-resistant prostate cancer. *Cancer Res* 2007;67(10):5033-5041.
172. Yeap BB, Krueger RG, Leedman PJ. Differential posttranscriptional regulation of androgen receptor gene expression by androgen in prostate and breast cancer cells. *Endocrinology* 1999;140(7):3282-3291.
173. Tyagi RK, Lavrovsky Y, Ahn SC, Song CS, Chatterjee B, Roy AK. Dynamics of intracellular movement and nucleocytoplasmic recycling of the ligand-activated androgen receptor in living cells. *Mol Endocrinol* 2000;14(8):1162-1174.
174. Bilhartz DL, Tindall DJ, Oesterling JE. Prostate-specific antigen and prostatic acid phosphatase: biomolecular and physiologic characteristics. *Urology* 1991;38(2):95-102.
175. Bonaccorsi L, Nosi D, Quercioli F, Formigli L, Zecchi S, Maggi M, Forti G, Baldi E. Prostate cancer: a model of integration of genomic and non-genomic effects of the androgen receptor in cell lines model. *Steroids* 2008;73(9-10):1030-1037.
176. Cinar B, Mukhopadhyay NK, Meng G, Freeman MR. Phosphoinositide 3-kinase-independent non-genomic signals transit from the androgen receptor to Akt1 in membrane raft microdomains. *J Biol Chem* 2007;282(40):29584-29593.
177. Hakariya T, Shida Y, Sakai H, Kanetake H, Igawa T. EGFR signaling pathway negatively regulates PSA expression and secretion via the PI3K-Akt pathway in LNCaP prostate cancer cells. *Biochem Biophys Res Commun* 2006;342(1):92-100.
178. Kawamura S, Sato I, Wada T, Yamaguchi K, Li Y, Li D, Zhao X, Ueno S, Aoki H, Tochigi T, Kuwahara M, Kitamura T, Takahashi K, Moriya S, Miyagi T. Plasma membrane-associated sialidase (NEU3) regulates progression of prostate cancer to androgen-independent growth through modulation of androgen receptor signaling. *Cell Death Differ*.
179. Yang L, Egger M, Plattner R, Klocker H, Eder IE. Lovastatin causes diminished PSA secretion by inhibiting AR expression and function in LNCaP prostate cancer cells. *Urology*;77(6):1508 e1501-1507.
180. Hamed H, Mitchell C, Park MA, Hanna D, Martin AP, Harrison B, Hawkins W, Curiel DA, Fisher PB, Grant S, Yacoub A, Hagan MP, Dent P. Human chorionic

- gonadotropin (hCG) interacts with lovastatin and ionizing radiation to modulate prostate cancer cell viability in vivo. *Cancer Biol Ther* 2008;7(4):587-593.
181. Oh HY, Leem J, Yoon SJ, Yoon S, Hong SJ. Lipid raft cholesterol and genistein inhibit the cell viability of prostate cancer cells via the partial contribution of EGFR-Akt/p70S6k pathway and down-regulation of androgen receptor. *Biochem Biophys Res Commun*;393(2):319-324.
 182. Reaven E, Leers-Sucheta S, Nomoto A, Azhar S. Expression of scavenger receptor class B type 1 (SR-BI) promotes microvillar channel formation and selective cholesteryl ester transport in a heterologous reconstituted system. *Proc Natl Acad Sci U S A* 2001;98(4):1613-1618.
 183. Kellner-Weibel G, de La Llera-Moya M, Connelly MA, Stoudt G, Christian AE, Haynes MP, Williams DL, Rothblat GH. Expression of scavenger receptor BI in COS-7 cells alters cholesterol content and distribution. *Biochemistry* 2000;39(1):221-229.
 184. Grewal T, de Diego I, Kirchhoff MF, Tebar F, Heeren J, Rinninger F, Enrich C. High density lipoprotein-induced signaling of the MAPK pathway involves scavenger receptor type BI-mediated activation of Ras. *J Biol Chem* 2003;278(19):16478-16481.
 185. Zhang Y, Ahmed AM, McFarlane N, Capone C, Boreham DR, Truant R, Igdoura SA, Trigatti BL. Regulation of SR-BI-mediated selective lipid uptake in Chinese hamster ovary-derived cells by protein kinase signaling pathways. *J Lipid Res* 2007;48(2):405-416.
 186. Mineo C, Yuhanna IS, Quon MJ, Shaul PW. High density lipoprotein-induced endothelial nitric-oxide synthase activation is mediated by Akt and MAP kinases. *J Biol Chem* 2003;278(11):9142-9149.
 187. Zhu W, Saddar S, Seetharam D, Chambliss KL, Longoria C, Silver DL, Yuhanna IS, Shaul PW, Mineo C. The scavenger receptor class B type I adaptor protein PDZK1 maintains endothelial monolayer integrity. *Circ Res* 2008;102(4):480-487.
 188. Al-Jarallah A, Trigatti BL. A role for the scavenger receptor, class B type I in high density lipoprotein dependent activation of cellular signaling pathways. *Biochim Biophys Acta*;1801(12):1239-1248.
 189. Rentero C, Evans R, Wood P, Tebar F, Vila de Muga S, Cubells L, de Diego I, Hayes TE, Hughes WE, Pol A, Rye KA, Enrich C, Grewal T. Inhibition of H-Ras

- and MAPK is compensated by PKC-dependent pathways in annexin A6 expressing cells. *Cell Signal* 2006;18(7):1006-1016.
190. Zhang Q, Zhang Y, Feng H, Guo R, Jin L, Wan R, Wang L, Chen C, Li S. High Density Lipoprotein (HDL) Promotes Glucose Uptake in Adipocytes and Glycogen Synthesis in Muscle Cells. *PLoS One*;6(8):e23556.
 191. Nieland TJ, Penman M, Dori L, Krieger M, Kirchhausen T. Discovery of chemical inhibitors of the selective transfer of lipids mediated by the HDL receptor SR-BI. *Proc Natl Acad Sci U S A* 2002;99(24):15422-15427.

APPENDICES

APPENDIX A: PROTEIN CONTENT IN CELL LINES

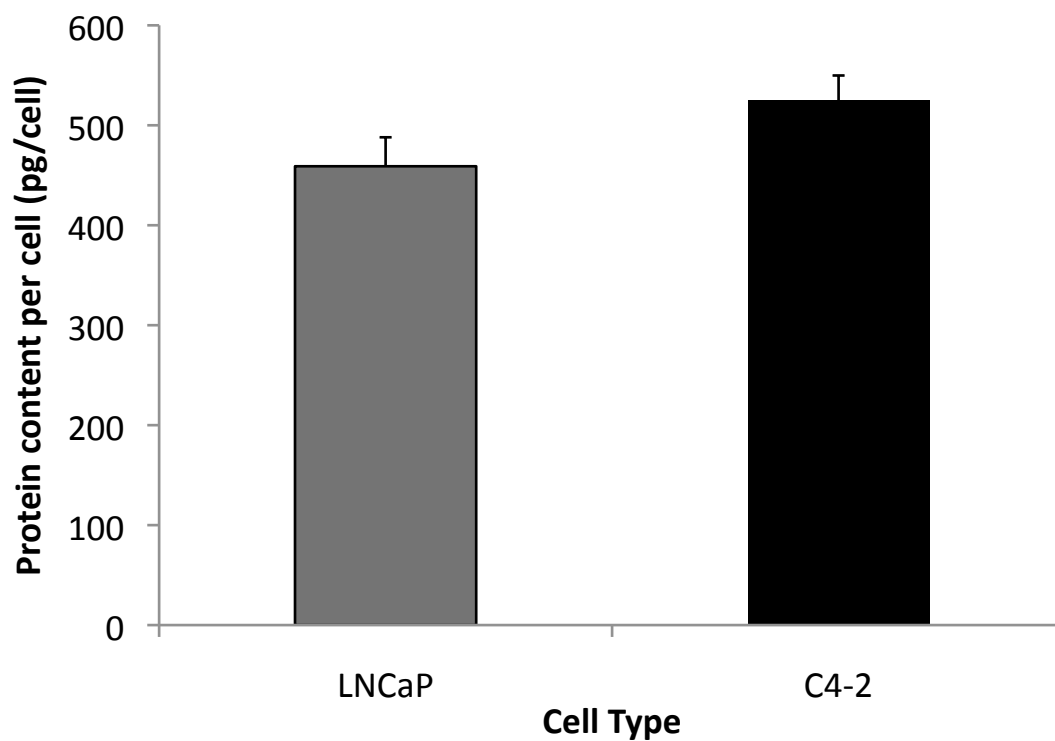


Figure A: Picograms of protein per cell; LNCaP (grey column) and C4-2 (black column). Columns, mean (n=3); bars, +/- SEM.

APPENDIX B: SIRNA METHOD DEVELOPMENT

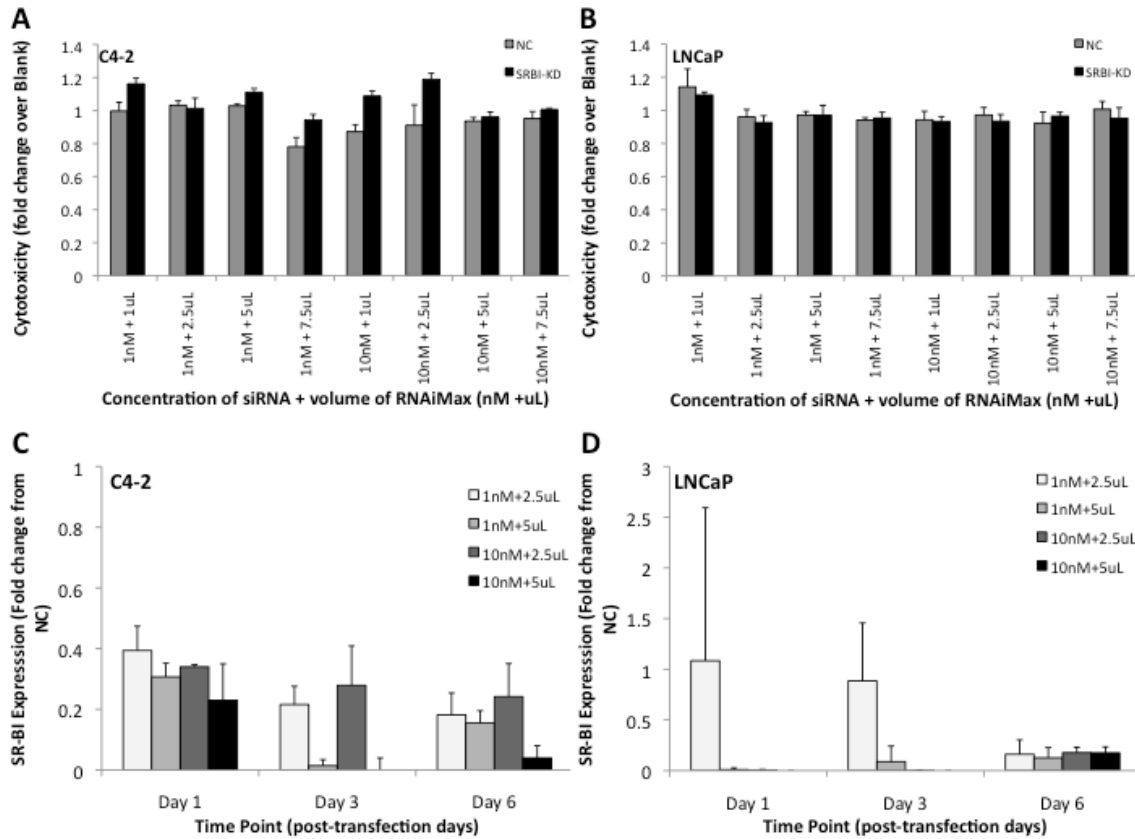


Figure B. A-D: Cell cytotoxicity is displayed in C4-2 (A) and LNCaP (B) cells treated with 1 and 10nM final concentration of negative control (NC, grey columns) and SR-BI (SRBI-KD, black columns) siRNA with 1-7.5 μ L of RNAiMax; a cationic delivery system. Values are expressed as fold change in LDH release (cytotoxicity) from an untreated control group. The lowest cytotoxic dose with the least difference between NC and SRBI-KD (1 or 10nM siRNA + 2.5 or 5.0 μ L RNAiMax) groups were tested using western blots for the most efficient and persistent reduction in SR-BI expression. The optimal dose of 10nM final concentration of siRNA with 5.0 μ L of RNAiMax was chosen. In addition, 25nM and 50nM siRNA with a different cationic delivery system (Lipofectamine® 2000) were tested but are not shown here because they were quickly ruled out due to lack of expression changes and significant toxicity.

APPENDIX C: SIRNA METHOD DEVELOPMENT

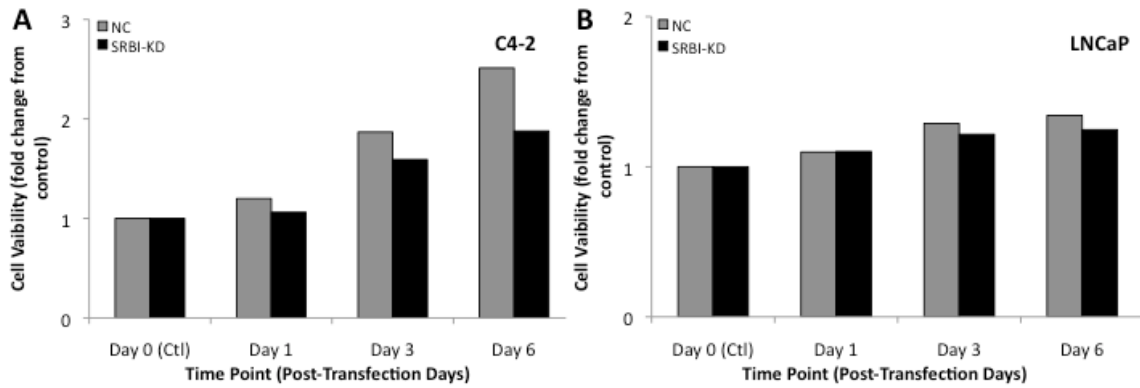


Figure C. A-B: Cell viability of cells grown in 5% CSS as opposed to 1%FBS is demonstrated as fold change in viability from the pre-transfection (Day 0) control in C4-2 (A) and LNCaP (B) cells treated with SR-BI siRNA (SRBI-KD, black columns), a negative control siRNA (NC, grey columns) at Day 1, 3 and 6 post-transfection. Columns, mean (n=2); bars, +/-SEM.

APPENDIX D: LIPOPROTEIN METHOD DEVELOPMENT

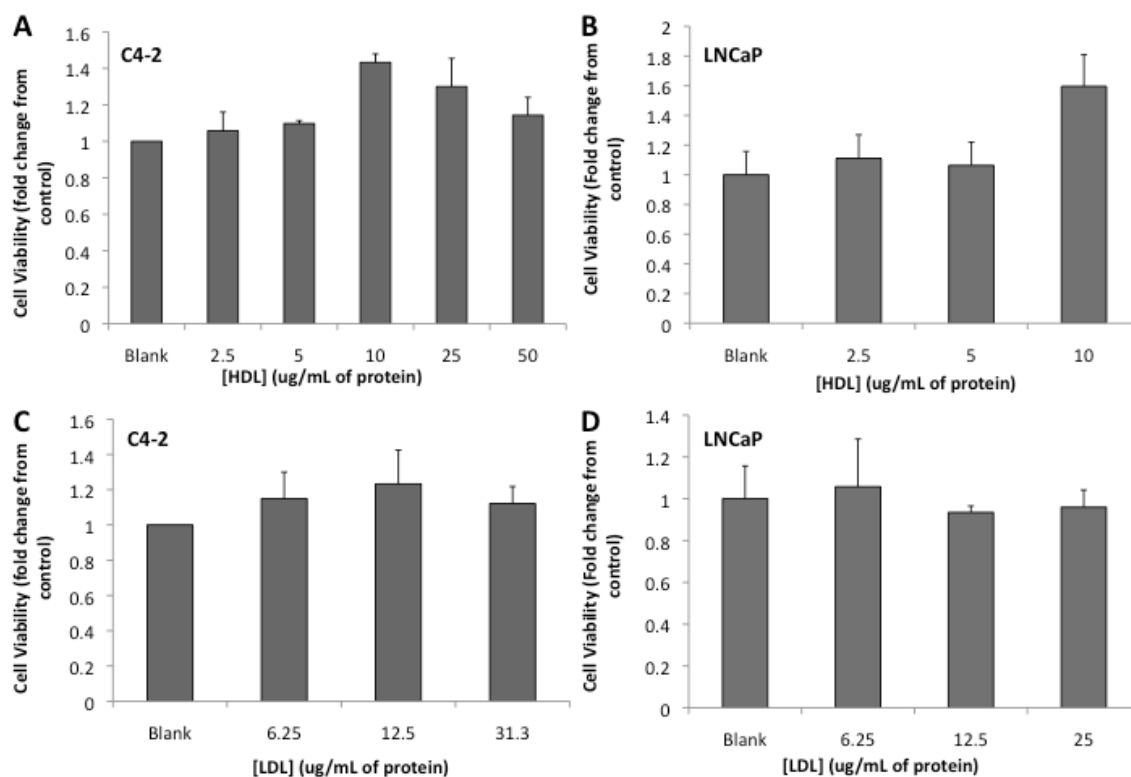


Figure D. A-D: Cell viability of LNCaP and C4-2 cells in response to increasing doses of HDL (A, C4-2 and B, LNCaP) and LDL (C, C4-2 and D, LNCaP) is demonstrated as fold change from untreated controls (Blank). Measures were taken using an MTS assay 24hrs after the addition of 0-50µg/mL HDL or 0-31.3µg/mL LDL. Columns, mean (n=3); bars, +/-SEM.

APPENDIX E: LDL-INDUCED VIABILITY

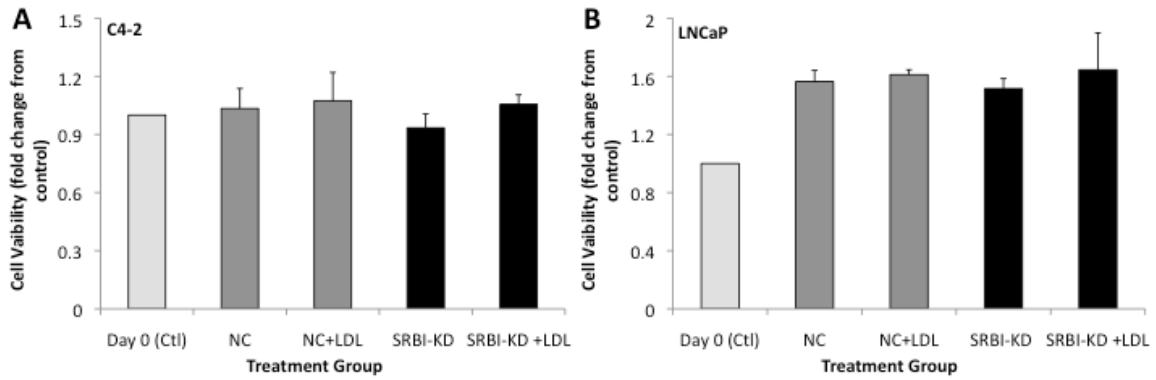


Figure E. A-B: Cell viability is demonstrated as fold change from Day 0 (white column) in C4-2 (A) and LNCaP (B) cells as above. Measures were taken 24hrs after the addition of 6.25ug LDL (+LDL) which was added immediately post-transfection to NC (grey columns) and SRBI-KD (black columns) cells. Columns, mean (n=3); bars, +/-SEM.

APPENDIX F: INTRACELLULAR CHOLESTEROL

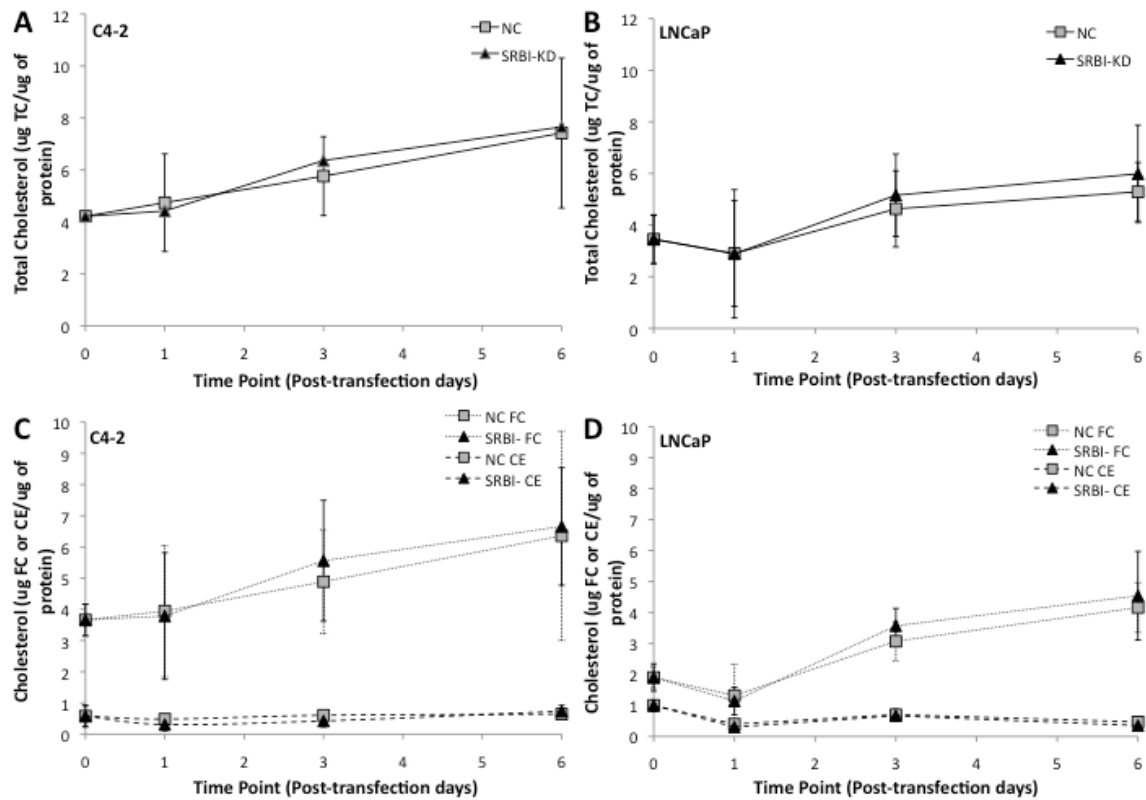


Figure F. A-D: Total cholesterol is shown as μg cholesterol per μg protein in intracellular samples of C4-2 (A) and LNCaP (B) cells treated with SR-BI siRNA (SRBI-KD, black triangles) and negative control (NC, grey boxes) siRNA at Day 0 (pre-transfection) and Day 1, 3 and 6 post-transfection. Free cholesterol (FC, dotted lines) and cholesteryl ester (CE, broken lines) concentration (μg FC or CE/ μg of protein) is shown in C4-2 (C) and LNCaP (D) cells. Curve, mean ($n=3$); error bars, \pm SD.

APPENDIX G: CHOLESTEROL SYNTHESIS DAY 3

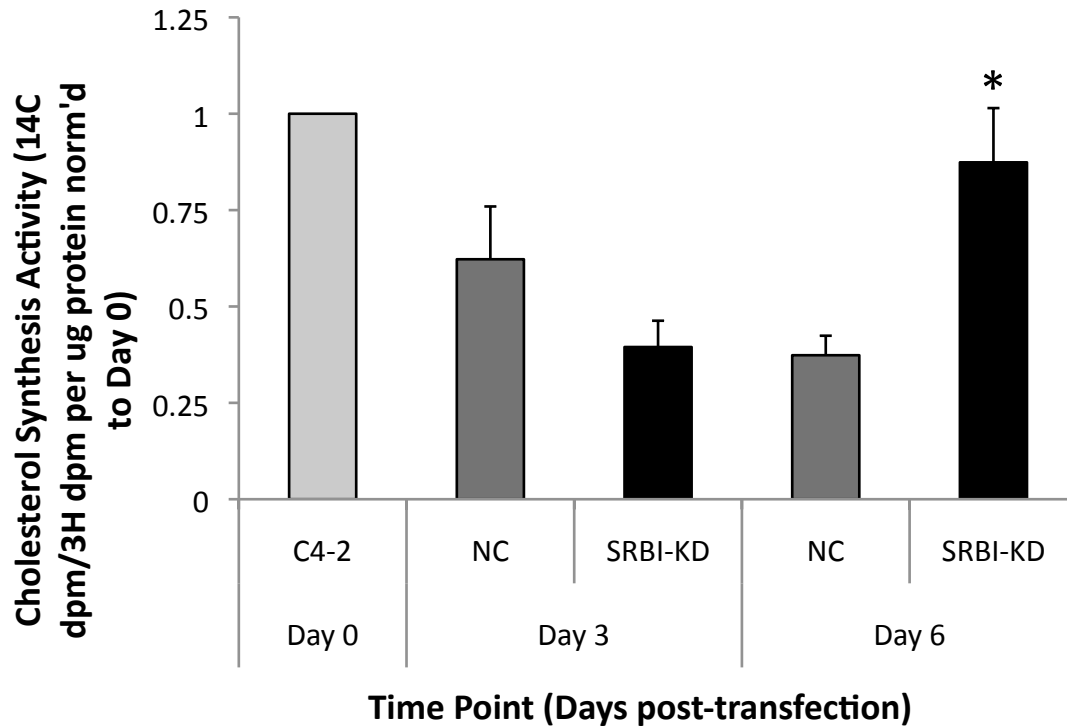


Figure G. Cholesterol synthesis was measured by following the incorporation of ^{14}C -acetate into cellular cholesterol as measured by scintillation counting after separation by thin layer chromatography in C4-2 at Day 0 (light grey column) and Day 3 and 6 post-transfection with negative control siRNA (NC, grey columns) and SR-BI siRNA (SRBI-KD, black columns). All values are corrected by ^3H -cholesterol control counts (dpm) and the amount of protein in each sample well (ug). Columns, mean (n=3); bars, +/- SEM. *, p<.05 Day 6 SRBI-KD vs Day 6 NC.

APPENDIX H: FUTURE STUDIES

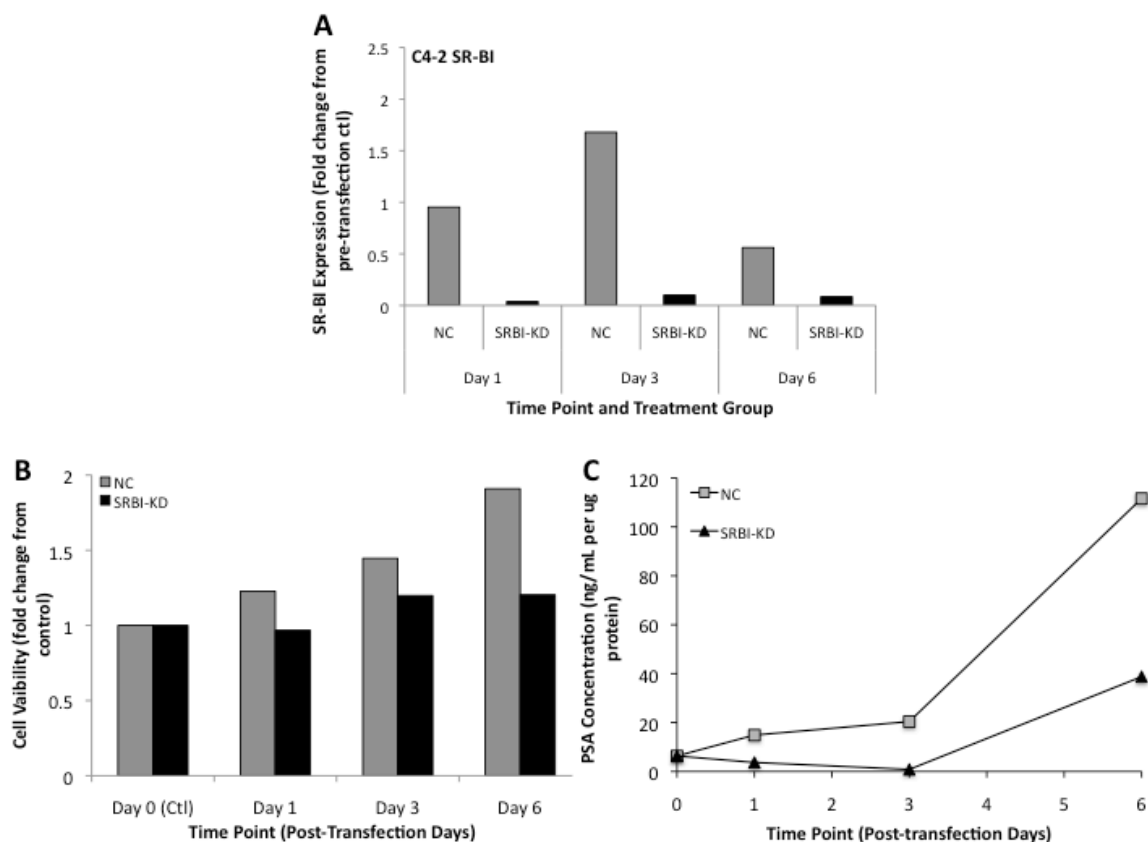


Figure H. A-C: Depicted in this figure is SR-BI expression (A), cell viability (B) and PSA secretion (C) results from a 2-dose siRNA protocol in C4-2 cells. Cells were treated with 10nM NC and SR-BI siRNA for 5 hours and then again, 24 hours following the first transfection. Western blot, MTS and PSA assays were completed 1, 3 and 6 days after the 2nd transfection. The expression data shows an improved silencing at Day 1 (SRBI-KD cells), a greater reduction in cell viability at Day 6 (SRBI-KD) and similar PSA secretion as compared to the single dose protocol. Columns/curves, mean (n=1).